ARKIV FÖR KEMI Band 11 nr 54

Communicated 11 September 1957 by Einar Hammarsten and Erik Jorpes

A comparative study of physico-chemical properties of hyaluronic acid prepared according to different methods and from different tissues

By Torvard C. Laurent

With 4 figures in the text

The shape of the hyaluronic acid molecule has been the subject of many investigations. Blix and Snellman [1], in their streaming birefringence studies, found it to be a long asymmetric molecule. The length varied between 1000 and 10,000 Å in samples prepared from different sources. More recent studies on hyaluronic acid from the vitreous body have confirmed their results [2, 3]. By means of light-scattering, Blumberg and Oster [4] found a spherical shape, which is at variance with the results of Laurent and Gergely [5] and Rowen *et al.* [6], who arrived at a random coil structure. Ogston and Stanier [7], in studying the hydrodynamic properties and sedimentation of a hyaluronic acid–protein complex from synovia, found almost spherical particles, which they assumed to be highly hydrated coils.

The different results of the shape studies seem at first glance to be greatly divergent, but they could all be explained by a highly solvated coil structure, which easily becomes deformed by a shearing force, thus giving an asymmetric particle.

The molecular weight determinations, including such methods as sedimentation [7–12], osmotic pressure [13] and light-scattering measurements [4, 5, 6, 12, 14], have given widely differing results, varying between 5.6×10^4 and 10^7. These differences appear to depend upon three main factors: the tissue from which hyaluronic acid has been prepared, the method of preparation and the method of determination. Osmotic pressure studies give number averages, while sedimentation velocity and light-scattering measurements give the weight averages of the molecular weight[1].

The physico-chemical property of hyaluronic acid that has been studied most is the viscosity [1, 7, 14–20]. This has been found to decrease during the course of different methods of preparation, which has been judged to be a depolymerization of the molecule [15].

In order to test how the method of preparation will affect the molecular characteristics and to study the degree of polymerization of hyaluronic acid prepared from different tissues, the following investigation was undertaken. Hyaluronic acid from

[1] For a system of i components of molar concentration m_i and molecular weight M_i, the number average molecular weight is defined as $M_n = \Sigma m_i M_i / \Sigma m_i$; the weight average as $M_w = \Sigma m_i M_i^2 / \Sigma m_i M_i$, and the z-average as $M_z = \Sigma m_i M_i^3 / \Sigma m_i M_i^2$.

human umbilical cord [21] was isolated according to three different methods. Preparation *A* was prepared according to Blix and Snellman [1], and its characteristics have been reported earlier [5]. Preparation *B* was obtained by digestion of proteins with pancreatic and intestinal enzymes [22, 23], and preparation *C*I was obtained by papain digestion and precipitation with cetylpyridinium chloride according to Scott [24]. Hyaluronic acid was further isolated according to Scott from ox vitreous body, *C*II [25], ox synovia, *C*III [26], cock's comb, *C*IV [27], and pigskin, *C*V [28].

Light-scattering and viscosity measurements have been used to characterize the preparations.

Methods

Light-scattering was measured and evaluated according to Zimm as described earlier [5]. The solutions were centrifuged at 50,000 × *g* for three hours to remove dust. Viscosity was measured in an Ostwald viscometer at 20°C. The values were corrected for kinetic error. The velocity gradient for distilled water was 400 sec^{-1}. The limiting viscosity number[1] is defined as $\lim_{c \to 0} (\eta - \eta_0)/\eta_0\ c$, where η and η_0 are the viscosities of the solution and the solvent respectively, and c the concentration of polysaccharide in g/cc. The concentration determinations are based on analysis of nitrogen, instead of hexosamine as earlier [5, 14], and are expressed in terms of dry and ash-free preparations. All measurements were performed in 0.1 *M* sodium chloride in the absence of buffer at a pH of approximately 5.5.

Material

Preparations

Sample *A* was prepared according to Blix and Snellman [1]. Samle *B* was obtained according to Gardell [22, 23] with some modifications. Because of these modifications, the procedure is reported below.

1500 g of human umbilical cords, freed from blood and blood-vessels, were boiled for 15 minutes, cut into pieces, and homogenized in a Waring blender. The homogenate was digested for three weeks with pancreatic and intestinal extracts, which were added in 1 cc portions daily, at 37°C and pH 8.5. Toluene was added to prevent bacterial growth. The toluene was distilled off and the hyaluronic acid was precipitated in 70 % ethanol. The precipitate was shaken over night in 1000 cc 90 % phenol and then washed with ethanol and ether. It was dissolved in 2000 cc of 0.2 *M* sodium sulphate, chondroitinsulphate was precipitated with an excess of cetylpyridinium chloride and the solution was centrifuged. The hyaluronic acid fraction was precipitated by 70 % ethanol, dissolved in distilled water and precipitated with cetylpyridinium chloride. The precipitate was dissolved in 0.4 *M* sodium chloride and the polysaccharide reprecipitated in 70 % ethanol. It was dissolved in distilled water for 48 hours, centrifuged at 30,000× *g* for 30 minutes and lyophilized. The amount of hyaluronic acid obtained was 1.6 g.

Preparations *C*I–V were obtained according to Scott [24]. The procedure was as follows:

---

[1] The term intrinsic viscosity was used in earlier papers [5, 14] and the concentration expressed in grams per 100 cc.

2000 g of human umbilical cords, 1200 cc of ox vitreous body (prepared from cattle eyes as described earlier [14]), 3000 g of pigskin, 500 g of cock's comb and 1500 cc of ox synovia were used. The skin was ground in a meat grinder and the subcutaneous fat was extracted with aceton at 65°C. The other tissues were homogenized in a Waring blender. The tissues were digested for 16 hours at 65°C in a 0.1 *M* phosphate citrate buffer pH 6.0, which was 0.005 *M* in versen and cystein hydrochloride, with 0.5 % crude papain (Hopkin and William Ltd., London). The volume of the umbilical cord extract was 5000 cc, of skin 3000 cc and of cock's comb 1500 cc. After the digestion the solutions were centrifuged at 30,000 × *g* for 30 minutes. The polysaccharides were precipitated from the supernatant by adding ethanol to a final concentration of 70 %, and redissolved in 0.2 *M* potassium chloride. The solutions were treated with an excess of cetylpyridinium chloride to precipitate chondroitinsulphate, and centrifuged. Hyaluronic acid was then precipitated from the supernatant by addition of ethanol to a final concentration of 70 %, redissolved in distilled water, centrifuged, and reprecipitated with cetylpyridinium chloride. To obtain hyaluronic acid as a potassium salt, the precipitate was dissolved in 0.2 *M* potassium chloride, reprecipitated twice in 70 % ethanol, dissolved in distilled water, dialysed for 48 hours against distilled water, centrifuged at 30,000 × *g* for 30 minutes and lyophilized. The yield from the umbilical cords was 4.4 g, from the vitreous body 0.4 g, from the pigskin 0.4 g, from cock's comb 1.0 g and from the synovia 0.5 g.

The main part of the preparations was performed at 4°C (besides the digestions). However, cetylpyridinium chloride has a very low solutbility at 4°C and the cetylpyridinium precipitations were made at room temperature.

Analyses

The analysis values of the different preparations are tabulated in Table 1. They are compared with the theoretical values for an ash-free and moisture-free preparation.

Table 1. Chemical analysis of the different hyaluronic acid preparations compared with theoretical values calculated from the formula $(C_{14}O_{11}H_{21}N)_n$.

	Analytical method (reference)	Human umbilical cord *B*	Human umbilical cord *CI*	Ox vitreous body *CII*	Ox synovia *CIII*	Cock's comb *CIV*	Pigskin *CV*	Theoretical values
Moisture %		11.5	9.2	13.7	14.1	11.9	14.5	
Ash %		10.7	11.6	10.1	5.9	9.5	9.7	
The following data are calculated as per cent of dry and ash-free preparation:								
Total hexosamine %	(29)[a]	41.7	44.5	42.5	42.2	43.3	44.3	47.2
Galactosamine %	(30)	3.1	1.9	1.2	—	0.4	0.2	—
CO_2 after decarboxylation %	(31)	11.9	11.9	11.6	11.8	11.2	11.6	11.6
Nitrogen %	(32)	4.2	4.1	4.2	4.6	4.2	4.5	3.7

[a] The method of Blix was used with minor modifications.

Results

The results are summarized in Table 2. Each value of molecular weight and radius of gyration[1] is an average of two to six determinations. The mean deviation of the separate values from their average is 7.3 %.[2] The results for preparation *CV* from pigskin are uncertain because of the difficulties which arise in making rectilinear exptrapolations of the scattering values to zero angle. The interaction constant, B,[3] obtained from the limiting slope of $K \times c/R_0$ versus concentration were in all determinations zero or slightly positive.

Table 2. Molecular weights, radii of gyration and limiting viscosity numbers of the different hyaluronic acid preparations.

Preparation	Molecular weight	Radius of gyration Å	Limiting viscosity number
Human umbilical cord (*A*)	3.4×10^6	2200	3360
Human umbilical cord (*B*)	3.0×10^6	2050	2020
Human umbilical cord (*CI*)	5.8×10^6	2600	1330
Ox vitreous body (CII)	3.0×10^5	850	380
Ox synovia (*CIII*)	1.6×10^6	1600	910
Cock's comb (*CIV*)	1.3×10^6	1600	950
Pigskin (*CV*)	(7.2×10^6)	(2500)	1420

Discussion

Chemical analyses of the preparations

In order to characterize the preparations, the following constituents were determined: hexosamine, uronic acid (decarboxylation method) and nitrogen.

The total hexosamine values were somewhat lower than the theoretical value for an acetylglucosamine–glucuronic acid polymer. This has been observed also by other authors and explained as an incomplete hydrolysis of the polysaccharide [33].

Scott's method does not fully separate the galactosamine containing polysaccharides in the preparations from umbilical cord and vitreous body. Galactosamine occurs in the hyaluronic acid preparation from the vitreous body in about the same proportions as found in unprepared vitreous [34]. It would therefore seem to belong not to chondroitinsulphuric acid, which was well separated from skin by Scott's method, but rather to another polysaccharide.

The uronic acid contents are close to the theoretical value.

The nitrogen analysis gave high values indicating the presence of other nitrogen containing compounds besides hexosamine, most probably proteins. The Sewag technique used by Blix and Snellman [1] seems to remove the protein in a larger degree, and the nitrogen content of preparation *A* was only 3.2 % [5].

[1] The term root-mean-square radius was used in earlier papers [5, 14].

[2] If the values of preparation *A*, obtained at different pH's [5], are excluded, the mean deviation is 6.5 %.

[3] B is an expression for the interaction between solute particles and between solute and solvent. $K = 4.58 \times 10^{-7}$ (for hyaluronic acid); c = concentration (g/cc); R_0 = the reduced intensity of scattering in the direction of the direct beam.

Physico-chemical properties

The shape of the hyaluronic acid molecule from umbilical cord (Preparation *A*) as determined by light-scattering, was discussed in an earlier paper [5]. The molecule was assumed to have a moderately stiff coil configuration. The root-mean-square end-to-end distance of a random coil (h) (without stiffness) is according to Kuhn [35]:

$$h^2 = f\,l^2 = v\,u\,d^2, \tag{1}$$

where l is the length of the statistical element in the chain and f the number of statistical elements. d is the length of the monomer (monosaccharide in hyaluronic acid), u the amount of monomers in the statistical unit, and v the total number of monomers in the chain.[1]

As may be seen, the square of the length of a random coil should be proportional to the degree of polymerization, i.e. the molecular weight. The square of the radius of gyration is plotted versus the molecular weight in Fig. 1. Points corresponding to all the different preparations, except *C*V, follow an approximately straight line, which is predicted for a random coil model. The values of *C*V are uncertain, because of difficulties in the extrapolation procedure in the determinations.

Fig. 2 shows the log-log plot of the radius of gyration versus the molecular weight. The experimental values have been compared with lines having slopes corresponding theoretically to rigid rod, random coil and spherical shapes.[2] The hyaluronic acid values indicate a shape between a coil and a sphere. It is however also consistent with a coil model with a certain degree of stiffness. The latter should be most marked at low degrees of polymerization, leading to higher values of the radius of gyration than predicted for a random coil, for low molecular weight species. (The Gaussian statistics is no longer applicable.) This interpretation is in agreement with the findings that preparation *A* had a somewhat stiff coil configuration [5].[3]

If it is assumed that hyaluronic acid can be fairly represented by the line in Fig.1,[4] it is possible to calculate the length of the statistical unit, l, from Eq. (1) by using the relationship for a random coil that $h^2 = 6\,(\overline{r^2})$ where $(\overline{r^2})^{\frac{1}{2}}$ is the radius of gyration [36]. If the monosaccharide length, d, is 5 Å [37], the statistical unit will contain about 60 monosaccharides and have a length of 300 Å.[5] A statistical element of this magnitude indicates stiffness of the glucosidic linkages.

The viscosity of a random coil has been the topic of intense discussion and several different equations have been proposed. Those best known [38–40] predict that the limiting viscosity number of a non-solvent draining randomly coiled polymer should

---

[1] The rotation between the real monomers is not completely free, but the chain can be treated with statistical methods, provided that it is long enough, if it is assumed to be made up of hypothetical links, the so-called statistical elements, which are freely jointed.

[2] Obtained from the relations

$$(\overline{r^2})^{\frac{1}{2}} = K_1 M \text{ (rod)}; \quad (\overline{r^2})^{\frac{1}{2}} = K_2 M^{\frac{1}{2}} \text{ (coil)}: \quad (\overline{r^2})^{\frac{1}{2}} = K_3 M^{\frac{1}{3}} \text{ (sphere)},$$

$(\overline{r^2})^{\frac{1}{2}}$ being the radius of gyration, K_1, K_2 and K_3 constants, and M the molecular weight.

[3] A deduction of the shape from Fig. 2 presumes that the preparations have about the same degree of polydispersity ($M_z : M_w$ = constant).

[4] This assumption is reasonable as the calculated end-to-end length of preparation *A* is only 2 % greater than the length of a Gaussian coil with the same radius of gyration.

[5] The value of l has been calculated for the case in which the preparations are monodisperse. The correct value is obtained if 300 Å is divided by $M_z^2/(M_w M_n)$. l will get a value of 70 Å for a polydispersity of $M_z : M_w : M_n = 3:2:1$.

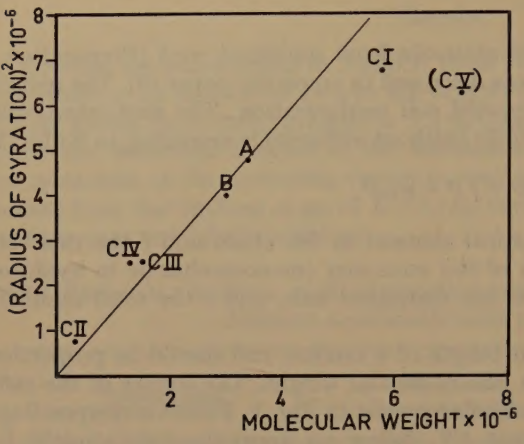

Fig. 1. The square of the radius of gyration for the different preparations plotted versus their molecular weights. The point *C*V is uncertain.

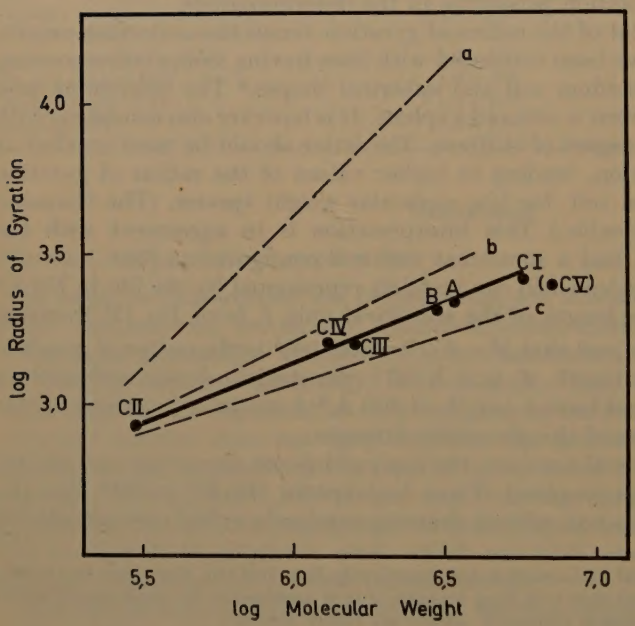

Fig. 2. The logarithm of the radius of gyration is plotted versus the logarithm of the molecular weight. The slope of line *a* corresponds to a rod, of *b* to a random coil and of *c* to a spherical configuration.

be proportional to the square-root of the molecular weight, which means that it is also proportional to the radius of gyration. In Fig. 3, the limiting viscosity numbers of the different preparations are plotted versus the radius of gyration. The different hyaluronic acid samples prepared according to Scott follow a straight line, but the hyaluronic acid from umbilical cord prepared according to Blix and Snellman and to Gardell have appreciably higher viscosities than the other preparations. Hyaluronic acid prepared according to Scott from different tissues would seem, therefore, to

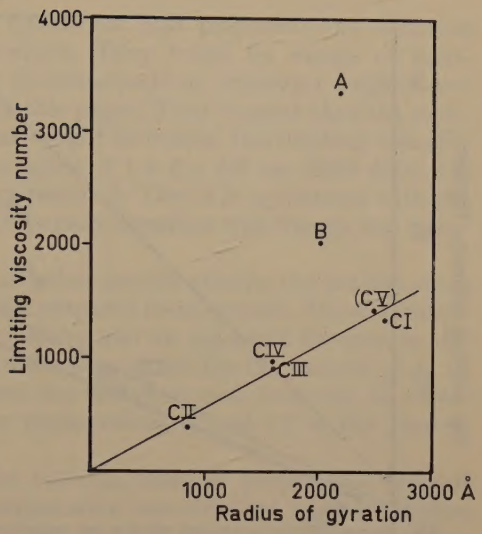

Fig. 3. The limiting viscosity number plotted versus the radius of gyration for the different preparations. The point *C*V is uncertain.

obey the relationship for a randomly coiled, non-solvent draining molecule.[1] An error might lie in the use of limiting viscosity numbers at 400 sec^{-1} and not at zero velocity gradient, and the relationship has therefore only a semiquantitative value. Sundblad [18] showed, however, that the viscosity of preparations of hyaluronic acid with limiting viscosity numbers of the same magnitude as those of *C*I–V were very little shear dependent at the velocity gradients used here.

The logarithm of the molecular weight was plotted versus the logarithm of the limiting viscosity number in Fig. 4. The values for *C*I–V follow a straight line, with a slope close to that of a non-solvent draining coil. For comparison, lines are also drawn with slopes corresponding to free solvent draining coils and rigid spheres.[2]

The high viscosities of the preparations *A* and *B* are of great interest. The preparation *A* was measured in *M*/15 phosphate buffer at the velocity gradient 800 sec^{-1}, while all the others were measured in 0.1 *M* sodium chloride at 400 sec^{-1}. The effect of the differences in ionic strength is, however, small,[3] and an increase in the streaming velocity should decrease rather than increase the viscosity. A possible explanation of the high viscosities of preparation *A* and *B* might be a changed ability for solvent draining through the molecules. This could be brought about by breaking weak intramolecular bonds with the more rough methods of preparation. Weak linkages binding the different parts of the molecular chain together, that break easily and will not reconstitute, might be the explanation of the phenomenon that the viscosity of hyaluronic acid decreases in the course of preparation [15]. It might also ex-

[1] This conclusion includes no assumption regarding the polydispersity, since the averages obtained from viscosity measurements are close to the weight averages [36].

[2] According to Einstein [41] the limiting viscosity number of a rigid sphere is independent of the molecular weight. A free draining coil should follow Staudinger's rule, i.e. direct proportionality between the viscosity and the molecular weight [42].

[3] The limiting viscosity number of preparation *B* in *M*/15 phosphate buffer is 7 % higher than in 0.1 *M* sodium chloride.

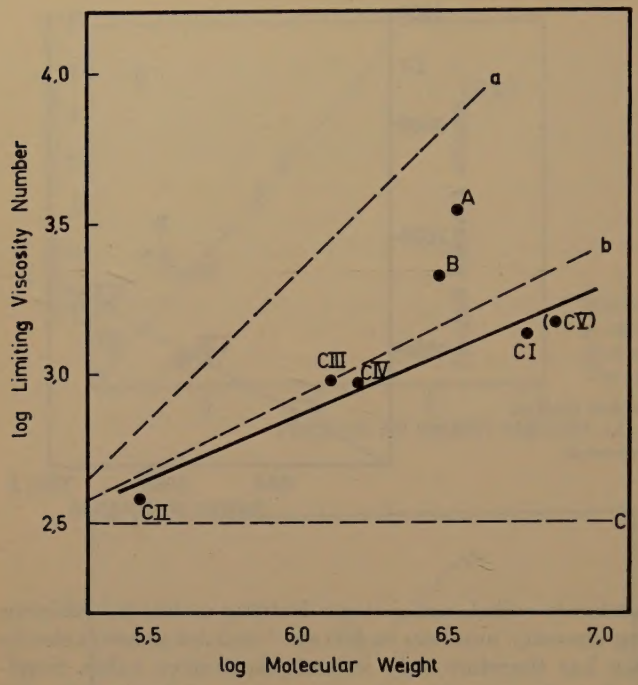

Fig. 4. The logarithm of the limiting viscosity number plotted versus the logarithm of the molecular weight. The slope of line *a* corresponds to a free solvent-draining coil, the slope of *b* to a non-solvent-draining coil and the slope of *c* to a spherical configuration.

plain the drop in the viscosity of preparation *B*, without any change in its molecular weight, after it had been dissolved as a cetylpyridinium salt in methanol [43].

Blix and Snellman [1] found a linear relationship between the length of the molecule and the limiting viscosity number. This is in agreement with the random coil model of the molecule. The molecular weight is then proportional to the square of the length, however, and not directly proportional, as was assumed by the authors.

The radius of gyration determined by light-scattering varies for the different preparations between 850 and 2600 Å, which means an end-to-end distance of 2100–6400 Å (calculated for a non-stiffened coil configuration), and the values obtained by streaming doublerefraction lie between 1000 and 10,000 Å [1–3, 12]. One also suspects that higher values would be obtained when the streaming force deforms and uncoils the molecules.

The molecular weight determinations give the highest values for human umbilical cord and pigskin hyaluronic acid, somewhat lower values for preparations from ox synovia and cocks' combs, and markedly lower values for the ox vitreous body sample. This agrees with the observations made by Blix and Snellman [1] that the umbilical cord preparations have the highest degree of polymerization and the vitreous humour the lowest. This has also been confirmed by the earlier light-scattering studies [5, 14]. Whether this is due to the presence of depolymerizing systems in the tissues and the action of these systems during the preparation procedure, or whether it is an intrinsic property of the tissue polysaccharide it has not yet been possible to establish with certainty.

Balazs *et al* [12] have recently studied hyaluronic acid prepared from different tissues by electrophoresis and electrodeposition. They found by means of light-scattering, sedimentation, and streaming doublerefraction, molecular weights and dimensions in the same range as reported in this paper. They suggest that the molecules coil up more and more as the molecular weight increases. The limiting viscosity numbers for preparations with molecular weights of $1.8–5 \times 10^6$ are 3050–4800, i.e. of the same magnitude as the value for preparation *A*. This is in agreement with the theory that the method of preparation with papain digestion will change the intramolecular structure.

Blumberg and Ogston [44] reported recently that papain attacks the protein component in the hyaluronic acid–protein complex prepared from synovia. The enzymatic hydrolysis was followed by a drop in the viscosity and an apparent decrease in the particle weight. They conclude that the protein is essential for the natural state of myaluronic acid. Digestion with trypsin and chymotrypsin had, however, no effect on the molecular characteristics. (Compare preparations *B* and *CI* of the present investigation.)

There is a great difference between the vitreous humour preparation studied earlier [14] and the present one. The first preparation was obtained by precipitation of the proteins at low and high ionic strengths, and the resultant preparation was estimated to contain 90 % hyaluronic acid. In light-scattering measurements the preparation appeared to be a multicomponent system, which gave the sample a relatively low molecular weight, but a large radius of gyration. This could be taken as a large polydispersity of the preparation. High molecular weight components in the vitreous humour preparations, or polydispersity of these preparations, have been observed also by other investigators [1, 2]. The present preparation does not show the high value of the radius of gyration, but it has about the same molecular weight. It has a higher viscosity value than the first preparation. This result indicates that the earlier preparation contained a large molecular weight component which is not present in this one. Large particles disturb the measurements of the radius of gyration to a greater extent than they disturb the measurements of the molecular weight, as the former is a z-average and the latter a weight-average. The high molecular weight fraction might be partly protein, as it disappears after papain digestion. These findings might explain the discrepancies between the light-scattering data of the first preparation and the sedimentation data [10, 14].

SUMMARY

Three hyaluronic acid samples prepared from human umbilical cord according to different methods have been compared by light-scattering and viscosity. It was found that the molecular weight and dimension did not change with different methods of preparation, but that the viscosity dropped with the enzymatic digestion methods. This has been assumed to be due to a change in the possibility for solvent draining through the molecule.

Hyaluronic acid was further prepared from five different tissues by papain digestion and fractionated precipitation with cetylpyridinium chloride. The radius of gyration and the viscosity as functions of the molecular weight follow the predictions for a randomly coiled molecule, which becomes increasingly stiff at lower degrees of polymerization and which immobilizes solvent within the coil.

ACKNOWLEDGEMENTS

The author wishes to thank Dr. Sven Gardell and Dr. Lennart Rodén for their guidance during the preparative work, and for the help received from Dr. Gardell in carrying out the hexosamine analyses. The investigation was supported by grants from *Stiftelsen Therese och Johan Anderssons minne.*

Department of Chemistry I, Karolinska Institutet, Stockholm.

REFERENCES

1. Blix, G., and Snellman, O., *Arkiv för Kemi, Mineral., Geol. 19A*, No. 32 (1945).
2. Brunish, R., Rowen, J. W., and Irvine, S. R., *Trans. Am. Ophtalm. Soc. 52*, 369 (1954).
3. Varga, L., and Gergely, J., *Biochim. Biophys. Acta 23*, 1 (1957).
4. Blumberg, B. S., and Oster, G., *Science 120*, 432 (1954).
5. Laurent, T. C., and Gergely, J., *J. Biol. Chem. 212*, 325 (1955).
6. Rowen, J. W., Brunish, R., and Bishop, F. W., *Biochim. Biophys. Acta 19*, 480 (1956).
7. Ogston, A. G., and Stanier, J. E., *Biochem. J. 52*, 149 (1952).
8. Fessler, J. H., Ogston, A. G., and Stanier, J. E., *Biochem. J. 58*, 656 (1954).
9. Jensen, C. E., and Djurtoft, R., *Acta Chem. Scand. 8*, 1659 (1954).
10. Varga, L., *J. Biol. Chem. 217*, 651 (1955).
11. Deutsch, H. F., *J. Biol. Chem. 224*, 767 (1957).
12. Balazs, E. A., Varga, L., and Gergely, J., *Ninth Intern. Congr. Rheum. Dis., Toronto, June* 1957.
13. Christiansen, J. A., and Jensen, C. E., *Acta Chem. Scand. 7*, 1247 (1953).
14. Laurent, T. C., *J. Biol. Chem. 216*, 263 (1955).
15. Jeanloz, R., and Forchielli, E., *J. Biol. Chem. 186*, 495 (1950).
16. Balazs, E. A., and Laurent, T. C., *J. Polym. Sci. 6*, 665 (1951).
17. Meyer, K. H., Fellig, J., and Fischer, E. H., *Helv. Chim. Acta 34*, 939 (1951).
18. Sundblad, L., *Acta Soc. Medicorum Upsaliensis 58*, 113 (1953).
19. Jensen, C. E., *Acta Chem. Scand. 8*, 937 (1954).
20. Blumberg, B. S., Oster, G., and Meyer, K., *J. Clin. Investig. 34*, 1454 (1955).
21. Meyer, K., and Palmer, J. W., *J. Biol. Chem. 114*, 689 (1936).
22. Gardell, S., *Arkiv för Kemi 4*, 449 (1952).
23. Gardell, S., and Rastgeldi, S., *Acta Chem. Scand. 8*, 362 (1954).
24. Scott, J. E., Thesis at Victoria University of Manchester (1956) and *Biochem. J, 62*, 31 p. (1956).
25. Meyer, K., and Palmer, J. W., *J. Biol. Chem. 107*, 629 (1934).
26. Meyer, K., Smyth, E. M., and Dawson, M. H., *J. Biol. Chem. 128*, 319 (1939).
27. Boas, N. F., *J. Biol. Chem. 181*, 573 (1949).
28. Meyer, K., and Chaffee, E., *J. Biol. Chem. 138*, 491 (1941).
29. Blix, G., *Acta Chem. Scand. 2*, 467 (1948).
30. Gardell, S., *Acta Chem. Scand. 7*, 207 (1953).
31. Tracey, M. V., *Biochem. J. 43*, 185 (1948).
32. Pregl, F., *Quantitative Organic Microanalysis.* J. and A. Churchill Ltd., London (1945).
33. Blix, G., and Gardell, S. *in* Hoppe-Seyler/Thierfelder, *Handbuch der physiologisch- und pathologisch-chemischen Analyse.* In print.
34. Balazs, E. A., Laurent, T. C., and Laurent, U., unpublished data.
35. Kuhn, W., and Kuhn, H., *Helv. Chim. Acta 26*, 1394 (1943).
36. Stacey, K. A., *Light-scattering in Physical Chemistry.* Butterworths Scientific Publications, London (1956).
37. Laurent, T. C., *Arkiv för Kemi 11*, 513 (1957).
38. Debye, P., and Bueche, A. M., *J. Chem. Phys. 16*, 573 (1948).
39. Kirkwood, J. G., and Riseman, J., *J. Chem. Phys. 16*, 565 (1948).
40. Kuhn, H., and Kuhn, W., *J. Polym. Sci. 9*, 1 (1952).
41. Einstein, A., *Ann. Physik. 19*, 289 (1906).
42. Debye, P., *J. Chem. Physik. 14*, 636 (1946).
43. Laurent, T. C., *Arkiv för Kemi 11*, 497 (1957).
44. Blumberg, B. S., and Ogston, A. G., *Biochem. J. 66*, 342 (1957).

Tryckt den 17 september 1957

Uppsala 1957. Almqvist & Wiksells Boktryckeri AB

ARKIV FÖR KEMI Band 11 nr 55

Communicated 11 September 1957 by Einar Hammarsten and Erik Jorpes

A study of cetylpyridinium hyaluronate in methanol solution

By Torvard C. Laurent

With 2 figures in the text

Hyaluronic acid behaves as a polyelectrolyte [1]. When it dissociates in aqueous solutions it becomes negatively charged. The charges affect the shape of the molecule and its interaction with surrounding macromolecules. Because of the large number of hydroxyl and carboxyl groups on the chain, it probably also interacts with the surrounding water via hydrogen bonds. The physico-chemical characteristics depend, to a large extent, on these properties. By coupling cetylpyridinium ions with the carboxyl groups of hyaluronic acid, a compound is formed which is insoluble in distilled water [2]. The compound is soluble in lower alcohols such as methanol, ethanol and propanol [3]. A hyaluronic acid derivative which is soluble in a solvent other than water can yield new information regarding the behaviour of this macromolecule. The following is a report on light-scattering and viscosity studies on cetylpyridinium hyaluronate.

Methods

Light-scattering measurements at the angles 30°–135° were performed in a Brice–Phoenix light-scattering instrument using blue light (4358 Å). The technique has been described earlier [4]. Dust was removed by centrifuging the solutions in a Spinco preparative ultracentrifuge for at least two hours at 50,000 × g. The refractive increment was measured with a Zeiss interferometer and was found to be 0.17 for sodium hyaluronate in water and 0.18 for cetylpyridinium hyaluronate in methanol.

Viscosity measurements were performed in two Ostwald viscometers, A and B, at 20°C. The capillaries were 29 and 188 mm long and had bores of 0.5 and 0.4 mm respectively. The bulbs contained 5 and 0.5 ml fluid. In viscometers A and B the outflow time (t) for water was 86.2 and 131.9 seconds and for methanol 67.9 and 95.5 seconds, the kinetic error $580/t$ and $13.3/t$ and the velocity gradient $272{,}000/t$ and $53{,}000/t$ sec^{-1} respectively.

The concentration of cetylpyridinium chloride was calculated from the optical density at 260 mμ measured in a Beckman DU spectrophotometer. Control curves for cetylpyridinium chloride were made in 0.1 M sodium chloride and in 100 % methanol. For cetylpyridinium hyaluronate control curves were made in 100 % methanol and, after centrifugation, in 80 % methanol to which had been added potassium chloride to 0.4 molarity. The different solvents did not change the optical density more than 3 %.

Nitrogen was determined as described earlier [4].

Material

Sodium hyaluronate from human umbilical cord was used. It was prepared by digestion with proteolytic enzymes and was fractionated from chondroitinsulphate as described elsewhere ([5], preparation *B*). For complete analysis values see this paper. The nitrogen content of the dry and ash-free polysaccharide was 4.2 %. All concentrations are expressed as dry and ash-free preparations.

Cetylpyridinium chloride was recrystallized twice from hot water solutions. Its nitrogen content was 4.3 % (theoretical value: 4.13 %). The optical density of a 0.01 % solution was 1.27.

The methanol used was nitrogen free and had a low optical density at 260 mμ.

Experimental

Experiment A

To 50 ml 0.25 % sodium hyaluronate was added 10 ml 1.7 % cetylpyridinium chloride (dissolved at 65°C), which is 1.5 times the stoichiometric equivalent of the hyaluronic acid carboxyl groups. The solution was centrifuged, and the white precipitate was washed twice with 5-ml portions of water at 65°C, dried in air and dissolved in 40 ml of methanol. The optical density of this solution corresponded to 0.287 % cetylpyridinium chloride. The nitrogen content was 0.0254 %. Of this, 0.0123 % belongs to cetylpyridinium chloride and the rest to hyaluronic acid. Thus the calculated polysaccharide concentration is 0.312 %. This corresponds to a ratio of 1.00:1.03 between disaccharides and cetylpyridinium chloride.

The methanol solution, which had become somewhat reduced and diluted during the physico-chemical measurements and the analysis, was used for regenerating the polysaccharide. One part of 2 *M* potassium chloride was added to four parts of the methanol solution. The potassium hyaluronate precipitate was centrifuged, redissolved in distilled water and reprecipitated twice in 60 % methanol, and then dissolved in 30 ml 0.1 *M* sodium chloride. The opitcal density of this solution at 260 mμ would correspond to a maximum residual cetylpyridinium chloride concentration of 0.002 %. The nitrogen analysis gave the value 0.0078 %, which means a polysaccharide concentration of 0.184 %.

Light-scattering and viscosity were measured on the original and on the regenerated sodium hyaluronate. Both samples were studied at various concentrations in aqueous solutions of 0.1 *M* sodium chloride. The cetylpyridinium hyaluronate was studied in methanol solution. The light-scattering measurements were made on solutions of less than 0.03 %.

The duration of the experiment was five days. The solutions were kept at 4°C when not used.

Experiment B

Cetylpyridinium hyaluronate was precipitated as in experiment *A*. The precipitate was then dissolved in methanol *containing 0.267 % free cetylpyridinium chloride*. Light-scattering measurements were performed on cetylpyridinium hyaluronate at concentrations less than 0.03 %. The concentration of this complex was calculated from the initial amounts of the polysaccharide, assuming that one cetylpyridinium ion was attached to every carboxyl group.

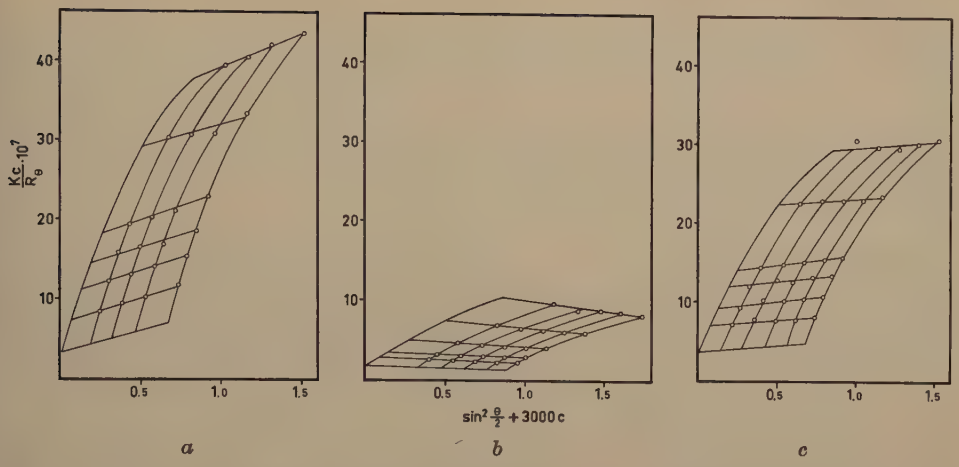

Fig. 1. Zimm plot of the original sodium hyaluronate (*a*), the cetylpyridinium hyaluronate (*b*) and the reconstituted sodium hyaluronate (*c*). *a* and *c* in 0.1 *M* NaCl, *b* in absolute methanol.

Table 1.

	Molecular weight	Radius of gyration Å	*B*
Sodium hyaluronate (original preparation) . . .	3.0×10^6	2030	1.6×10^{-3}
Cetylpyridinium hyaluronate in methanol	5.4×10^6	1185	-0.1×10^{-3}
Sodium hyaluronate (regenerated)	3.0×10^6	1800	0.6×10^{-3}

Results

The light-scattering values were evaluated according to Zimm [4].

Experiment A

The Zimm plots of the original sodium hyaluronate perparation, of the cetylpyridinium hyaluronate and of the reconstituted sodium hyaluronate are given in Fig. 1. In Table 1 the molecular weight values, the radii of gyration[1] and the interaction constant (*B*) are tabulated.

The viscosity number $((\eta - \eta_0)/\eta_0 c$; η and η_0 are the viscosities of the solution and solvent respectively and c the concentration in grams per ml) is plotted in Fig. 2 as a function of the concentration. The limiting viscosity number[2] obtained by extrapolation to zero concentration is tabulated in Table 2 for the two viscometers A and B.

[1] The term root-mean-square radius was used in earlier papers [4].

[2] The term intrinsic viscosity was used earlier, and the concentration was expressed in grams per 100 ml [4].

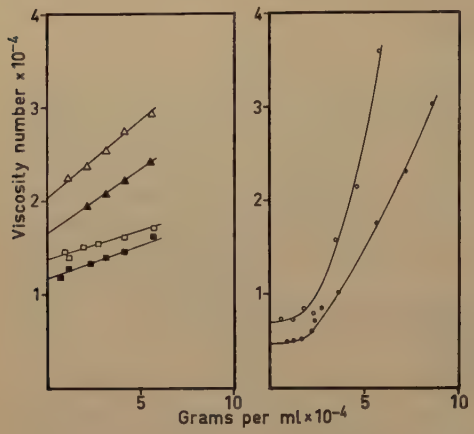

Fig. 2. The viscosity number is plotted vs. concentration for the original sodium hyaluronate (△ ▲), the reconstituted sodium hyaluronate (□ ■), and for cetylpyridinium hyaluronate in methanol (○ ●). Open marks for measurements in viscometer B, filled for viscometer A.

Table 2.

	Limiting viscosity number at velocity gradient	
	400 sec^{-1} (550 sec^{-1})[a]	3150 sec^{-1} (4000 sec^{-1})[a]
Sodium hyaluronate (original preparation)	2020	1660
Cetylpyridinium hyaluronate in methanol	670	450
Sodium hyaluronate (regenerated)	1360	1180

[a] For methanol solution.

Experiment B

0.267 % cetylpyridinium chloride in methanol showed strong scattering, indicating that micelles of cetylpyridinium chloride molecules had been formed in the solution. The molecular weight of these micelles was roughly estimated to be several millions. The size of the cetylpyridinium hyaluronate complex was difficult to determine because of the strong concentration dependence. However, it was estimated to be approximately 30×10^6.

Discussion

Hyaluronic acid is precipitated with equivalent amounts of cetylpyridinium chloride, and the compound formed is soluble in methanol. Both the chemical analysis and the light-scattering values confirm that about one cetylpyridinium ion is attached to each disaccharide unit of the hyaluronic acid molecule. The molecular weight of the complex: 5.4×10^6 shows an increase of 80 %. If the equivalent weight of the disaccharide of the hyaluronic acid is 379 and that of the cetylpyridinium hyaluronate is 683, it will correspond to an increase of 80 %. This is in agreement with the finding of J. E. Scott, i.e. it is possible to titrate the negative groups of hyaluronic acid with cetylpyridinium chloride.

The radius of gyration of the cetylpyridinium hyaluronate complex is only about 1200 Å, but the sodium hyaluronate molecule, with its lower molecular weight, has a radius of gyration of 2000 Å. This indicates that the molecular structure has col-

lapsed when the charges on the chain are neutralized and the solute–solvent (including the counter ion) interaction has changed. The lower limiting viscosity number of the cetylpyridinium hyaluronate as compared with the sodium hyaluronate confirms the decrease in size and change in shape.

The viscosity number of the cetylpyridinium hyaluronate is strongly dependent on the concentrations indicating aggregation (Fig. 2). This is also a probable explanation for the negative value of the interaction constant (B) in the light-scattering measurements.

From experiment B it is seen that cetylpyridinium chloride itself has a tendency to form micelles in methanol. An increase of the concentration of cetylpyridinium chloride in the presence of hyaluronic acid will increase the size of the cetylpyridinium hyaluronate complex. This results either from the adsorption of the cetylpyridinium molecules by the complex or from the aggregation of the complex. Therefore, studies on the cetylpyridinium hyaluronate must be performed in low concentrations and without excess of cetylpyridinium chloride.

The regenerated sodium hyaluronate had properties slightly different from those of the original hyaluronate. The viscosity is lower, and the radius of gyration and the interaction constant (B) are also lower. The molecular weight appeared, however, to be constant. There is a possiblity that weak intramolecular bonds have been broken during the procedure and the flexibility of the molecule has increased. This will be discussed elsewhere [5].

The viscosity is markedly dependent upon the velocity gradient, indicating either an ordering effect or a deformation of the molecules during oriented flow.

The ability to dissolve hyaluronic acid in solvents other than water gives us a tool which would be of great help in chromatographic, chemical and physico-chemical work. (See also Bera *et al.* [3]).

SUMMARY

When cetylpyridinium ions are coupled with carboxyl groups of hyaluronic acid a compound is formed which is soluble in alcohols. This has been studied in methanol solutions by light-scattering and viscosity. The molecular weight increases corresponding to the weight of the attached cetylpyridinium ions. The radius of gyration of the molecule decreases from 2000 Å to 1200 Å. This indicates a contraction of the molecule when the stabilizing effects of the charges and the interaction with water have disappeared.

This investigation was supported by grants from *Stiftelsen Therese och Johan Anderssons minne.*

Department of Chemistry I, Karolinska Institutet, Stockholm.

REFERENCES

1. Balazs, E. A., and Laurent, T. C., *J. Polym. Sci. 6,* 665 (1951).
2. Scott, J. E., *Biochim. Biophys. Acta, 18,* 428 (1955) and Thesis at Victoria University of Manchester 1956.
3. Bera, B. C., Foster, A. B., and Stacey, M., *J. Chem. Soc.* 3788 (1955).
4. Laurent, T. C., and Gergely, J., *J. Biol. Chem. 212,* 325 (1955).
5. Laurent, T. C., *Arkiv för Kemi 11,* 487 (1957).

Tryckt den 17 september 1957

Uppsala 1957. Almqvist & Wiksells Boktryckeri AB

ARKIV FÖR KEMI Band 11 nr 56

Communicated 11 September 1957 by Einar Hammarsten and Erik Jorpes

On the hydration of macromolecules

X-ray diffraction studies on aqueous solutions of hyaluronic acid

By Torvard C. Laurent

With 5 figures in the text

The solute–solvent interaction in macromolecular solutions has been the subject of many theories. Recently, a new hypothesis was put forward to explain the interaction between water and certain gel-forming substances, such as desoxyribonucleic acid and hyaluronic acid [1]. The hypothesis is based mainly on dielectric studies [1, 2] and proton magnetic resonance measurements on desoxyribonucleic acid solutions [3].

According to X-ray studies the normal water structure is four-coordinated [4, 5]. Every oxygen atom tries to surround itself by four other oxygen atoms by means of hydrogen bonds at a distance of about 2.9 Å. Different theories have been developed to explain the difference between water and the regular four-coordinated lattice structure of ice [4, 5, 6, 7]. One of them, proposed by Forslind [6], explains the difference in terms of thermal vibrations, lattice defects (Frenkel defects) and lone interstitial water molecules.

According to the hypothesis referred to, the hydration of the macromolecules stabilizes the normal water lattice and this stabilized structure extends a great distance from the surface of the macromolecules. When desoxyribonucleic acid and hyaluronic acid are dissolved in water, certain groups on the macromolecular chain combine with the water lattice. The thermal vibrations in the lattice are reduced and the amount of Frenkel defects decreases. Lone interstitial water molecules give the lattice about the same density as that of normal water. The effect is most prominent close to the macromolecular surface and decreases with increasing distance from the surface.

A decrease in the thermal vibrations and in the amount of Frenkel defects should give a more regular four-coordinated water structure. X-ray diffraction is the only unequivocal method to study a change in the four-coordination. It has been reported in a preliminary note that the effect of some gel-forming substances such as desoxyribonucleic acid, carboxymethylcellulose and dibenzoylcystin, on the diffractogram of water is the same as the effect of a temperature decrease [8].

This paper is a report of an extended X-ray investigation on aqueous solutions of hyaluronic acid supplemented by radial distribution analysis.

Methods

The diffractograms were obtained in three different cylindrical cameras (diameter 57.3 mm). These were built by Dr. B. Jacobson according to the Guinier principle for Cu K_α and Mo K_α radiation [9]. The exposures were made at 50 kV, 15 mA over the X-ray tube with molybdenum target and 40 kV, 15 mA over the copper tube. The camera was filled with helium during Cu K_α exposures.

The water solutions were kept in flat cells with thin mica windows in two of the cameras and the penetrating forward scattering was registered. In the third camera, constructed for Mo K_α exposures, the specimens were kept in thin glass capillaries and both the forward and the backward scattering were measured.

The intensity of the scattering was registered on photographic film within a range of $5° < 2\theta < 60°(160°)$ corresponding to a total s-interval of $0.36 < s < 17.41$. (2θ = the angle of diffraction; $s = (4\pi \sin\theta)/\lambda$ where λ = the wavelength of the radiation.) Ilford Industrial C and G X-ray films were used. The films were developed under standard conditions. The optical density was measured at individual points in a Zeiss microphotometer with a 0.15 × 1.0 mm slit. The slit width corresponds to a maximum of 0.04 s-units. The accuracy of the photometer was within 1 %. Industrial G X-ray film was preferred because of its greater speed and the better near linear relationship between the optical density and the exposing intensities.

The intensity of the diffractogram, measured as the optical density of the film at positions corresponding to different angles includes certain errors, some of which have to be corrected. *Background radiation* was obtained from exposures of empty cells and capillaries. It was corrected for absorption in the specimen and subtracted from the intensity of the diffractogram. Correction factors for *polarization* and *absorption* in flat and cylindrical specimens are given by Klug and Alexander [9]. The distance between the cell and the film in the flat-cell cameras changes with the angle and a correction factor for the *asymmetric position of the sample was used.*

Further errors depending on voltage fluctuations in the X-ray tubes and the photometer and on unevenness in the film as well as on differences in the cell windows and capillaries amount to about 1–2 % of the maximum intensity in the diffractograms. The error was decreased by combining several X-ray pictures and make photometer readings at short intervals.

The projection width on the film of the diffraction cones within the s-range used was at no angle larger than 0.08 s-units in the flat-cell cameras and 0.25 s-units in the capillary camera.

Material

Two preparations of sodium hyaluronate (I and II) from human umbilical cord were studied. Preparation I was obtained according to Blix and Snellman [10] and preparation II by enzymatic digestion of the proteins and precipitation with cetylpyridinium chloride ([11], Preparation *B*). The analysis values of preparation I were as follows: ash 9.5 %, moisture 7.9 %, and nitrogen 3.4 %. The same values for preparation II were as follows: ash 10.7 %, moisture 11.5 %, and nitrogen 3.3 %. The limiting viscosity numbers in 0.1 M sodium chloride were 4400 and 2020 respectively at a velocity gradient of 400 sec^{-1}.

Calculation of radial distributions

Only a short summary of radial distribution analysis is given below. For more details see Klug and Alexander [9] and Brosset [12].

Hydrogen atoms give very small scattering compared to oxygen atoms, and water can therefore be assumed to contain only one kind of atom from the point of view of X-ray diffraction. A radial distribution calculated for water gives the positions of other oxygen atoms around a reference atom.

When there is only one kind of atom present in a sample, e.g. oxygen, the intensity scattered from the sample will be given by the formula

$$I(s) = N_a f^2(s) \left[1 + \int_0^\infty 4\pi r^2 (\varrho_a(r) - \varrho_0)\, dr\, \frac{\sin sr}{sr}\right], \tag{1}$$

where $I(s)$ = the intensity of coherent scattering expressed in electron units; N_a = number of atoms in the sample; $f(s)$ = the atomic scattering factor for oxygen [13]; $\varrho_a(r)$ = the number of atoms per unit volume at the distance r from a reference atom; ϱ_0 = the average number of atoms per unit volume in the sample; r = the distance from the reference atom.

With the aid of the Fourier integral theorem the equation (1) can be converted to

$$4\pi r^2 \varrho_a(r) = 4\pi r^2 \varrho_0 + \frac{2r}{\pi} \int_0^\infty s\, i_a(s) \sin sr\, ds, \tag{2}$$

where

$$i_a(s) = \frac{I(s)}{N_a f^2(s)} - 1. \tag{3}$$

$4\pi r^2 \varrho_a(r)$ is the number of atoms in a shell with unit thickness at the distance r from the reference atom.

Finbak has shown that the results are more reliable if, instead of calculating the atomic distribution, one calculates the electronic radial distribution [14]. He defines his electronic radial distribution function:

$$\varrho_e(r) = C r \int_0^\infty s\, i_e(s) \sin sr\, ds \tag{4}$$

$$i_e(s) = I(s) - N_a f^2(s). \tag{5}$$

$\varrho_e(r)\, dr$ is the probability of finding electrons in the system at a mutual distance between r and $r + dr$. C is a constant.

Calculation of the radial distribution from observed scattering values consists of two main steps. The relative intensities obtained should be converted to the functions $i_a(s)$ and $i_e(s)$ and the integrals (2) and (4) should be calculated.

The experimental intensity values after due corrections, contain two components, coherent and incoherent scattering. The theoretical coherent and incoherent scattering, if the atoms scatter independently of each other, have been tabulated [13]. The experimental intensity data are adjusted to the total theoretical independent

scattering, $B(s)$,[1] at high s-values ($8 < s < 14$), and the difference between the measured and the theoretical values is $i_e(s)[N_a = 1]$. $i_a(s)$ is obtained by dividing $i_e(s)$ by $f^2(s)$.

The integrals (2) and (4) have been calculated with a digital electronic computer, which performed the summation

$$\frac{2r}{\pi} \sum_{s=0}^{s=p} s\, i(s) \sin sr\, \Delta s \qquad (6)$$

for r-values between 0–8 Å. $i(s)$ stands for $i_e(s)$ and $i_a(s)$ respectively. Δs was selected as 0.05, which gives good resolution at high r-values. The $s\, i(s)$ values below $s = 0.35$ were obtained by rectilinear extrapolation. At high s-values $i(s)$ approaches zero, and the summation can be limited to a finite s-value (p). The experimental errors will be more pronounced at high s-values. Therefore $p = 8.0$ was used for the electronic distribution and $p = 6.5$ in the atomic radial distribution calculations.

Results

The X-ray diffractogram of water, shown in Fig. 1, is in good agreement with the results of other investigations [4, 5, 15, 16, 17]. There are four peaks at the s-values 2.03, 2.85, 4.5 and 7.0. The second peak is less marked than in the diffractograms published by Morgan and Warren [4] and by Finbak [5]. The intensity of the third

[1] The scattering of the hydrogen atoms has been included in the calculations of the incoherent scattering.

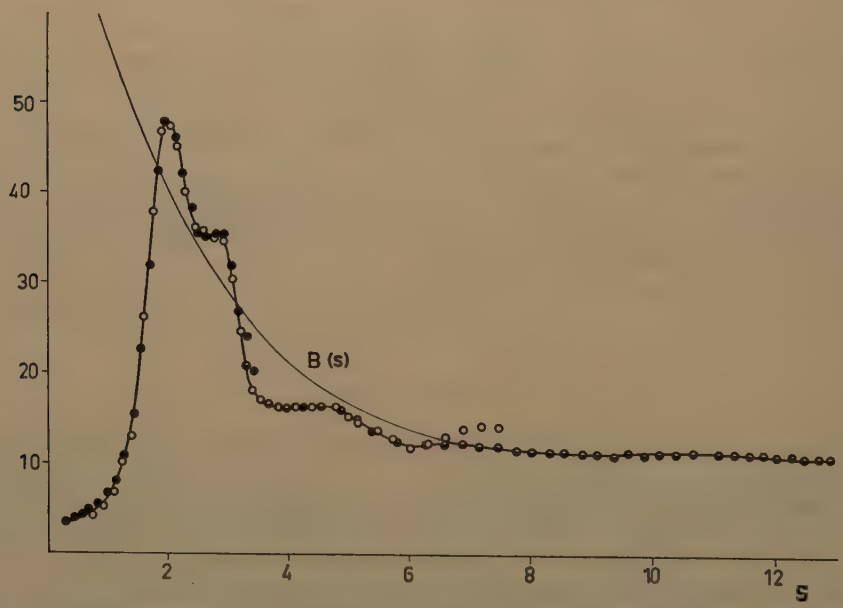

Fig. 1. The diffractogram of pure water. $B(s)$ represents the total independent scattering. The experimental points from the Cu $K\alpha$ (●) and Mo $K\alpha$ (○) flat-cell cameras and the capillary camera (◒) have been matched to the total independent scattering at high s-values.

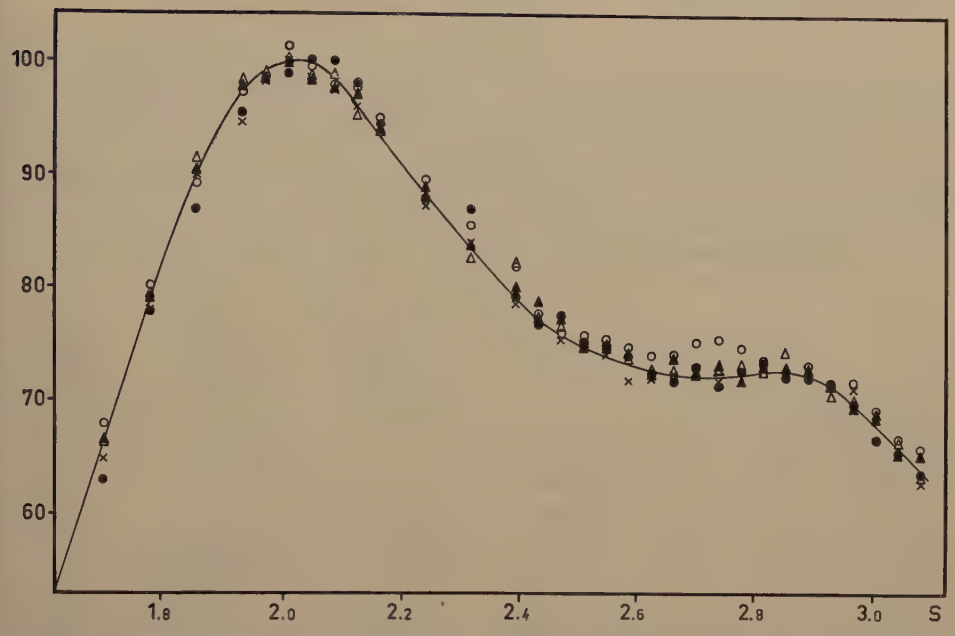

Fig. 2. The diffractogram of water in the interval $1.7 < s < 3.1$ is compared with the values from hyaluronic acid II solutions of the concentrations 0.25 % (×), 0.5 % (△), 1.0 % (▲), 1.5 % (○) and 2.0 % (●).

peak is lower than Finbak's value, but in good agreement with that of Morgan and Warren.

The electronic radial distribution is shown in Fig. 3. The first peak is at 3 Å, corresponding to the hydrogen bond distance. The next peak is a broad peak between 4 and 5 Å, corresponding to a second layer in a four-coordinated structure. There is a further peak at 7 Å.

The first peak of the atomic distribution ($4\pi r^2 \varrho_a(r)$) is at 2.9 Å (Fig. 4*a*). The area under the peak corresponds to 4.65 atoms. Morgan and Warren report 4.6 at 30°C. The maximum between 4 and 5 Å in the electronic radial distribution has been divided by a low minimum at 4.3 Å. This minimum was not reported earlier. There are reasons to believe that this minimum is an artefact, as no corresponding minimum is found in the electronic distribution, and it is possible to suppress it by cutting off the amplitude of the $i_a(s)$ function at high s-values, where the experimental errors are large.

The hyaluronic acid preparation I has been measured at the concentrations 0.3 % and 1.0 % and preparation II at 0.25 %, 0.5 %, 1.0 %, 1.5 % and 2.0 %.

The diffractograms of the hyaluronic acid solutions were compared with that of water in the interval $1.7 < s < 3.1$. The height of the main peak of all the diffractograms was set to 100 arbitrary units. The water diffractogram composed of five different molybdenum exposures is shown in Fig. 2. The individually measured points of the five concentrations of hyaluronic acid II are also plotted. Each point is the mean value of two separate exposures. The deviations of the hyaluronic acid points from the water diffractogram are tabulated in Table 1. The deviations have been given as per cent of the height of the main peak.

Table 1.

The mean deviation of the individually measured points of five different Mo K_α exposures of water has been calculated in the intervals $1.7 < s < 3.1$ and $2.5 < s < 3.1$. This is compared with the average deviation of the measured values of different hyaluronic acid solutions from the water diffractogram (columns I and III). The deviation is expressed as per cent of the height of the main peak.

The diffractograms have been calculated from the measured individual points for each hyaluronic acid concentration. In columns II and IV are given the mean deviation of the five water diffractograms and the deviation of the hyaluronic acid solutions from pure water (e.g., + 0.24 means that the curve as an average lies 0.24 % above the water curve).

	$1.7 < s < 3.1$		$2.5 < s < 3.1$	
	I Individual points	II Diffractogram	III Individual points	IV Diffractogram
H_2O (5 diffractograms)	±1.19	±0.66	±1.25	±0.73
Hyaluronic acid I				
1 %	1.28	+0.24	0.84	−0.51
0.3 %	0.99	−0.42	1.18	−1.17
Hyaluronic acid II				
2 %	1.08	−0.05	0.68	+0.23
1.5 %	1.47	+1.44	1.72	+1.72
1.0 %	0.71	+0.39	0.76	+0.59
0.5 %	0.75	+0.72	0.78	+0.64
0.25 %	0.81	−0.35	0.57	0.00

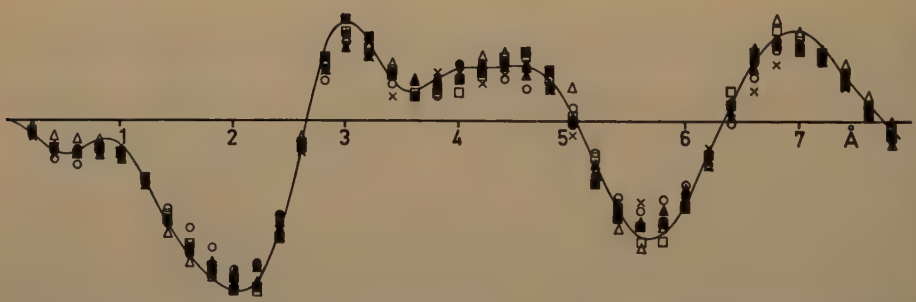

Fig. 3. The electronic radial distribution ($\varrho_e(r)$) for pure water is compared with hyaluronic acid solutions. Preparation I, 0.3 % (■) and 1.0 % (□); preparation II, 0.25 % (×), 0.5 % (△), 1.0 % (▲), 1.5 % (○) and 2.0 % (●).

As can be seen from Fig. 2, there is no significant shift of the first peak towards lower angles in the hyaluronic acid diffractograms. There is a small shift of the 2 % solution towards higher angles (about 0.03 s-units), but this is hardly significant. The increase in the height of the second peak is within the limit of the error, which is clearly shown in Table 1. The mean deviation of the individual water values from the curve is ±1.25 % in the interval $2.5 < s < 3.1$. The mean deviation from the water curve of the individual hyaluronic acid points are all lower except for the 1.5 % concentration, where it is of the same magnitude. It is impossible to distinguish any shift of the angle of the second peak.

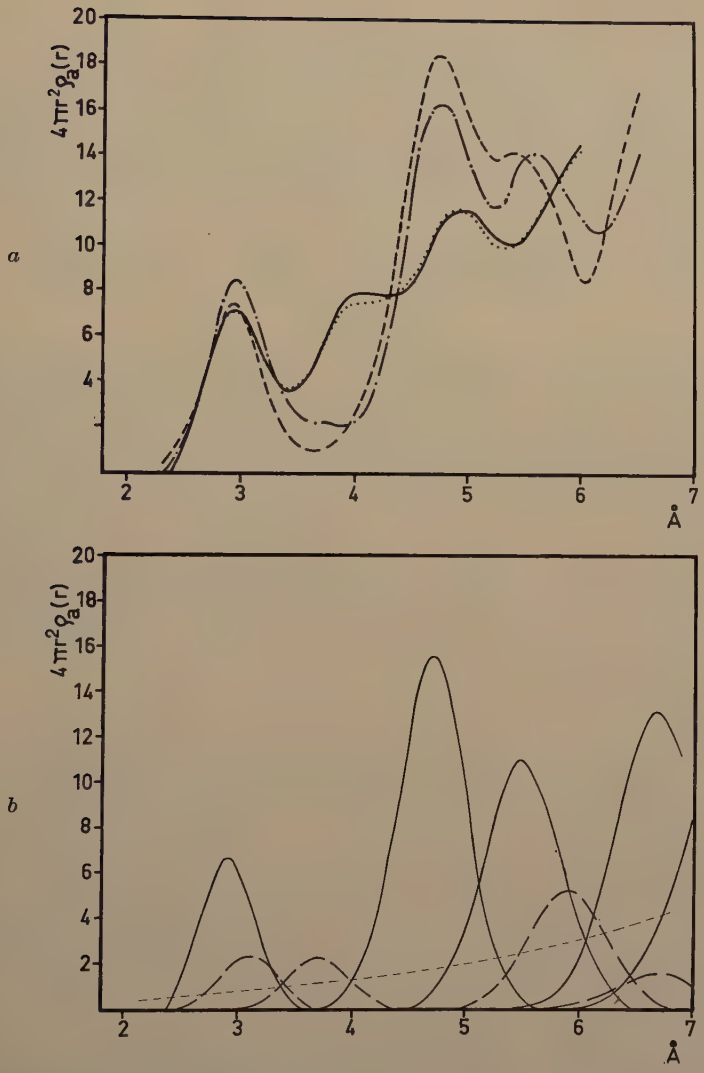

Fig. 4*a*. The experimental atomic radial distribution of pure water (———) compared with the distribution in a 1.0 % hyaluronic acid I solution (·····). The distribution for an ideal four-coordinated hexagonal lattice with lone interstitial molecules placed at random (– – –) or in the center of the interstices (–·–·–) has been calculated for comparison. For the calculations see text and Fig. 4*b*.

Fig. 4*b*. Calculation of a regular four-coordinated lattice according to Prins and Petersen. The lattice molecules (———) were placed 4 at 2.9 Å, 12 at 4.7 Å, 9 at 5.5 Å, 12 at 6.7 Å, and 9 at 7.2 Å. The lone interstitial molecules were either placed at random (– – –) or 1.5 at 3.1 Å, 1.5 at 3.7 Å, 4.5 at 5.9 Å, and 1.5 at 6.7 Å (— — —).

The second step was to compare the electronic radial distributions obtained for the hyaluronic acid solutions with that of pure water. The results are plotted in Fig. 3. The hyaluronic acid points are scattered around the water curve with rather

large deviations. However, there is no intrinsic tendency for the hyaluronic acid points to deviate in any special direction. The large deviations come from erroneous matching of the experimental values to the total independent scattering curve, $B(s)$, at high s-values. Finbak [14] has also pointed out the fact that it is possible to draw qualitative conclusions from the sites of the maxima in the radial distributions, but that one has to be careful in making quantitative deductions from the heights of the peaks.

The third step in the investigation was to calculate the atomic radial distribution for water and hyaluronic acid solutions. The results are shown in Fig. 4.

Discussion

The present investigation was performed in order to test the hypothesis that certain macromolecules should stabilize the normal water structure and give a more regular four-coordinated lattice. If pseudo-crystalline hydration shells, many times greater than the molecules they surround, are formed, one should find changes in the diffractograms. Changes which are smaller than 2 % cannot be attributed to structural changes in the water, as the scattering from the dissolved specimen will be of this order.

The results of the study of pure water are in good agreement with earlier reports. The minimum at $r = 4.3$ Å in the atomic radial distribution is most probably an artefact, as it does not appear in the electronic distribution. Finbak [14] has shown that erroneous peaks in the atomic distributions are easily obtained. As it does not disturb the conclusions, no investigation of its origin is needed.

From the studies on hyaluronic acid it has not been possible to verify the effects on the water diffractogram, which were reported for other gel-forming substances [8], as the differences found are within the limits of the experimental errors ($< 2\,\%$).

The electronic radial distribution was calculated for all concentrations of hyaluronic acid. This includes all measured values from $0.36 < s < 8.00$. If there were any major changes within this range, indicating an increased regularity in the four-coordinated lattice, they should show up in the distributions. There are no indications of this. However, the objection can be made that the Fourier summation was arbitrarily extended to $s = 8.0$. When the summation was extended to $s = 6.5$; 7.0; and 7.5; there were no appreciable changes in the distributions and 8.0 was therefore considered to be a safe limit.

What kind of changes can we expect in the radial distribution if there is an increased lattice order in the water? As long as we do not know the magnitude and nature of the hydration, we cannot predict the radial distribution. Assuming, however, that the thermal vibrations are randomly distributed and the amount of Frenkel defects are negligible throughout the bulk of the water, we can calculate an approximate atomic distribution. It may be pointed out that the thermal vibrations, at least in ice, are to a certain degree direction-dependent [18]. The distribution was calculated for an ideal four-coordinated "ice-like" structure with an oxygen–oxygen distance of 2.90 Å. To account for the correct density of water, lone interstitial water molecules were placed within the lattice. In one calculation they were placed at random and in another in the center of the lattice interstices. The distributions are calculated according to Prins and Petersen ([4] and [19]):

$$4\pi r^2 \varrho_a(r) = \sum_k \frac{N_k b}{(\pi r_k)^{\frac{1}{2}}} \exp\left(-(b^2/r_k)(r-r_k)^2\right), \tag{7}$$

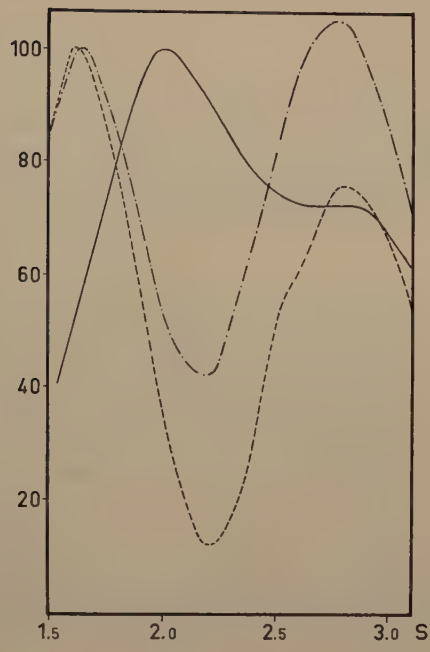

Fig. 5. A comparison of the experimental diffractogram of water (———) in the region $1.5 < s < 3.1$ with the calculated curves for a regular four-coordinated lattice with lone interstitial water molecules placed at random (– – –) or in the center of the interstices (–·–·–).

where N_k is the number of neighbours at a distance r_k, and b is a constant chosen so that the curve will fit to the first experimental peak. The atoms were placed as shown in Fig. 4*b*. In Fig. 4*a*, the calculated distributions are compared with the distribution for water and for a 1 % hyaluronic acid I solution. The atomic distribution of the water molecules in the hyaluronic acid solution closely follows the pure water distribution, and there is no definite change towards the distributions for the regular four-coordinated lattices.

The atomic distributions calculated for the two ideal four-coordinated lattices have been used to obtain the corresponding intensity curves in the range $1.5 < s < 3.1$ with the aid of Eq. (1). The integral was calculated as a summation comparable to Eq. (6) for $0 < r < 6.5$. The intensity curves are given in Fig. 5 compared with the experimentally obtained curve for water. Fig. 5 gives us an idea of in what direction we could have expected possible changes of the water diffractogram. The first peak should have moved towards lower s-values and the second peak should be more marked. These are also the changes obtained in the diffractogram when the temperature of the water is decreased [4]. No such changes have been found in the hyaluronic acid solutions.

The hypothesis that macromolecules should stabilize the water structure and increase the lattice order was based mainly on the dielectric and proton magnetic resonance properties of certain macromolecular solutions. As these properties are not directly correlated with the positions of the oxygen atoms in the lattice, but rather with the behaviour of the protons, it has been suggested that the stabilization of the water lattice involves a change in the mobility of the protons and their ability to take part in chain reaction jumps [20].

SUMMARY

The hydration of hyaluronic acid in solution in concentrations below 2 % does change the X-ray diffractogram of pure water only within the experimental errors (< 2 %). X-ray diffraction gives no support for the hypothesis that hyaluronic acid forms large hydration shells with an increased four-coordinated hexagonal lattice structure.

ACKNOWLEDGEMENTS

The author wishes to thank Dr. Bertil Jacobson, who introduced him to the problem, and who also built the cameras. Thanks are also due to Fil. lic. Gunnar Ehrling and "Statens Matematikmaskinnämnd" for aid with the Fourier analyses. The investigation was supported by grants from *Statens Medicinska Forskningsråd* and *Karolinska Institutets reservationsanslag.*

Department of Chemistry I, Karolinska Institutet, Stockholm.

REFERENCES

1. JACOBSON, B., *J. Am. Chem. Soc. 77*, 2919 (1955) and *Sv. Kemisk Tidskrift 67*, 1 (1955).
2. JACOBSON, B., and LAURENT, T. C., *J. Colloid Sci. 9*, 36 (1954).
3. JACOBSON, B., ANDERSON, W. A., and ARNOLD, J. T., *Nature 173*, 772 (1954).
4. MORGAN, J., and WARREN, B. E., *J. Chem. Phys. 6*, 666 (1938).
5. FINBAK, CHR., and VIERVOLL, H., *Tidskr. f. Kjemi, Bergvesen og Met. 3*, 36 (1943).
6. FORSLIND, E., *Proc. Swed. Cement and Concrete Res. Inst.* No. 16 (1952).
7. POPLE, J. A., *Proc. Roy. Soc. A 205*, 163 (1951).
8. JACOBSON, B., *Acta Chem. Scand. 9*, 192 (1955).
9. KLUG, H. P., and ALEXANDER, L. E., *X-ray Diffraction Procedures.* John Wiley and Sons Inc., New York (1954).
10. BLIX, G., and SNELLMAN, O., *Arkiv f. Kemi, Mineral., Geol. 19A*, No. 32 (1945).
11. LAURENT, T. C., *Arkiv f. Kemi. 11*, 487 (1957).
12. BROSSET, C., *Arkiv f. Kemi 1*, 353 (1949).
13. COMPTON, A. H., and ALLISON, S. K., *X-rays in Theory and Experiment.* D. Van Nostrands Co. Inc., New York (1935), pp. 781–782.
14. FINBAK, CHR., *Acta Chem. Scand. 3*, 1279 (1949).
15. MEYER, H. H., *Ann d. Physik 5*, 701 (1930).
16. STEWART, G. W., *Phys. Rev. 37*, 9 (1931).
17. SIMONS, L., *Soc. Scient. Fenn. Comm. Phys. Math. 10*, 9 (1939).
18. OWSTON, P. G., *Acta Cryst. 2*, 222 (1949).
19. PRINS, J. A., and PETERSEN, H., *Physica 3*, 147 (1936).
20. JACOBSON, B., personal communication.

Tryckt den 17 september 1957

Uppsala 1957. Almqvist & Wiksells Boktryckeri AB

ARKIV FÖR KEMI Band 11 nr 57

Communicated 11 September 1957 by Einar Hammarsten and Erik Jorpes

The amorphous X-ray diffractogram of hyaluronic acid

By Torvard C. Laurent

With 4 figures in the text

X-ray diffraction is the most suitable method for structural analysis of crystalline materia. It can also be applied to amorphous compounds, such as liquids, but the only information obtained in these cases is the probability that certain interatomic distances may occur in the sample. Most polymers can be treated as amorphous compounds if the molecules in the specimen are unoriented. X-ray studies of different amorphous polymers are reported in the literature (see e.g. Klug and Alexander [1]), and the diffractograms have been Fourier-analysed in a few cases [1, 2, 3]. This is a report on the X-ray diffractogram of hyaluronic acid and the information obtained from it.

Theory

Finbak [4] has shown that the distribution of distances between electrons belonging to different atoms in an amorphous compound is given by the expression:

$$\varrho_e(r) = C r \int_0^\infty i(s)\, s\, (\sin sr)\, ds, \qquad (1)$$

where $\varrho_e(r)dr$ is the probability of finding two electrons belonging to different atoms at a distance from each other of r to $r + dr$. C is a constant; $s = (4\pi \sin\theta)/\lambda$; 2θ = the angle of diffraction and λ = the wavelength of the radiation. $i(s)$ is given by:

$$i(s) = i_{exp}(s) - B(s), \qquad (2)$$

where $i_{exp}(s)$ is the diffracted intensity obtained experimentally, corrected for polarization, and adjusted at high s-values to the function $B(s)$, which is the sum of the total independent coherent and incoherent scattering calculated theoretically.

Methods

The X-ray diffractograms were measured in a Philips Wide Range Goniometer [1] at the angles $3° < 2\theta < 156°$, which correspond to $0.21 < s < 7.97$. Cu K_α radiation was monochromatized by a 0.021 mm thick nickel filter. The voltage and current over the X-ray tube were kept at 20 kV and 36 mA respectively.

The intensity was registered by a GM-counter-ratemeter with a scaler attached. A time constant of 16 seconds was used. The scanning speed was $\frac{1}{2}°$ per minute. A $\frac{1}{6}°$

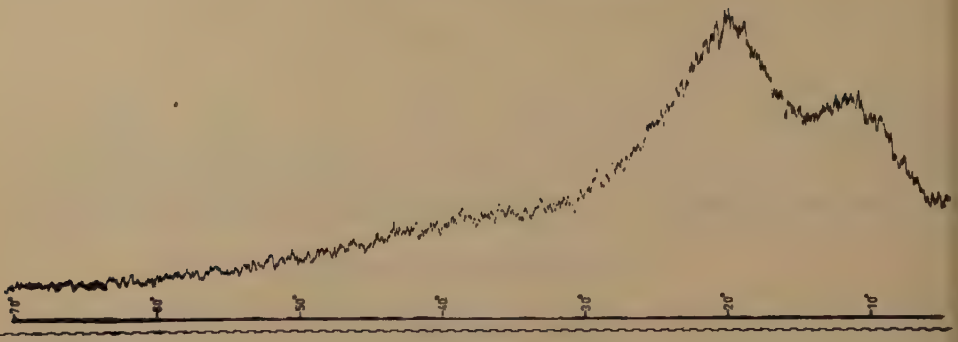

Fig. 1. The amorphous X-ray diffractogram of lyophilized hyaluronic acid in the interval $3° < 2\theta < 70°$. (Cu K_α irradiation. Time constant 16 seconds. Scanning rate $\frac{1}{2}°$ per minute. Divergent slit $\frac{1}{6}°$. Receiving slit 0.2°.)

divergent slit was used in the interval $3° < 2\theta < 30°$, and a 1° slit in the interval $30° < 2\theta < 156°$. The receiving slit was 0.2°.

The number of counts per second varied between 15 and 50, i.e. the number of counts for every 2° (corresponding to an s-interval of about 0.1) is at least 3600. The standard deviation for this count is ± 1.67 %. The mean deflexion from the curve will however be as much as 4.6 % [5] which will be seen clearly in Fig. 1.

The samples used were pressed to flat squares (10 × 20 mm). The thickness (t) fulfilled the condition

$$t > \frac{3.2}{\mu} \sin \theta$$

which gives a beam of maximum intensity [1]. μ is the linear absorption coefficient.

The total independent scattering ($B(s)$) was calculated as the sum of the coherent and incoherent scattering from the different elements in the specimen. For tabulated values of independent scattering see e.g. Compton and Allison [6]. The experimental intensity values were read from the curves (Fig. 1) with s-intervals of 0.1. They were corrected for polarization and background scattering. The absorption is independent of the angle, and no correction was made for it [1]. The experimental values were adjusted to $B(s)$ in the interval $6.5 < s < 8.0$ by multiplication with a suitable factor. $i(s)$ values were obtained according to Eq. (2), and Eq. (1) was solved by a digital electronic computer [7].

Material

Hyaluronic acid from umbilical cord was prepared by enzymatic digestion of proteins and precipitation of the polysaccharide as a cetylpyridinium salt. The procedure and analysis values are given elsewhere ([8], Preparation *C*I). Chondroitinsulphate prepared from the rib cartilage of young calves was kindly supplied by Dr. Sven Gardell. The preparations were dissolved in 0.2 % solution and shaken with a cation exchange resin (Dowex 50, H-form, 20–40 mesh). The supernatant was lyophilized. The ash contents of the dry preparations were found to be 0.76 % of the hyaluronic acid and 0.92 % of the chondroitinsulphuric acid. The lyophilized preparations were easily pressed to flat squares suitable for measurements.

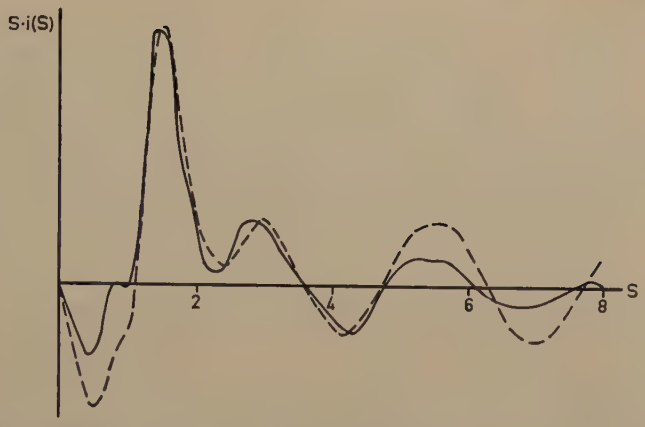

Fig. 2. The $si(s)$ function of lyophilized hyaluronic acid (———) and chondroitinsulphuric acid (– – –).

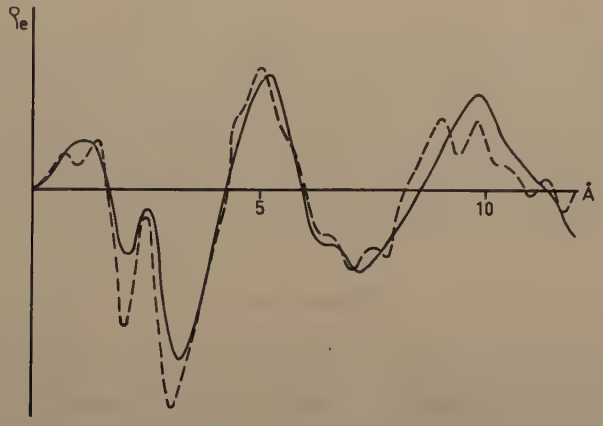

Fig. 3. Electronic radial distribution in lyophilized hyaluronic acid (———) and chondroitinsulphuric acid (– – –).

A quantity of hyaluronic acid was dissolved in distilled water and titrated to neutrality with 0.1 N sodium hydroxide. One portion of the sodium hyaluronate was lyophilized and another precipitated in 70 % ethanol. The densities of the two preparations when pressed to flat squares were 0.6 and 1.2 g/cm³ respectively.

Results

The X-ray diffractograms of hyaluronic acid, chondroitinsulphuric acid and sodium hyaluronate were very much alike, and a typical diffractogram is shown in Fig. 1. There are two main peaks at the angles $2\theta = 11.5°$ and 20.0° and a rather flat peak at about 40°.

For the computation of the radial distributions according to Eq. (1), the $si(s)$ values were tabulated with intervals of 0.1 s-units. A rectilinear extrapolation was

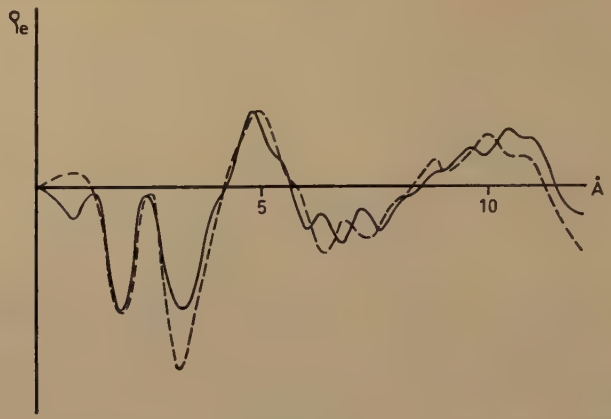

Fig. 4. Electronic radial distribution in lyophilized (– – –) and ethanol-precipitated (———) sodium hyaluronate.

made from $s = 0.3$ to zero. It was assumed that the integration of Eq. (1) could be performed to $s = 8.0$ instead of to infinity. The $si(s)$ functions of hyaluronic acid and chondroitinsulphuric acid are shown in Fig. 2. The curves have prominent maxima at about 0.85 $Å^{-1}$, 1.5 $Å^{-1}$, 2.9 $Å^{-1}$ and 5.5 $Å^{-1}$. The corresponding radial distributions after the Fourier transforms are given in Fig. 3. In Fig. 4, the Fourier transforms of sodium hyaluronate prepared by lyophilization and ethanol precipitation are compared. The main characteristics in all the electron distributions are peaks at about 1.3–1.5 Å, 2.5 Å, 5 Å and 10 Å.

Discussion

The present technique was found to be preferable to the photographic technique for liquid diffraction described in an earlier paper [7]. The measuring takes less time and the error in the photometry is eliminated. The technique gives a very good resolution of the peaks in the diffractogram, and the different s-intervals are well resolved by using different scale factors on the scaler. Because of the experimental set-up, the absorption is not dependent on the angle, and needs no correction factor.

The measuring range goes to low s-values ($s = 0.2$), which is of importance in measuring large interatomic distances. The upper limit ($s = 8.0$) is about the same as that which Björnhaug *et al.* [9] found to be useful for cellulose. It is probable, however, that an increased s-range would make adjustment to $B(s)$ more accurate.

A large ratemeter time constant was used to decrease the fluctuations in the curve contour. The retarded response by which this was attended did not seem to disturb the values, since there are no sharp peaks in the diffractogram.

The X-ray scattering from an amorphous organic material is low and the uncertainty in the measurements with a ratemeter increases. The error is in the order of two per cent, i.e. the same as with the photographic method [7].

The irregularity of the hyaluronic acid structure decreases the amplitude of the intensity function, ($i(s)$ in Eq. (2)), which increases the influence of the error of the measurements. An error in the intensity function or in the adjustment of the experimental values to the theoretical independent scattering, may give erroneous peaks

in the calculated radial distribution. Finbak [4] has shown that the positions of the real peaks usually are correct, but that their height easily might deviate from the theoretical height. An incorrect adjustment to $B(s)$ gives erroneous peaks at low r-values. These facts call for caution when drawing conclusions.

Like other carbohydrate compounds, hyaluronic acid has a complicated structure, and only very dominating interatomic distances will be revealed in the radial distribution. There are two kinds of interatomic distances, intra- and intermolecular. The present technique does not allow of any distinguishment between the two.

The result shows one peak at about 1.3–1.5 Å corresponding to the carbon–carbon (1.54 Å) and carbon–oxygen (1.43 Å) distances. The peak is badly resolved from an artefact at low r-values in two of the radial distributions given. The artefact depends on incorrect adjustment of the experimental intensity function to $B(s)$. (See Finbak [4].) The next peak at 2.5 Å corresponds to the next nearest neighbour distance (C–C–C, C–O–C, C–C–O). The occurrence of these two peaks shows the reliability of the method. The same peaks have been demonstrated in several other polymers, e.g. in cellulose and alginic acid [2, 9].

A plausible explanation of the peaks at 5 Å and 10 Å would be the smooth interferences from inter-chain distances. It has been shown that the chain–chain distance in cellulose has given dominating peaks in the $\varrho_e(r)$ curve at 5.3 Å and 9.7 Å [9]. In order to test this possibility, the sodium hyaluronate preparation was measured in lyophilized and ethanol-precipitated state. Judging from the densities, the chain–chain distances might be considerably different in the two preparations. The difference in the radial distributions is however mainly a displacement of the broad peak at 10 Å, and not a change of the 5 Å peak. The difference is small, and is more probably due to coiling of the molecular chain rather than to a change in the chain–chain distance. Furthermore, if the density is used to calculate the chain–chain distance in the lyophilized preparation, assuming a hexagonal packing, one arrives at a value of 11.3 Å.

The repeating unit of the hyaluronic acid polymer is a disaccharide of glucuronic acid and N-acetylglucosamine. The monosaccharides are probably united by 1–3 linkages [10]. So far nothing is known about the steric building of the polysaccharide chain. The distance between the centers of gravity of two neighbour monosaccharides in the chain is in the order of 5 Å. If the chain is mobile in the glucosidic linkages, the result in the $\varrho_e(r)$ curve of the interferences between the monosaccharides should be a smooth peak at about 5 Å and a second peak at about 10 Å. The 5 Å peak can therefore be taken as an expression for the link length of the chain.

The chondroitinsulphuric acid and hyaluronic acid have similar radial distributions, indicating that the relationship between the two molecules is not purely organochemical.

The difference between hyaluronic acid and its sodium salt is revealed by the presence of several small peaks in the distribution of the salt. The significance of the peaks may be debatable but the agreement between the two sodium hyaluronate preparations is striking, except for the peaks at 6–7.5 Å. With a more refined technique the small peaks may become more reliable, and can then be used for further structural studies of the polymer.

SUMMARY

A one-dimensional Fourier analysis of the amorphous X-ray diffractogram of hyaluronic acid reveals main peaks at 1.3–1.5 Å, corresponding to the carbon–carbon and carbon–oxygen distances, 2.5 Å corresponding to the next nearest neighbour distance, 5 Å and 10 Å. 5 Å seems to be a characteristic periodicity of the sample. Sodium hyaluronate and chondroitinsulphuric acid give radial distributions similar to those of hyaluronic acid.

ACKNOWLEDGEMENTS

The author is grateful to "Statens Matematikmaskinnämnd" for aid with the Fourier analyses. The investigation was supported by grants from *Karolinska Institutets reservationsanslag.*

Department of Chemistry I and Department of Medical Physics, Karolinska Institutet, Stockholm.

REFERENCES

1. Klug, H. P., and Alexander, L. E., *X-ray Diffraction Procedures.* John Wiley and Sons Inc., New York 1954.
2. Björnhaug, A., Ellefsen, Ö., and Tönnesen, B. A., *J. Polym. Sci. 12,* 621 (1954).
3. Riley, D. P., and Arndt, U. W., *J. Colloid Sci. 1,* 57 (1954).
4. Finbak, Chr., *Acta Chem. Scand. 3,* 1279 (1949).
5. Hägg, G., *Fasanalys och identifiering med röntgendiffraktion.* Uppsala 1954.
6. Compton, A. H., and Allison, S. K., *X-rays in Theory and Experiment.* D. Van Nostrands Co. Inc., New York 1935, pp. 781–782.
7. Laurent, T. C., *Arkiv för Kemi 11,* 503 (1957).
8. Laurent, T. C., *Arkiv för Kemi 11,* 487 (1957).
9. Björnhaug, A., Ellefsen, Ö., and Tönnesen, B. A., *Norsk Skogsindustri 7,* 171 (1953).
10. Weissmann, B., and Meyer, K., *J. Am. Chem. Soc. 76,* 1753 (1954).

Tryckt den 17 september 1957

Uppsala 1957. Almqvist & Wiksells Boktryckeri AB

ARKIV FÖR KEMI Band 11 nr 58

Communicated 5 June 1957 by Arne Fredga

On the thiophene analogues of mandelic acid

By Salo Gronowitz

With 6 figures in the text

In connection with work on optically active thiophene compounds, it was of interest to study the thiophene analogues of mandelic acid. Seventy years ago Ernst (1) claimed to have prepared the 2-isomer, 2-thienylglycolic acid, by reduction of 2-thienylglyoxylic acid with sodium amalgam. No experimental details were given. He states that the melting point is 116°. The 3-isomer has recently been prepared by Campaigne and Bourgeois (2) through the cyanohydrin synthesis from 3-thiophenecarboxaldehyde in low yield. The cyanohydrin synthesis of α-hydroxy acids, which is the most convenient route to mandelic acid (3), when applied to 2-thiophenecarboxaldehyde gives only tars on hydrolysis of the cyanohydrin and no 2-thienylglycolic acid could be isolated, even when the hydrolysis was carried out under mild conditions. Thus, the cyanohydrin synthesis is not a practical route for the preparation of thienylglycolic acids. It may, however, be possible that the modifications of the cyanohydrin synthesis worked out by Nerdel (4) for the preparation of 2-furylglycolic acid may also be useful for the thiophene compounds.

A convenient synthesis of the thienylglycolic acids was, however, found in the quantitative rearrangement of the thienylglyoxals into these acids in aqueous alkali. 2-Thienylglyoxal has earlier been prepared in several ways (5, 6); the most convenient synthesis seems to be the method by Kipnis and Ornfelt (7) who prepared it through SeO_2 oxidation of 2-acetothienone in 43 % yield, especially as the present author in several experiments found that yields between 70–75 % could be reached. The 2-thienylglyoxal was further characterized through the quinoxaline prepared by the reaction with *o*-phenylenediamine (8).

2-Thienylglycolic acid was prepared from 2-thienylglyoxalhydrate by dissolving it in 1 *N* sodium hydroxide solution and refluxing for 10 minutes. After acidification and extraction with ether an acid was obtained which had a m.p. of 81–82° even after several recrystallizations from benzene. As mentioned above, Ernst gave a m.p. of 116°. The acid obtained by the present author analyses correctly for 2-thienylglycolic acid and gives upon desulphurization with Raney-Nickel alloy α-hydroxycaproic acid. Any isomerization during the rearrangement of 2-thienylglyoxalhydrate is also improbable, as Neville (9) through C_{14} tracer studies of the rearrangement of phenylglyoxal to mandelic acid has shown that no rearrangement of the carbon skeleton occurs and that the reaction thus proceeds by a shift of the aldehydic hydrogen. Several attempts were made to crystallize the acid from different solvents and to innoculate with mandelic acid

in case the 2-thienylglycolic acid obtained is polymorphic. However, the same melting point was always obtained. In order to solve this discrepancy the experiments of Ernst were repeated.

2-Thienylglyoxylic acid, obtained through permanganate oxidation of 2-acetothienone (10), was reduced with 5 % sodium amalgam. The acid obtained in 70 % yield had the same melting-point as the 2-thienylglycolic acid obtained from 2-thienylglyoxal, gave no melting-point depression with this acid and had the same IR-spectrum which was free from the characteristic maxima of 2-thienylglyoxylic acid. The route via the glyoxal is, however, the better method of synthesis as 2-thienylglyoxylic acid can only be obtained in small portions as the oxidation of 2-acetothienone has to be made in dilute solutions. It can also be obtained through the ethoxalylation of thiophene with ethoxalyl chloride (11) followed by hydrolysis. This, however, is a much more cumbersome method.

2-Thienylglycolic acid is difficult to crystallize and rather an unstable compound. When heated for a few minutes on a boiling water bath it polymerizes readily to a dark tar and it also darkens rapidly when allowed to stand in day-light. This instability may perhaps be the reason for the difficulty to obtain the acid via the cyanohydrin synthesis. The acid was resolved into its optical antipodes. The (−)-form was obtained through fractional crystallization of the cinchonidine salt and the (+)-form through the crystallization of the (−)-phenylethylamine salt. $[\alpha]_D^{25} = 98^\circ$ in water and m.p. 83–84° was obtained for the pure antipodes. Further details will be given in a later publication.

When this work was completed it was found by chance that Fujise (5) already in 1931 had obtained optically active levorotatory 2-thienylglycolic by treating 2-thienylglyoxal with yeast. This result cannot be found through the registers of Chemical Abstracts. It should also be noted that Steinkopf (12) in his monograph on thiophene erroneously states that Fujise obtained 2-thienylglyoxylic acid in his reaction and the same error appears also in the monograph by Hartough (13). Fujise did not make any check to find out if he had obtained the optical pure antipode. This was, however, the case as he gives the same specific rotation as the present author now has found.

3-Thienylglyoxal has to the best of the author's knowledge now been prepared for the first time by SeO_2 oxidation of 3-acetothienone. It was characterized as the hydrate, semicarbazone osazone and quinoxaline. It was almost quantitatively rearranged to 3-thienylglycolic acid. It had the same m.p. 107.5–108.5° as given by Campaigne and Bourgeois (2). The 3-acetothienone was synthezised according to Campaigne and LeSuer (14) from dimethylcadmium and 3-thenoylchloride. However, the present author has earlier found that 3-thiophenecarboxylic acid is best synthezised from 3-thienyllithium (15). Investigations are therefore in progress to use 3-thienyllithium directly for the synthesis of 3-thienyl-substituted ketones.

Contrary to the 2-isomer 3-thienylglycolic acid is a stable, easily crystallizable compound. It is unchanged by heating at 100° for several hours.

It is thus obvious that the instability of the 2-isomer does not depend on the reactivity of the remaining α-position, for in such a case the 3-isomer should be even more reactive, but instead on the difference in influence of the 2- and 3-thienyl nucleus on the side-chain. Differences between the influence of the 2- and 3-thienyl nucleus on the side-chain reactivity have earlier been found by the present author in the racemization of the isomeric thienylsuccinic acids (16).

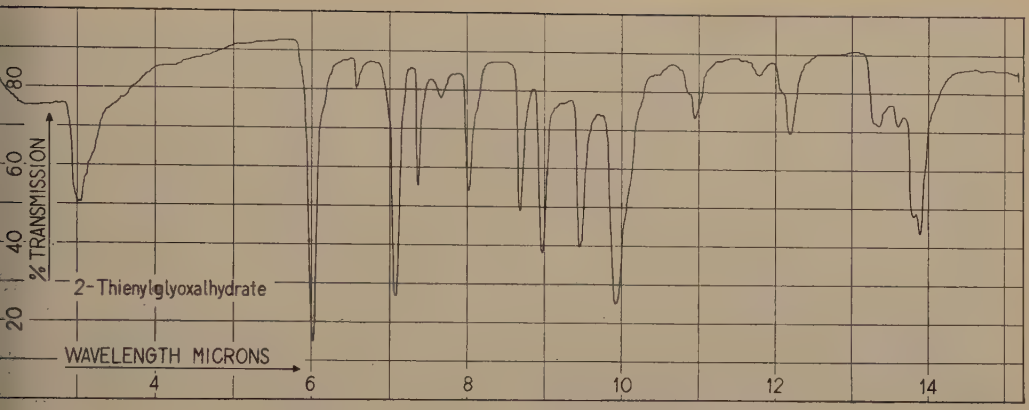

Fig. 1. IR-spectrum of 2-thienylglyoxalhydrate.

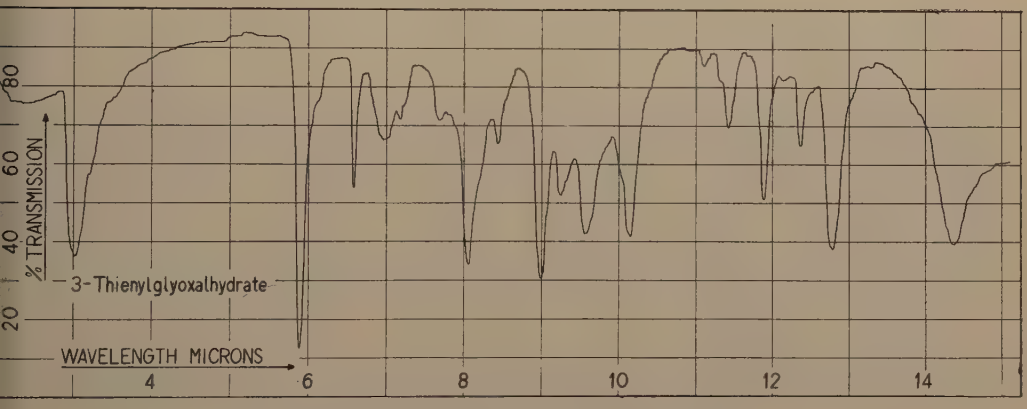

Fig. 2. IR-spectrum of 3-thienylglyoxalhydrate.

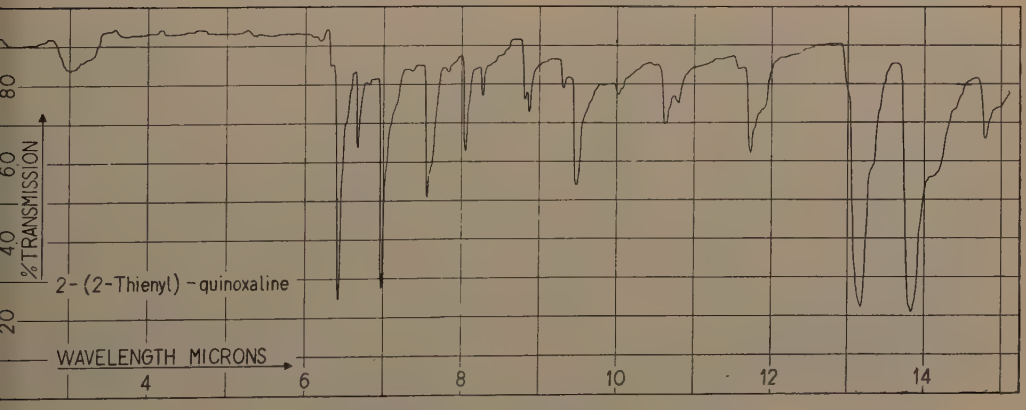

Fig. 3. IR-spectrum of 2-(2-thienyl)-quinoxaline.

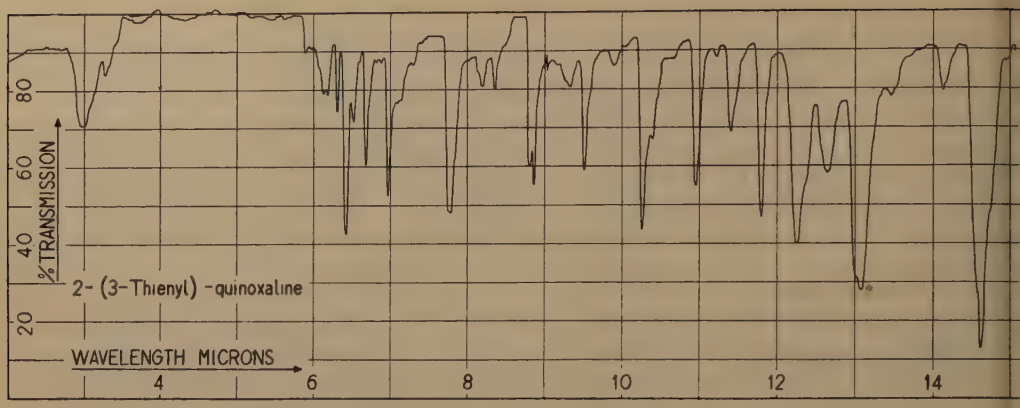

Fig. 4. IR-spectrum of 2-(3-thienyl)-quinoxaline.

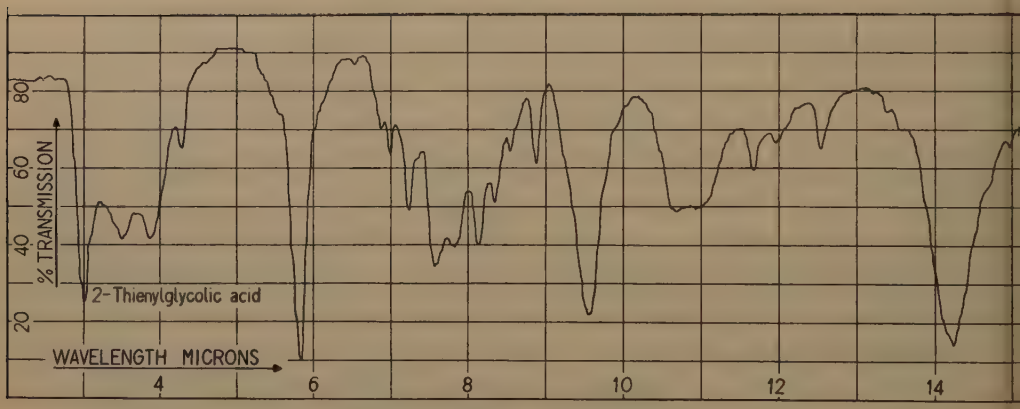

Fig. 5. IR-spectrum of 2-thienylglycolic acid.

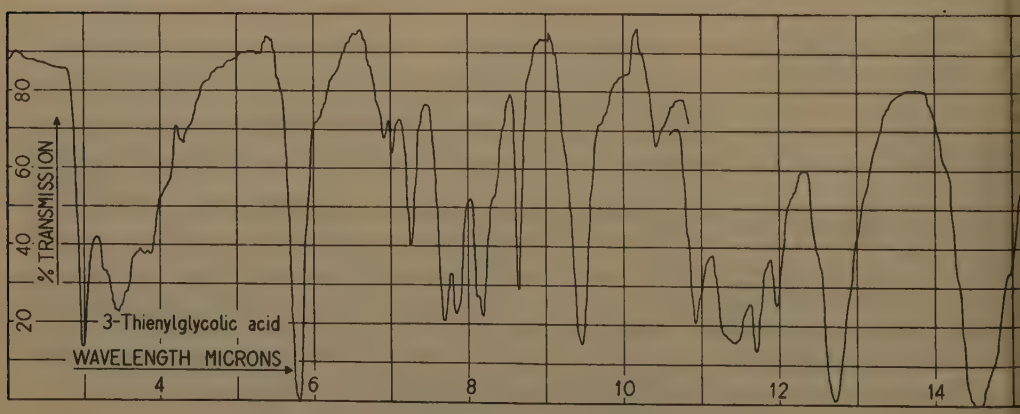

Fig. 6. IR-spectrum of 3-thienylglycolic acid.

With respect to stability 3-thienylglycolic acid thus resembles mandelic acid, while the 2-isomer resembles dioxy- and dimethoxy-substituted mandelic acids (17, 18) and of course 2-furylglycolic acid (4) which also are rather unstable compounds.

The IR-spectra of the isomeric thienylglyoxalhydrates, 2-(thienyl)-quinoxalines and thienylglycolic acids are given in figs. 1–6. The 3-thienyl-substituted glyoxal and glycolic acid show like many other 3-substituted thiophenes a characteristic strong band in the 12.75–13.20 μ region, which most probably can be ascribed to aromatic C–H deformation. However, in the 2-(thienyl)-quinoxalines the 2-isomer also absorbs in this region. This may be due to the aromatic hydrogen in the quinoxaline nucleus, since four adjacent aromatic hydrogens in benzene absorb in this region (19). It is interesting to note that the carbonyl band in the glyoxals shows the same difference in conjugation between the 2- and 3-isomer as has earlier been found for the isomeric carboxaldehydes and carboxylic acids (20). In dilute chloroform solution the C = O stretching frequency is 1673 cm^{-1} for the 2-isomer and 1689 cm^{-1} for the 3-isomer.

Experimental

2-Thienylglyoxal.—This compound was prepared according to Kipnis and Ornfelt (7). The only difference was that the reaction product was not filtered through a layer of Hyflo Supercel. From 94 g (0.75 moles) 2-acetothienone (21) and 83 g (0.75 moles) SeO_2, 75 g 2-thienylglyoxal (72 %) was obtained b.p. 101–102°/16 mm Hg. The glyoxal was immediately converted to the hydrate in the usual manner. It was washed with petroleum ether and recrystallized from benzene.

2-(2-Thienyl)-quinoxaline.—This compound was prepared in the usual way from 2-thienylglyoxalhydrate and *o*-phenylenediamine. Pale yellow crystals m.p. 118–119°.

Anal. 7.980 mg: 19.790 mg CO_2 and 2.837 mg H_2O; 7.686 mg: 19.078 mg CO_2 and 2.665 mg H_2O; – 6.377 mg: 0.835 mg N_2; 6.110 mg: 0.798 mg N_2; – 4.928 mg: 2.28 ml *N*/50 J.

$C_{12}H_8SN_2$ (212.2)	calc.	C 67.92,	H 3.80,	S 15.08, N 13.20;
	found	C 67.68,	H 3.98,	S 14.83, N 13.09;
	found	C 67.74,	H 3.88,	N 13.06.

2-Thienylglycolic acid.—48 g (0.3 moles) 2-thienylglyoxalhydrate was dissolved in one liter 1 *N* NaOH and then refluxed for ten minutes. After cooling, the alkaline solution was extracted with ether twice in order to remove possible nonacidic products. The water phase was then acidified in the cold with 6 *N* hydrochloric acid saturated with sodium chloride and extracted with ten 150 ml portions of ether. The ether phase was shaken with decolorizing carbon and dried with magnesium sulphate. The ether was removed *in vacuo* and after inoculation the residue crystallized. Yield 47 g (98 %). After one recrystallization from benzene 44 g of the acid crystallized in colourless prisms m.p. 81–82°. It seems essential to use 2-thienylglyoxalhydrate free from 2-acetothienone, as otherwise strongly coloured solutions are obtained and it is then more difficult to obtain a colourless product. The strongly coloured contamination is most probably formed through an aldol-type condensation between the glyoxal and the ketone.

Anal. 0.13327 g: 8.32 ml 0.1014 *N* NaOH; 0.13669 g: 8.50 ml 0.1014 *N* NaOH; – 4.430 mg: 7.41 mg CO_2 and 1.57 mg H_2O; 4.588 mg: 7.70 mg CO_2 and 1.66 mg H_2O; – 5.063 mg: 3.25 ml *N*/50 J; 4.578 mg: 2.92 ml J.

$C_6H_6O_3$ (158.2) calc. Equiv. wt. 158.2, C 45.56, H 3.82, S 20.27;
found „ „ 158.0, C 45.64, H 3.97, S 20.58;
found „ „ 158.6, C 45.80, H 4.05, S 20.45.

Desulphurization of 2-thienylglycolic acid.—A solution of 2 g 2-thienylglycolic acid in 90 ml 20 % sodium hydroxide solution was cooled in ice-water. A few drops of octanol were added in order to avoid frothing and 25 g of Raney-Nickel alloy was added in small portions with stirring during one hour. It was then carefully heated to reflux temperature and refluxed for five hours. The hot solution was filtered and the nickel washed with a little water. The alkaline solution was extracted twice with ether and then added to excess 6 *N* hydrochloric acid. The water phase was extracted eight times with ether, dried and the ether distilled off. The residue was recrystallized from petroleum ether (b.p. 38–42°) giving 1.15 g (69 %) of white prisms m.p. 59.5–61.5° which did not depress the m.p. of an authentic sample of α-hydroxycaproic acid (22).

Reduction of 2-thienylglyoxylic acid.—7.5 g 2-thienylglyoxylic acid (10) was dissolved in 75 ml 1 *N* soda solution and cooled in ice-water, 5 % sodium amalgam was added in small portions under frequent shaking. The amalgam liquidified rapidly and only slight evolution of hydrogen was noticeable. When further addition of amalgam did not lead to liquidification the addition was stopped and the solution allowed to remain in contact for a few hours with the amalgam under frequent shaking. The solution was then decanted from the amalgam which was washed with bicarbonate solution. The combined alkaline phases were extracted with ether to remove neutral products and then acidified in the cold with 6 *N* hydrochloric acid, saturated with sodium chloride and extracted ten times with ether. The ether solution was dried over magnesium sulphate. The ether was removed *in vacuo*. Yield 5.2 g (70 %). The acid was recrystallized from benzene and 4.5 g of 2-thienylglycolic acid, m.p. 80–81° was obtained.

3-Thienylglyoxal.—This compound was prepared in the same manner as the 2-isomer. From 20 g (0.16 moles) 3-acetothienone (14) and 17.6 g (0.16 moles) SeO_2, 14 g (63 %) 3-thienylglyoxal b.p. 95–98°/12 mm Hg was obtained. It was at once converted into the hydrate which was crystallized from benzene and water, m.p. 86–90°; the hydrate seems to dissociate when recrystallized from organic solvents. The yellow colour of the glyoxal returns as well as its characteristic piercing odour. This compound did not analyze correctly for $3\text{-}C_4H_3SCOCHO \cdot H_2O$, but for a somewhat lower water content. Similar results were obtained by Fujise (5) for the 2-isomer. He found the analysis to be correct for a half-hydrate. This was not the case in our analyses and it is probable that the product is a mixture of the hydrate and the water-free ketoaldehyde. The derivatives prepared, however, analyzed correctly.

Anal. $(C_6H_4O_2S) \cdot \frac{1}{2} H_2O$ calc. C 48.32, H 3.38, S 21.52;
found C 47.59 ± 0.10, H 3.62 ± 0.03, S 20.96 ± 0.09.

2-(3-Thienyl)-quinoxaline.—Matted needles m.p. 86–87°.

Anal. 5.690 mg: 14.103 mg CO_2 and 1.935 mg H_2O; 6.016 mg: 14.848 mg CO_2 and 2.060 mg H_2O; – 6.718 mg: 0.863 mg N_2; 0.5447 mg: 0.697 mg N_2; – 4.700 mg: 2.21 ml *N*/50 J.

$C_{12}H_8SN_2$ (212.2) calc. C 67.92, H 3.80, S 15.08, N 13.20;
found C 67.64, H 3.81, S 15.07, N 12.85;
found C 67.35, H 3.83, N 12.80.

3-Thienylglyoxalsemicarbazone.—White matted needles m.p. 238–240° dec.

Anal. 5.521 mg: 8.611 mg CO_2 and 1.848 H_2O; 7.811 mg: 12.183 mg CO_2; 2.568 mg H_2O; – 7.012 mg: 1.528 mg N_2; 6.133 mg 1.335 mg N_2.

$C_7H_7N_3O_2S$ (197.2). calc. C 42.63, H 3.58, N 21.30;
found C 42.56, H 3.74, N 21.79;
found C 42.56, H 3.68, N 21.77.

3-Thienylglyoxalosazone.—Golden-yellow matted needles m.p. 164–166° dec.

Anal. 4.042 mg: 1.27 ml *N*/50 J; – 3.385 mg: 0.506 cm^3 N_2 (20.5°, 756.5 mm).

$C_{12}H_{10}SN_4$ (321.3) calc. S 9.98, N 17.44;
found S 10.07, N 17.31.

3-Thienylglycolic acid.—5.5 g 3-thienylglyoxalhydrate was dissolved in 125 ml 1 *N* sodium hydroxide and then refluxed for 10 minutes. The cooled solution was extracted once with ether and worked up as described for the 2-isomer. Yield 5.4 g (98 %). After one recrystallization from benzene 4.5 g pure 3-thienylglycolic acid was obtained in white flakes m.p. 107.5–108.5°.

Anal. 161.19 mg: 9.94 ml 0.1021 *N* NaOH; 115.77 mg: 8.16 ml 0.1021 *N* NaOH; 4.304 mg: 7.16 mg CO_2 and 1.37 mg H_2O; 4.499 mg: 7.49 mg CO_2 and 1.44 mg H_2O; – 5.940 mg: 3.72 ml 0.02 *N* J; 3.195 mg: 2.03 ml 0.02 *N* J.

$C_6H_6O_3S$ (158.2) calc. Equiv. wt. 158.2, C 45.56, H 3.82, S 20.27;
found „ „ 158.8, C 45.40, H 3.56, S 20.08;
found „ „ 158.4, C 45.43, H 3.58, S 20.37.

All melting-points were determined in a Kofler hot-stage microscope. A Perkin Elmer model 21 spectrophotometer equipped with sodium chloride prism was used for the IR absorption spectra. The solid substances were examined as solid pressed potassium bromide plates according to the method described by Schiedt and Reinwein (23).

SUMMARY

New methods for the synthesis of 2- and 3-thienylglycolic acid have been worked out.

ACKNOWLEDGEMENTS

The author is greatly indebted to Professor Arne Fredga for valuable discussions. Thanks are also due to the head of this institute, Professor Nils Hellström, for his kind interest and for all facilities put at the author's disposal. The IR-spectra were recorded by Mr. Stig Bergvall and the microanalysis partly by Dr. Alfred Bernhardt at Mikroanalytisches Laboratorium, Max Planck Institut, Mülheim, and partly by Dr. A. Bengtsson of the Analytical Department of the Chemical Institute, University of Uppsala. A grant from the *Swedish Natural Science Research Council* is gratefully acknowledged.

Institute of Organic Chemistry, Royal Agricultural College, Uppsala, May 1957.

REFERENCES

1. ERNST, F., Ber. *19*, 3280 (1886).
2. CAMPAIGNE, E., and BOURGEOIS, P. C., J. Am. Chem. Soc. *75*, 2702 (1953).
3. Organic Syntheses. Collective Volume I, p. 336.
4. NERDEL, F., KLEEBERG. W., and SCHONEWALD, G., Ber. *87*, 276 (1954).
5. FUJISE, S., Biochem. Z. *236*, 241 (1931).
6. KRÖHNKE, F., and BÖRNER, E., Ber. *69*, 2006 (1936).
7. KIPNIS, F., and ORNFELT, J., J. Am. Chem. Soc. *68*, 2734 (1946).
8. VEIBEL, S., The Identification of Organic Compounds, p. 108. Copenhagen, 1954.
9. NEVILLE, O. K., J. Am. Chem. Soc. *70*, 3499 (1948).
10. RUFFI, H., Ber. *20*, 1740 (1887).
11. STEINKOPF, W., and WOLFRAM, A., Ann. *437*, 27 (1924).
12. STEINKOPF, W., Die Chemie des Thiophens, p. 89. Dresden und Leipzig, 1941.
13. HARTOUGH, H. D., Thiophene and Its Derivatives, p. 32. New York, 1952.
14. CAMPAIGNE, E., and LESUER, W. M., J. Am. Chem. Soc. *70*, 1555 (1948).
15. GRONOWITZ, S., Arkiv Kemi *7*, 361 (1954).
16. GRONOWITZ, S., Arkiv Kemi 11, 361 (1957).
17. BARGER, G., and EWINS, A. J., J. Chem. Soc. *95*, 557 (1909).
18. VANZETTI, L., Atti reale accad. Lincei 5, 12, II, 633 (1903).
19. BELLAMY, L. J., The Infra-red Spectra of Complex Molecules, p. 66. London, 1954.
20. GRONOWITZ, S., and ROSENBERG, A., Arkiv Kemi *8*, 23 (1955).
21. HARTOUGH, H. D., and KOSAK, A. I., J. Am. Chem. Soc. *69*, 3093 (1947).
22. NARWEL, C. S., MACCORQUIODALE, D. W., KENDALL, F. E., and LAZIER, W. A., J. Am. Chem. Soc. *46*, 2840 (1924).
23. SCHIEDT, U., and REINWEIN, H., Z. Naturforsch. *7* b, 270 (1952).

Tryckt den 2 oktober 1957

Uppsala 1957. Almqvist & Wiksells Boktryckeri AB

ARKIV FÖR KEMI Band 11 nr 59

Communicated 5 June 1957 by Arne Fredga

On the reactivity of ions and ion-pairs in the Dieckmann condensation

By Arne Brändström

With 3 figures in the text

In a recent paper the present author (1) has demonstrated that both ions and ion-pairs are active in the alkylation of alkali ethoxides and some related reactions. From a kinetic investigation of the reaction of ethyl diacetoacetate with acetic acid using various metal compounds as a catalyst, the present author (2) has further drawn the conclusion that a condensation reaction of the Claisen type, e.g. a Dieckmann condensation, is not affected by the dissociated part of the catalyst but exclusively by the undissociated part, e.g. a chelated part or an ion-pair. In order to see if this theory is correct, the present investigation has been undertaken.

Most condensations of the Claisen type can only be performed in solvents such as hydrocarbons or ethers where the solubility of a condensation agent usually is not sufficient to permit a study of the condensation reaction in a homogeneous solution. For such a study a condensation which takes place by means of alkali ethoxides in an alcoholic solution seems to be suitable. Such condensations are, however, rather uncommon, and if condensations which proceed almost quantitatively are desired, there are only very few such reactions that can be used. The most convenient of these seems to be the reaction

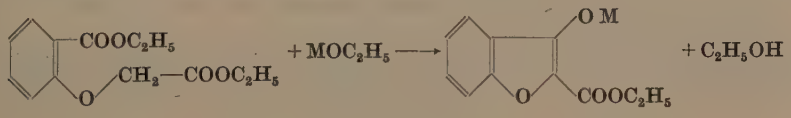

which is the one chosen in this investigation.

When treated with a solution of ferric chloride in 99.5 per cent alcohol the condensation product obtained in the reaction (2-carbethoxy-3-hydroxybenzofuran) gives a strong colour, thus providing a very simple and accurate method of following the progress of the condensation.

The water unavoidably present in the alcoholic solutions causes, however, a complication as ethyl *o*-carbethoxyphenoxyacetate is very rapidly hydrolysed in an alcoholic solution containing an alkali hydroxide. A solution in 99.5 per cent alcohol being 0.1 normal both in sodium hydroxide and in ethyl *o*-carbethoxyphenoxyacetate is hydrolysed to over 95 per cent in 2 minutes at 15°. As the condensation reaction is several hundred times slower it can be assumed that all

the water present in the reaction mixture is used up in the hydrolysis in the first few minutes. The reaction then proceeds as if no water is present and the concentrations of the ethoxide and the ethyl *o*-carbethoxyphenoxyacetate are reduced with a quantity equivalent to the concentration of water initially present. As the concentration of water in the solutions can be kept rather low, usually 0.01–0.015 normal, and further accurately determined by means of Karl Fischer titrations it is possible to make an exact correction for the water content.

It was further found that the concentration of water determined by a Karl Fischer titration was exactly the same as the difference between the concentration of the component not in excess and the end concentration of the condensation product taken after about 24 hours. This means that the condensation is practically quantitative and that the water content of the solution is most exactly calculated from a measurement of the concentration of the condensation product after about 24 hours. This has also been done in all cases where the condensation product did not crystallize from the reaction solution after standing for 24 hours.

The condensation reaction was found to be of the second order with the velocity proportional to both the concentration of the ethoxide and the ethyl *o*-carbethoxyphenoxyacetate. The velocity constant K_n obtained from the different measurements varied considerably with the initial concentration of the ethoxide, but the fraction $K_n/(1-\alpha)$, where α is the degree of dissociation of the alkali ethoxide (1) (in pure alcohol), was perfectly constant for all solutions containing the same alkali ion, thus proving that the ion-pair of the alkali ethoxide is the condensation agent and that the free ethoxide ion appears to be totally inactive, just as predicted by Brändström (2).

As the ion-pair is the condensation agent the nature of the alkali ion in the ion-pair must be of great importance for the velocity of the reaction. In good agreement with this the fraction $K_n/(1-\alpha)$ is more than two and one half times higher for KOC_2H_5 than for $LiOC_2H_5$. $NaOC_2H_5$ has a value slightly lower than that of KOC_2H_5. Although no values for the degree of dissociation are available for $RbOC_2H_5$ and $CsOC_2H_5$ and only very approximative kinetic measurements have been done with these ethoxides the value of $K_n/(1-\alpha)$ for $RbOC_2H_5$ seems to be close to that for KOC_2H_5 and that for $CsOC_2H_5$ about 50 per cent higher.

For the ethoxides of Li, Na, and K the reactivities in the condensation reaction is thus increasing with an increasing distance between centers of different charges in the ion-pair of the alkali ethoxides (1). This is in good agreement with the mechanism given for a smaller distance gives rise to a higher internal neutralisation of the charges and hence a lower reactivity of the ion-pair.

Experimental

Dry alcohol was prepared in the following way:

2 kg of 99.5 per cent alcohol "spectro grade" was refluxed with 25 g of calcium hydride for 6 hours in a 5 liter flask fitted with an efficient reflux condenser the top of which was connected to a condenser set for distillation. During the whole preparation a stream of pure dry nitrogen was passed through the liquid. After 6 hours the water jacket of the reflux condenser was emptied and the alcohol distilled. The first 100 and the last 500 ml were rejected and the main fraction taken up in a buret flask which had been carefully dried and filled with pure dry nitrogen.

The ethyl *o*-carbethoxyphenoxyacetate was redistilled at about 0.1 mm Hg just before use thus removing any trace of water from it.

The ethoxide solutions were prepared by dissolving the pure alkali metal in pure alcohol avoiding contact with the atmosphere as far as possible. In this operation an inverted test tube placed over the neck of the volumetric flask containing the alkali metal and the alcohol was found to be a very convenient vapor seal. The concentration of the ethoxide solution was determined by titrations against standard hydrochloric acid.

The kinetic measurements were made at 15.00° in a water thermostat at days when the humidity was very low in the laboratory.

A run was performed in the following way: A total volume of 15.00 ml of pure alcohol and ethoxide solution was placed in a carefully dried 25-ml volumetric flask. After it had been allowed to come to 15.00°, 5.00 ml of a 1.000 molar solution of ethyl *o*-carbethoxyphenoxyacetate in pure alcohol was added. The flask was quickly stoppered and shaken. Each third minute a sample was taken with a 1-ml pipette (in the most dilute solutions a 2-ml pipette) which could be emptied in one second. The sample was quickly transferred to a flask containing 20.00 ml of a solution containing 2.2 g of acetic acid in 1-liter of 99.5 per cent alcohol "spectro grade" and the pipette was well rinsed with the acid solution. Volumes from 0.500 to 3.000 ml of the resulting solutions were mixed in a 25 ml volumetric flask with 20 ml portions of a solution containing 1.62 g of $FeCl_3 + 6H_2O$ in one liter of 99.5 per cent alcohol "spectro grade" and the solutions made up to the mark with 99.5 per cent alcohol "spectro grade". The colour of the resulting solutions were measured in a Hilger filter fotometer of the type Spekker using filter H 606. The concentration of 2-carbethoxy-3-hydroxybenzofuran was calculated from a standard graph. The time for the first sample was taken as the arbitrary zero time.

The results of the measurements are given in Tables 1–15 and in Figs. 1–3, where a, b, and x are the concentrations of the ethyl *o*-carbethoxyphenoxyacetate, the ethoxide and 2-carbethoxy-3-hydroxybenzofuran respectively, a_0 and b_0 the concentrations of the same compounds immediately after mixing, and W the concentration of water; K_n is the velocity constant measured, t the time in minutes.

Tables 1–3. Condensations using lithium ethylate.

Table 1

$a_0 = 0.2500$; $b_0 = 0.3956$
$W = 0.0140$

t (min.)	x	$\int_0^t \frac{dx}{ab}$
0	0.0244	0
4.98	0.0420	0.255
9.98	0.0576	0.508
15.00	0.0734	0.802
24.93	0.0967	1.324
32.45	0.1129	1.772

$K_n = 0.0532$

Table 2

$a_0 = 0.2500$; $b_0 = 0.1978$
$W = 0.0140$

t (min.)	x	$\int_0^t \frac{dx}{ab}$
0	0.0113	0
5.03	0.0208	0.233
10.02	0.0290	0.477
15.03	0.0368	0.719
20.07	0.0431	0.955
24.95	0.0483	1.153
27.45	0.0518	1.277

$K_n = 0.0470$

Table 3

$a_0 = 0.2500$; $b_0 = 0.0989$
$W = 0.0102$

t (min.)	x	$\int_0^t \frac{dx}{ab}$
0	0.00527	0
4.93	0.00923	0.207
9.87	0.01304	0.419
14.90	0.01685	0.654
19.90	0.02010	0.864
24.97	0.02307	1.068
29.97	0.02578	1.260

$K_n = 0.0427$

Tables 4–6. Condensations using sodium ethoxide.

Table 4

$a_0 = 0.2500$; $b_0 = 0.4008$
$W = 0.0140$

t (min.)	x	$\int_0^t \frac{dx}{ab}$
0	0.0294	0
2.98	0.0483	0.276
6.00	0.0669	0.594
9.01	0.0831	0.881
12.11	0.0945	1.177
15.00	0.1033	1.399
18.00	0.1164	1.776
21.01	0.1235	2.006
23.95	0.1320	2.310
27.08	0.1364	2.481
30.03	0.1452	2.840
33.00	0.1518	3.174

$K_n = 0.0955$

Table 5

$a_0 = 0.2500$; $b_0 = 0.2004$
$W = 0.0134$

t (min.)	x	$\int_0^t \frac{dx}{ab}$
0	0.0146	0
2.83	0.0232	0.235
5.90	0.0313	0.487
8.83	0.0390	0.729
11.85	0.0455	0.962
14.85	0.0521	1.217
17.96	0.0589	1.502
20.91	0.0631	1.691
23.95	0.0690	1.978
27.01	0.0747	2.277
29.95	0.0777	2.434
32.91	0.0802	2.593

$K_n = 0.0818$

Table 6

$a_0 = 0.2500$; $b_0 = 0.1002$
$W = 0.0130$

t (min.)	x	$\int_0^t \frac{dx}{ab}$
0	0.0106	0
2.82	0.0143	0.223
5.84	0.0174	0.417
8.84	0.0209	0.655
11.82	0.0236	0.847
14.87	0.0255	0.991
18.05	0.0281	1.195
20.85	0.0308	1.422
23.79	0.0329	1.608
26.90	0.0359	1.887
29.89	0.0371	2.006

$K_n = 0.0689$

Tables 7–12. Condensations using potassium ethoxide.

Table 7

$a_0 = 0.2500$; $b_0 = 0.4076$
$W = 0.0165$

t (min.)	x	$\int_0^t \frac{dx}{ab}$
0	0.0345	0
3.00	0.0547	0.311
6.02	0.0727	0.634
9.00	0.0916	1.040
11.95	0.1030	1.324
15.03	0.1147	1.658
17.94	0.1219	1.886
20.94	0.1327	2.261
23.95	0.1399	2.564
26.95	0.1457	2.821
30.02	0.1514	3.099
33.04	0.1591	3.515

$K_n = 0.1068$

Table 8

$a_0 = 0.2500$; $b_0 = 0.3057$
$W = 0.0165$

t (min.)	x	$\int_0^t \frac{dx}{ab}$
0	0.0218	0
2.97	0.0380	0.301
6.05	0.0512	0.591
9.05	0.0655	0.942
11.97	0.0749	1.207
15.12	0.0855	1.538
18.00	0.0940	1.836
21.04	0.1013	2.154
27.00	0.1151	2.725
30.02	0.1208	3.014
33.00	0.1265	3.328

$K_n = 0.1023$

Table 9

$a_0 = 0.2500$; $b_0 = 0.1974$
$W = 0.0165$

t (min.)	x	$\int_0^t \frac{dx}{ab}$
0	0.0120	0
2.96	0.0211	0.257
6.02	0.0305	0.548
8.95	0.0388	0.835
12.03	0.0460	1.107
14.96	0.0529	1.391
18.08	0.0587	1.652
21.00	0.0649	1.956
23.96	0.0692	2.183
26.98	0.0738	2.443

$K_n = 0.0917$

Table 10

$a_0 = 0.2500$; $b_0 = 0.0987$
$W = 0.0163$

t (min.)	x	$\int_0^t \frac{dx}{ab}$
0	0.0061	0
2.98	0.0098	0.218
5.96	0.0132	0.436
8.96	0.0170	0.694
11.96	0.0205	0.952
14.96	0.0237	1.171
17.90	0.0260	1.395
21.08	0.0291	1.669
24.00	0.0316	1.903
27.00	0.0343	2.177

$K_n = 0.0788$

Table 11

$a_0 = 0.2500$; $b_0 = 0.05095$
$W = 0.0125$

t (min.)	x	$\int_0^t \frac{dx}{ab}$
0	0.00314	0
3.05	0.00460	0.181
6.10	0.00639	0.413
9.07	0.00780	0.608
12.04	0.00895	0.774
15.12	0.01044	1.001
17.94	0.01131	1.141
21.14	0.01246	1.335
24.12	0.01349	1.515
27.09	0.01476	1.747
33.14	0.01582	2.185

$K_n = 0.0635$

Table 12

$a_0 = 0.2500$; $b_0 = 0.02468$
$W = 0.0122$

t (min.)	x	$\int_0^t \frac{dx}{ab}$
0	0.00164	0
3.00	0.00199	0.133
5.98	0.00240	0.292
8.90	0.00277	0.446
11.96	0.00321	0.634
14.95	0.00352	0.779
17.91	0.00392	0.962
20.88	0.00426	1.127
23.88	0.00457	1.285
27.02	0.00482	1.420

$K_n = 0.0526$

Table 13. Condensations with lithium ethoxide.

b_0	K_n	α	$K_n/(1-\alpha)$
0.3956	0.0532	0.212	0.0675
0.1978	0.0470	0.296	0.0668
0.0989	0.0427	0.390	0.0700

Table 14. Condensations with sodium ethoxide.

b_0	K_n	α	$K_n/(1-\alpha)$
0.4008	0.0955	0.344	0.1456
0.2004	0.0818	0.439	0.1458
0.1002	0.0689	0.527	0.1457

Table 15. Condensations with potassium ethoxide.

b_0	K_n	α	$K_n/(1-\alpha)$
0.4076	0.1068	0.396	0.1768
0.3057	0.1023	0.427	0.1785
0.1974	0.0917	0.474	0.1743
0.0987	0.0788	0.555	0.1771
0.05095	0.0635	0.631	0.1721
0.02468	0.0526	0.704	0.1777

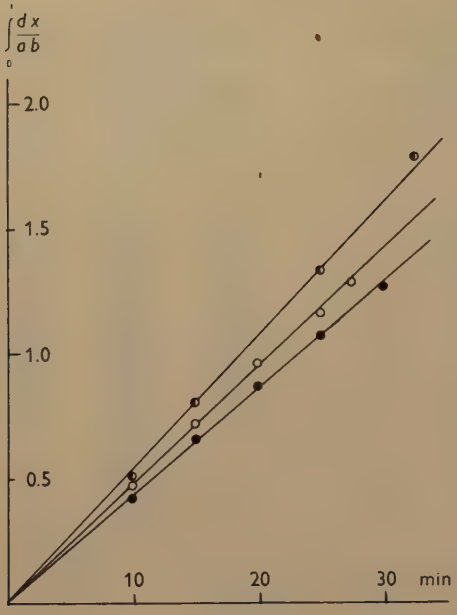

Fig. 1. Condensations using lithium ethoxide.

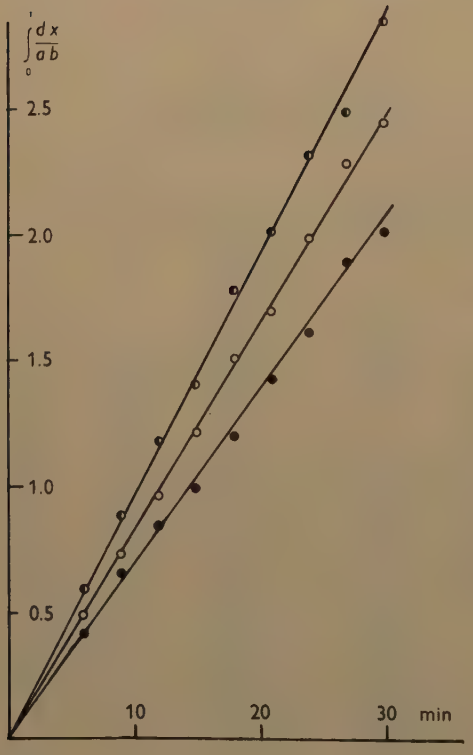

Fig. 2. Condensations using sodium ethoxide.

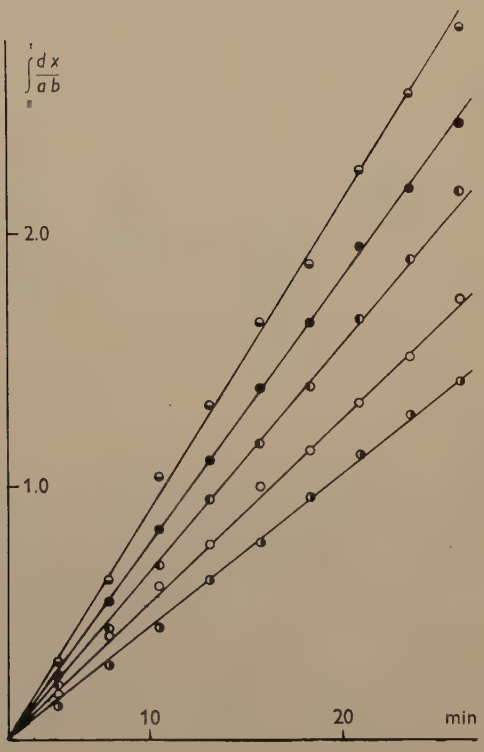

Fig. 3. Condensations using potassium ethoxide.

SUMMARY

The velocity of the Dieckmann condensation of ethyl *o*-carbethoxyphenoxyacetate to 2-carbethoxy-3-hydroxybenzofuran by means of alkali ethoxides in pure alcohol has been measured. The condensation agent was found to be the ion-pair of the alkali ethoxide. The free ethoxide ion is not a catalyst in this condensation.

The author is indebted to Wolfgang Kirsten who worked out the method of analysis and to Messrs. Pharmacia Ltd. for permission to publish this work.

Research Laboratory of Pharmacia Ltd., Uppsala, June 1957.

REFERENCES

1. A. Brändström, Arkiv f. Kemi, in press.
2. —— Arkiv f. Kemi *7*, 188 (1954).

Tryckt den 2 oktober 1957

Uppsala 1957. Almqvist & Wiksells Boktryckeri AB

ARKIV FÖR KEMI Band 11 nr 60

Communicated 24 April 1957 by Arne Fredga and Arne Ölander

A flash photolysis apparatus for photochemical studies at very high light intensities and energies

By Stig Claesson and Lars Lindqvist

With 25 figures in the text

In 1949 Norrish and Porter (1) introduced the use of very intense light flashes for photochemical investigations, as a means of studying short-lived states directly. The high light intensity made it possible to obtain such a high concentration of transient products that it became feasible to investigate them by recording their absorption spectra photographically. These techniques, now known as flash photolysis and flash spectroscopy, have proved to be extremely powerful research tools. A large number of valuable investigations have been performed with these methods, for instance the study of free radicals and excited molecules, reaction mechanisms and kinetics of fast reactions, such as explosions. The already extensive literature in these fields is reviewed in an article by Norrish and Thrush (2). The references (3)–(9) cover more recent papers.

The experimental arrangement described in detail by Porter (10) is shown in Fig. 1. Only minor modifications have been introduced by subsequent investigators. The photolysis flash lamp *A*, which is connected across a high capacity condenser *B*, consists of a straight quartz tube with heavy tungsten electrodes. The tube is filled with a rare gas under such a pressure (about 50 mm Hg) that it will withstand the voltage (about 4 kV) to which the condenser *B* is charged without firing spontaneously. The lamp is fired by applying a high voltage pulse to a third triggering electrode. The intense light flash produced will give rise to a high concentration of transient products from a photo-active substance contained in the cuvette *C*. As mentioned above, these products can be studied by recording their absorption spectra photographically. The necessary light for the short exposure-times required is obtained from a smaller flash lamp *D*.

Absorption spectra are photographed at different times after the photolysis flash by having a suitable synchronizing system for firing the lamp *D*. This has the advantage that the whole spectrum is recorded at each exposure, but the drawback that under normal experimental conditions only one such spectrum can be obtained after each photolysis flash. Sometimes it is advantageous to follow the changes in absorption within a narrow spectral region. This can be done by replacing the lamp *D* and the spectrograph *E* with a constant intensity light source and a monochromator. Recordings are then made by means of a phototube connected to an oscilloscope.

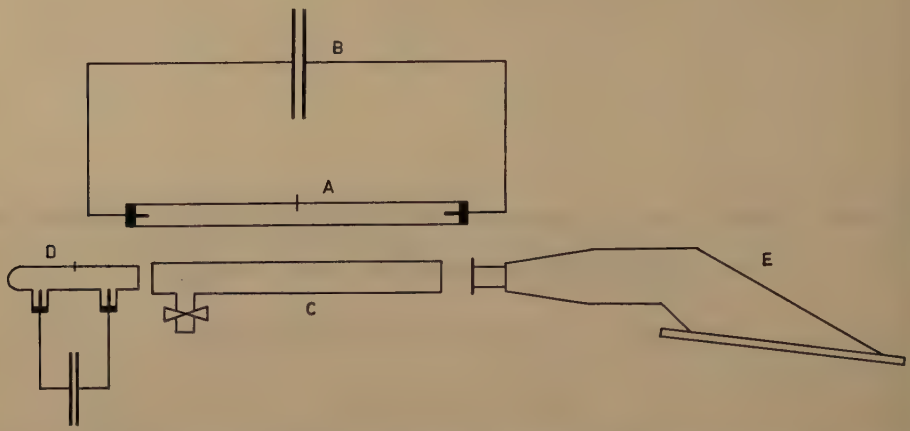

Fig. 1. Flash photolysis apparatus. *A*, photolysis flash lamp; *B*, condenser bank; *C*, reaction vessel; *D*, spectrograph flash lamp; *E*, spectrograph.

The present paper deals with a flash photolysis apparatus which has been constructed at this Institute and which embodies the fundamental principles described above. We were fortunate enough to receive a large condenser bank as a gift from ASEA, AB Liljeholmens Kabelfabrik, Stockholm. This provided a source of very high energies, which under special conditions could be used so as to extend the potentialities of the flash photolysis method. Thus we have obtained both higher light energies and light intensities (more than tenfold) than hitherto reported. This development required the construction of specially designed heavy-duty discharge tubes, which should be strong enough to endure a large number of flashes lasting about 10^{-4} sec with an average power of more than 10^8 W. Systematic investigations on the behavior of such lamps at these high energies and powers have been performed.

It therefore seems to us that a rather detailed description of our apparatus may be of interest— even if it is similar in principle to the original design of Norrish and Porter.

The description will be divided in sections, based on the block diagram, Fig. 2. The block diagram shows the apparatus mounted for photographic recording of absorption spectra by the "flash spectroscopy" method. In a separate section an arrangement for continuous recording with phototube and oscilloscope will be described. In the section on photolysis flash lamps are included the results of the study of their characteristic properties.

The condenser bank

The condenser bank consists of 70 units (Liljeholmens Kabelfabrik, type CKT-E5) in their standard mounting for use in power stations. Each unit has a capacity of about 20 μF and is designed for continuous use at 2.4 kV ac. They have been tested in the factory at 6.9 kV ac for 1 minute and are used by us at a maximum voltage of 7 kV dc. The total capacity of the condenser bank is 1370 μF and consequently the maximum energy stored is 33,600 joules. The dimensions of the condenser bank,

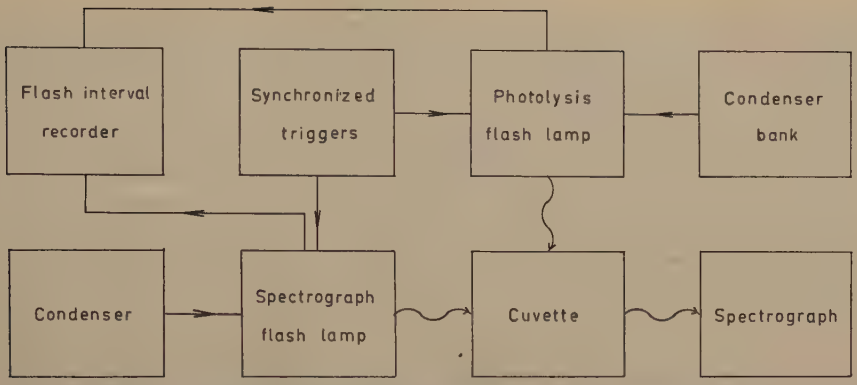

Fig. 2. Block diagram of flash photolysis apparatus together with spectrograph for photographic recording of absorption spectra. ———, Electrical connections; ~~~~, light.

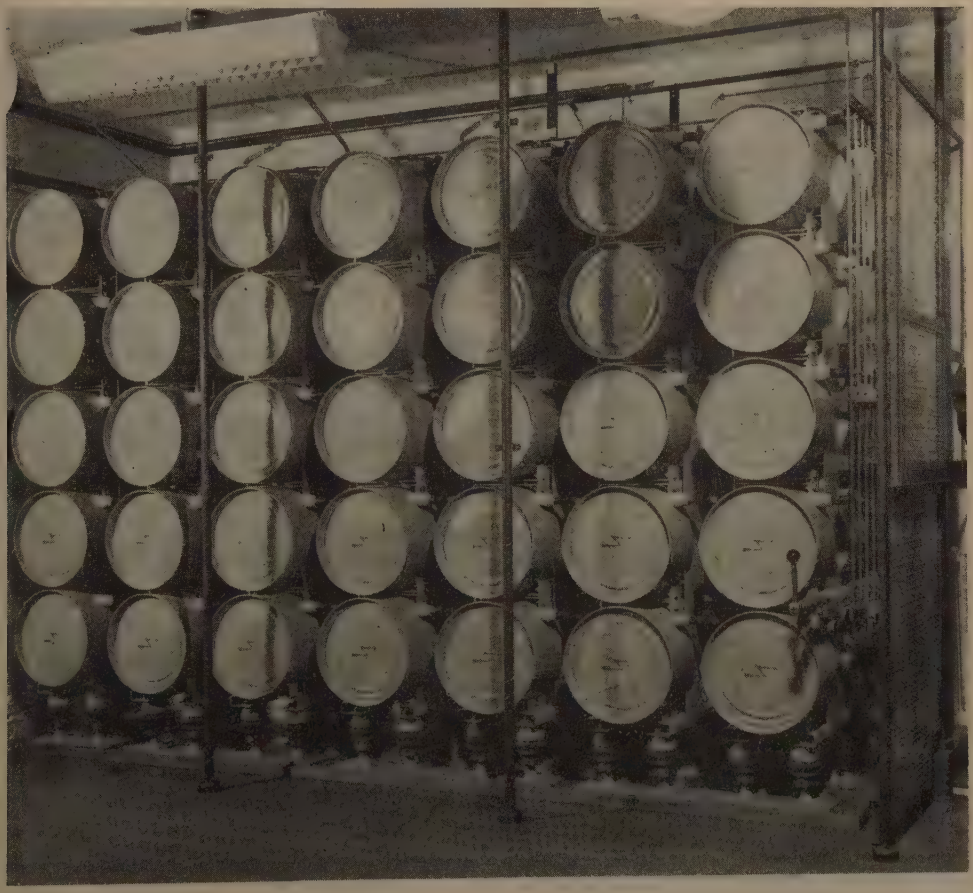

Fig. 3. The condenser bank, 70 units of total capacity 1370 μF and maximum voltage 7 kV. One side is seen with safety screen removed.

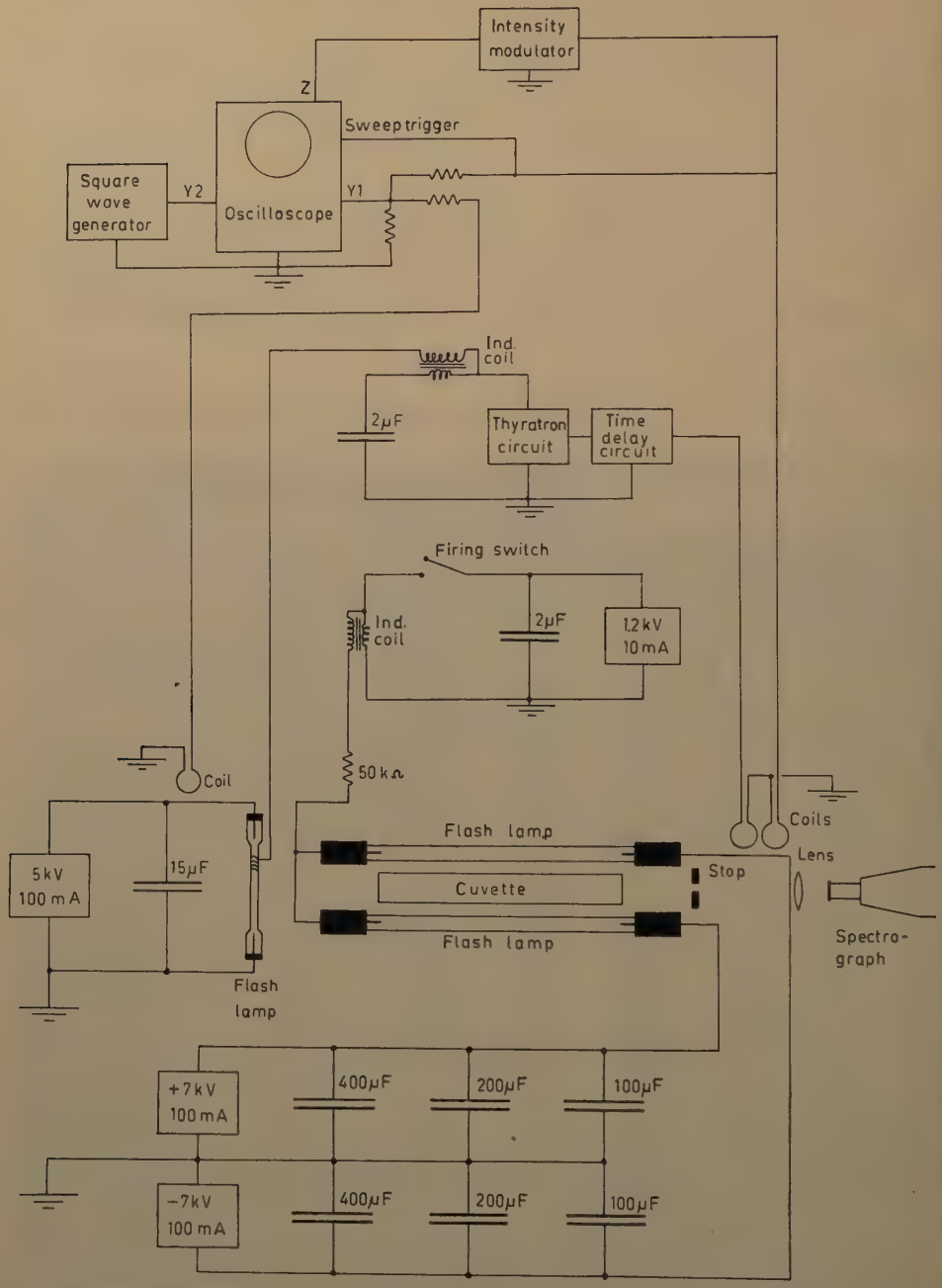

Fig. 4. Schematic diagram of the complete flash photolysis apparatus. It can be used together with either a spectrograph (this fig.) or a monochromator and phototube (Fig. 21) for recording of absorption spectra. The thyratron and time delay circuits and the intensity modulator are shown in detail in Figs. 19 and 20.

shown in Fig. 3, make it immediately obvious that extremely short discharge times cannot be realized. The units are interconnected by straight copper bars (5×25 mm in cross section). The connections are such that six units are formed with capacities of approximately 100, 100, 200, 200, 400, and 400 μF respectively. These units are connected to a compact switch-board, from which a heavy coaxial cable leads to the lamp. The inductance of this cable is 1 μH and the total inductance of the discharge circuit, the lamps excluded, amounts to 4–6 μH, depending upon the number of condenser groups used. Two separate charging units are used (max. current 0.1 A, voltage continuously variable to +7 kV and −7 kV respectively) and the maximum energy can therefore be realized either as 1370 μF at 7 kV or as 340 μF at 14 kV across the lamp. This arrangement is seen in Fig. 4, which represents schematically the whole flash photolysis apparatus.

Because of the high energies and voltages employed, rather elaborate safety devices have been worked out and all controls and instrumentation are in an adjacent room. The condenser bank is automatically grounded through suitable resistances by safety relays before one can enter the room where it is mounted together with the photolysis lamps and related equipment.

The photolysis flash lamps

When a condenser bank of the above-mentioned size is discharged rapidly through a flash lamp, the latter is subjected to very great strains; care must therefore be exercised in designing the lamps. In order to arrive at the most suitable type of lamp systematic experiments were performed.

For spectroscopic work with gases and dilute solutions long optical paths are necessary and it was therefore convenient to employ rather long lamps alongside of which the cuvette is placed. To combine maximum strength with low inductance the lamps were made from straight quartz tubes, which were provided with a heavy electrode at each end. Different tube dimensions, electrode seals and gas fillings were tried. The lamps were in all cases triggered by means of a high voltage pulse.

Electrodes

It was found that commercially available types of fused quartz electrode seals were not able to withstand the high currents through the lamp. Therefore an attempt was made to cement the electrodes to the lamp. This was done in such a way that the discharge could not reach the vacuum seal directly. Two different types of seals have been tried. In one type (Fig. 5A) a conical ground joint is used. The ground joint is used to prevent the discharge from reaching the Apiezon W seal. The male part is made from invar, which has the same coefficient of thermal expansion as quartz. The other type (Fig. 5B), with a cylindrical cemented joint, is suitable when the lamp material consists of thick-walled quartz tubing, which is difficult to work up. Both these types proved very convenient. Overloaded lamps never showed any tendency to break at the electrodes but exploded violently in the middle of the tube. The use of cement has not given rise to any unfavourable effects due to impurities. In fact, it is unnecessary to use spectroscopically pure gases in lamps of this type, because in any case silicon vapour and oxygen are produced at each flash. It might be mentioned that the use of aluminium as the material for the electrode holder was not

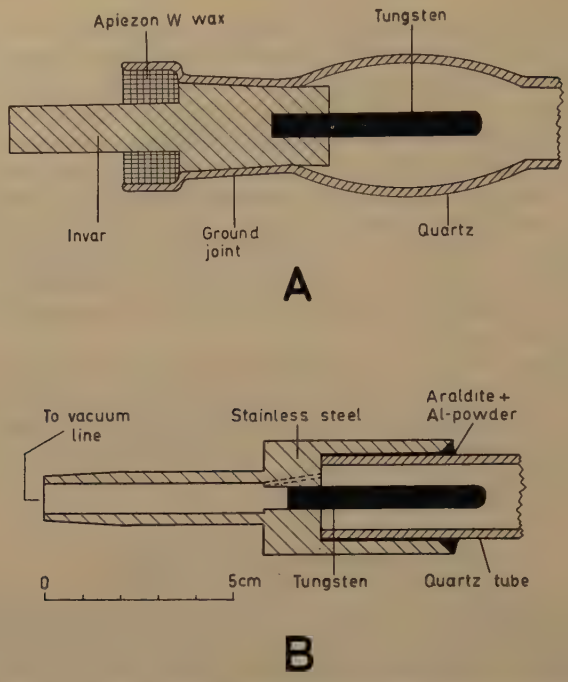

Fig. 5. The photolysis flash lamp electrodes, A with conical ground joint, B with cylindrical cemented joint.

possible, since the lamp then became filled with aluminium droplets already at the first flash.

In the first types of photolysis flash lamps (L 1–5 in Table 1) a side tube was sealed to the middle of the discharge tube for introducing the trigger electrode (a 1 mm W-wire) and also for connexion to the vacuum line. Later the lamps were evacuated through a hole in one of the electrode holders (shown in Fig. 5 B). The trigger electrode was then wound around the middle of the quartz tube (type L6 and L7). In the final modification of the lamp system with two lamps in series, the interconnected electrodes function as trigger electrode (see below).

Lamp dimensions and mounting

In order to determine the most suitable lamp dimensions a number of lamps of different sizes were constructed and the discharge energy increased until they exploded. Some pertinent data are collected in Table 1. All lamps were made of transparent quartz of medium quality.

From these data it was concluded that it would not be feasible to construct a practically useful photolysis flash lamp through which all the available energy could be discharged. Therefore, in the final assembly two lamps (type L7 in Table 1) were used, one placed on each side of the cuvette and electrically connected in series.

The two interconnected electrodes are grounded through a high resistance and the other two are connected to the condenser bank, which is divided into two equal

Table 1. Dimensions and energy tolerance of the photolysis flash lamps

Lamp type	Quartz tube: Inner diameter (mm)	Quartz tube: Wall thickness (mm)	Electrode separation (mm)	Electrode design, according to Fig. 5	Energy input tolerated	Energy input resulting in breakage
L1	24	2	610	A	1400 μF, 5 kV	100 μF, 11 kV
L2	25	2	330	A	1200 μF, 5 kV	1300 μF, 5 kV
L3	9	1.5	310	A	700 μF, 5 kV	900 μF, 5 kV
L4	22	2	610	A	1400 μF, 5 kV 350 μF, 8 kV 250 μF, 10 kV	350 μF, 10 kV
L5	18	2	610	A	600 μF, 6 kV	700 μF, 6 kV
L6	18	2	610	B	350 μF, 10 kV	350 μF, 11 kV
L7	17	3	610	B	350 μF, 11 kV	350 μF, 12 kV

parts (each of capacity $C/2$) and grounded in the middle (see Fig. 4). The two parts are charged to a voltage of $+V$ and $-V$ respectively. The total energy discharged through the two lamps can then be expressed by a voltage V at a total capacity C, or as a voltage $2\ V$ and a capacity $C/4$. As the voltage V is the actual accelerating voltage across each lamp we will in the following always give the voltage and capacity values corresponding to V and C.

Fig. 6 shows the lamp and cuvette assembly which is mounted inside a magnesium oxide coated reflector. This arrangement gives symmetrical illumination of the cuvette and small light losses. It has the further advantage that the two interconnected electrodes can be used as an internal trigger electrode.

In our case this mounting of two lamps in series did not noticeably increase the discharge time compared to that of one single lamp used under the same conditions as one of the lamps in the pair. From the data in Table 1 it is seen that the lamp pair has enough safety margin against explosion to be convenient for routine work. These lamps stand thousands of flashes, the only signs of deterioration being that some quartz distils off and condenses on the cooler parts of the lamp and that small disrupted particles from the tungsten electrodes melt into the quartz. However, the condensation only takes place at the ends of the lamps behind the tips of the W electrodes and therefore the light output is not reduced.

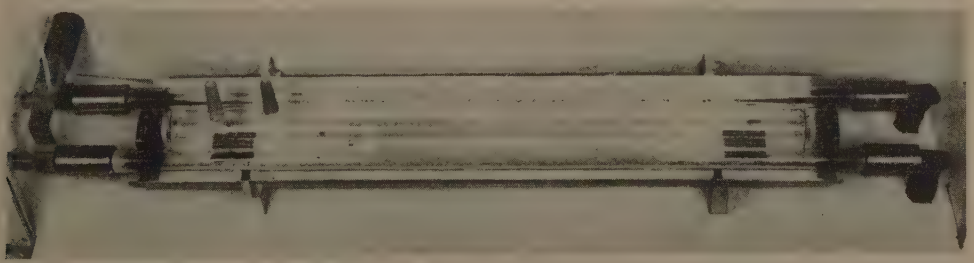

Fig. 6. Photograph of the lamp system showing the cuvette in place between the two photolysis flash lamps (L7, Table 1) inside the magnesium oxide coated reflector. The upper half of the reflector is removed.

Flash characteristics

The lamps have been investigated in relation to their more characteristic properties. Flash duration times and time lags between the triggering pulse and the start of flash were followed by means of a phototube and oscilloscope. Light outputs were measured by means of chemical actinometry. Emission spectra were obtained photographically.

As the lamps have to stand a fairly high voltage (7 kV) without spontaneously firing they must be filled with a gas at a relatively high pressure (about 30 mm Hg for argon or 5 mm Hg for oxygen). On the other hand, as the lamp is fired by means of a high voltage pulse of limited triggering efficiency the pressure must be confined to a value permitting reliable triggering. Rare gases are commonly used for filling this type of lamp. However, at the high energies we have used, some oxygen gas was produced in the lamp at each flash by dissociation of the quartz. When using rare gas fillings this oxygen contamination had a poisoning effect, so that it became more and more difficult to fire the lamp and consequently the pressure had to be reduced after almost every flash. We therefore tried pure oxygen as a lamp filling, and it proved to be very suitable. In this case the oxygen developed[1] during the flashes causes no difficulties as this means only a small relative increase in the oxygen pressure.

In order to improve the constancy of the composition and pressure of the gas filling in the lamp a glass flask of about 2 litres volume was mounted as a ballast immediately outside the lamp.

The only disadvantage with oxygen compared to argon is that the time lag between the initiation of the flash by the triggering pulse and the start of the flash is longer. For oxygen this time lag varies in an irreproducible way from 0.4 to 1 msec. This is no disadvantage as long as the current rise at the start of the flash and not the triggering pulse is used for starting the succeeding sequence of events (spectrograph flash, oscilloscope sweep, etc.).

When the spectrograph shutter wheel, described on p. 551, is used, more reproducible time lags are needed because in this case the shutter is necessarily synchronized with the triggering pulse. Some argon can then be added to the oxygen. This reduces the time lag to 100 ± 50 μsec.

Bardócz and Klatsmányi (11) have described a method of triggering two lamps in series by short-circuiting one lamp through a resistor. The whole voltage will then be placed over the other lamp causing it to fire spontaneously. This will in its turn cause the first lamp to fire. We have tried this system with our lamp-pair; for our particular lamp dimensions it gave no improvement in firing characteristics compared to those of the ordinary pulse. The time lag obtained is inherent in the nature of the discharge build-up but can be eliminated by pre-ionizing the gas filling (12).

Flash duration times

The duration of the flash was studied by means of a phototube and oscilloscope. The phototube (935) was provided with a filter transmitting 360–380 mμ (Zeiss WG 1,

[1] At the higher energies (>400 μF at 5 kV) oxygen is consumed during the flash and since the effects of consumption and evolution of oxygen cancel each other at about 400 μF and 5 kV, the pressure in the lamp remains almost unchanged even after a large number of flashes at this energy.

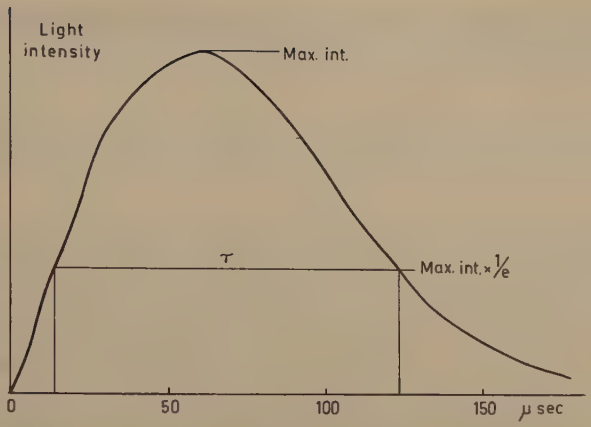

Fig. 7. The light intensity during the flash as a function of time for the lamps in Fig. 6. Capacity 800 μF, voltage 5 kV. Lamp filling, oxygen and argon, 2 and 20 mm Hg resp. The definition of the flash duration time τ is illustrated.

WG 2, WG 3, GG 13, GG 18, 2 mm each, total transm. 0.1%) and mounted close to the oscilloscope (Furzehill 0.100 bandwidth 0–1 Mc/sec). The load resistance was 50 kΩ and stray capacity 100 pF. A typical oscillogram is shown in Fig. 7.

It is seen that the light intensity does not oscillate. The light is emitted during a length of time which approximately corresponds to the time of a half-period calculated for the resonance frequency of the lamp circuit using the values of its inductance given on p. 539.

It may also be mentioned that we have found from phototube measurements with a monochromator that the variation in intensity with time during the flash is somewhat different for different regions of the spectrum. This effect has been studied in more detail by Cloupeau (12) using a rotating mirror technique. In our case the region 360–380 mμ was chosen as lying in the middle of the photochemically useful spectral range.

By the duration of the flash, τ, we mean the time interval from $1/e$ of maximum light intensity on the rising part of the curve to the corresponding point on the descending part. (About 80% of the light energy lies within this time interval.)

The time τ has been measured as a function of the voltage V at constant capacity C. As a lower voltage necessitates a lower pressure in the lamp, the effect of pressure on the flash duration is implicit in Fig. 8 where some results are collected. It is seen that the flash duration time increases only slowly with increasing voltage in the useful voltage range. It is therefore advantageous to use higher voltages in order to get higher light intensities. The curve was obtained for the lamp-pair of type L7 with a mixture of oxygen and argon in the lamp (ca. 20 mm Hg of A and 2 mm Hg of O_2). For pure oxygen (5 mm Hg) the discharge time is somewhat shorter, thus showing the effect of decreased pressure.

The time τ has also been measured as a function of the capacity at constant voltage. A curve for $V=5$ kV is given in Fig. 9. The deviation of the points from a smooth curve is real and due to the fact that the bars connecting the different parts of the condenser bank are of different length giving rise to different inductances in the circuit. It is seen that even at the highest capacities the duration of the flash is

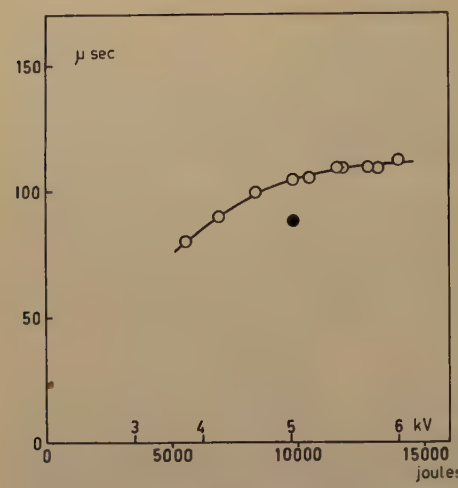

Fig. 8. The flash duration time as a function of voltage at constant capacity, 800 μF, for the lamps in Fig. 6. Lamp filling: ○, oxygen and argon, 2–5 and 20 mm Hg resp.; ● pure oxygen, 5 mm Hg.

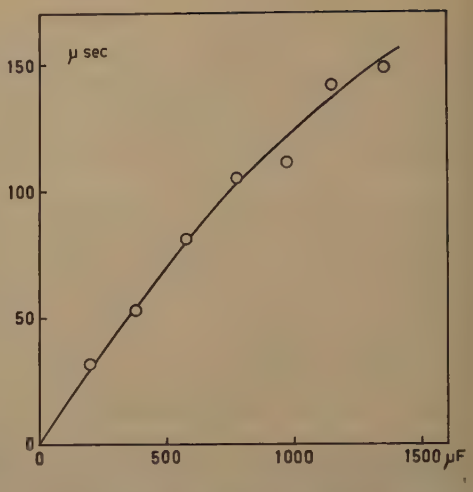

Fig. 9. The flash duration time as a function of capacity at constant voltage, 5 kV, for the lamps in Fig. 6. Lamp filling, oxygen and argon, 2 and 20 mm Hg resp.

short enough to make our apparatus very useful for the study of rapid reactions. It is also obvious that the flash duration does not increase in proportion to the increase in capacity, and even at the high energies used one gains in intensity by increasing the capacity at constant voltage. From Fig. 8 it is equally obvious that for a fixed energy the duration of the flash becomes shorter if a smaller capacity is used at a higher voltage.

Spectral distribution

The spectral distribution of the total light emitted is seen qualitatively from the spectrum in Fig. 10 obtained with a Hilger medium spectrograph on Ilford Selochrome plate. Due to the high temperature and pressure in the lamp during the flash a strong continuum is developed. This continuum contains absorption lines from silicon as well as superimposed emission lines mainly from the gas-filling and the oxygen derived from the quartz. No lines from the tungsten electrodes show up in the spectrogram. The intensity of the light is, as already pointed out by Christie and Porter (13), rather constant throughout the quartz ultraviolet and visible regions.

For quartz, the rapidly increasing absorption at shorter wave lengths causes a cut off of the emission from the photolysis flash lamps at about 200 mμ. By using synthetic saphire for the tubes of the photolysis flash lamps Nelson and Ramsay (7) were able to get photolysis effects at wavelengths shorter than those in quartz ultraviolet.

It may also be mentioned that Mains, Roebber and Rollefson (3) produced flash discharges between Al electrodes in high vacuum and got the *line* spectrum of the aluminium spark. That is particularly valuable as filters can then be used for isolating certain lines. However, these spark discharges have the disadvantage of a low light yield.

Fig. 10. The emission spectrum of the photolysis flash lamp L5. Capacity 600 μF, voltage 5 kV. Lamp filling, oxygen, 5 mm Hg. Hilger medium quartz spectrograph, Ilford Selochrome plate.

Light output

The light output has been studied by means of chemical actinometry.

A uranyl oxalate actinometer according to Forbes and Heidt (14) was used. The concentration was 0.001 *M* in uranyl oxalate and 0.004 *M* in oxalic acid. A value of 0.6 for the quantum yield has been used throughout the absorption region. The titrations were made with ceric sulfate as follows.

A weighed amount (25 g) of the actinometer solution was rendered CO-free by a stream of nitrogen at 70° C for 20 min. After cooling, it was mixed with a weighed amount (28 g) of 0.01 *M* ceric sulfate solution (0.01 *M* $Ce(SO_4)_2 \cdot 2(NH_4)_2SO_4$ in 2 *M* sulfuric acid) so that the final solution contained a small amount of ceric ions.

This amount of ceric ions, which depends upon the decomposition of the actinometer, is then determined by titration with 0.0025 *M* arsenic solution using osmium tetroxide as catalyzer and ferroin as indicator. In order to get a sharp indicator change it is necessary to add a slight excess of arsenic and then back-titrate with a 0.0025 *M* ceric sulfate solution. The titrating solutions used are very stable and the method described proved to be convenient and accurate. The reproducibility is about 0.1 %, which means that the light absorbed can be determined with a relative accuracy of 1 % if it decomposes one tenth of the oxalate.

Recently Hatchard and Parker (15) have developed the potassium ferrioxalate actinometer. We have used it for extending the uranyl oxalate actinometer measurements as it is sensitive at longer wave lengths. The absorption spectra of the two actinometers are given in Fig. 11. The concentration of the ferrioxalate actinometer solution used was 0.025 *M* and the specifications given by Hatchard and Parker were followed closely. An average value of 1.2 has been used for the quantum yield in the calculations.

First it was ascertained that the lamp dimensions and gas fillings were not critical —variation of these parameters did not noticeably affect the number of quanta obtained for a given amount of electrical energy. For instance, two lamps (type L2 and L3) of equal length, 30 cm, but with different inner diameters, 9 mm and 25 mm respectively, gave actinometer decompositions of 10.2% and 10.0% respectively at 700 μF and 5 kV; no reflector was used and the cuvette with actinometer solution was mounted in such a way that it absorbed the same fraction of the emitted light in both cases. The light output was also shown to be constant along the whole length of the lamp.

The effect of gas filling and pressure on the light output at constant energy, 500 μF, 6 kV, for a lamp of type L5 is seen in Fig. 12. At pressures of 50 mm Hg and less, traces of oxygen were added to the argon in order to avoid spontaneous firing. It is seen that the oxygen and argon points lie on a smooth curve. It is also seen that the light output increases somewhat for increasing pressure. However, in practice it is nevertheless preferable to work at low pressures as the lamp can then stand a higher energy without exploding. As mentioned above the flash duration is shorter at lower pressures and consequently no loss in intensity is caused by reducing the pressure.

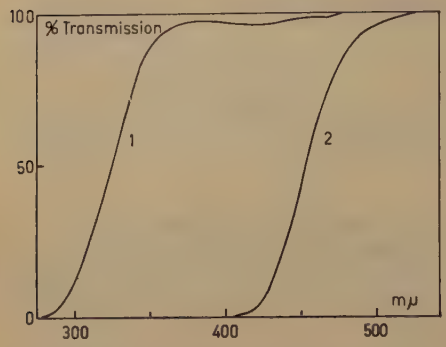

Fig. 11. The light transmission curves for a one-cm layer of the actinometer solutions used. *1*, Uranyl oxalate; *2*, potassium ferrioxalate.

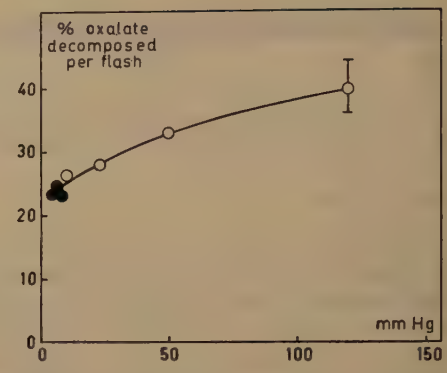

Fig. 12. The effect of gas filling and pressure on the light output at constant energy, 500 μF, 6 kV, for the photolysis flash lamp L5. Lamp filling: ●, oxygen; ○, argon.

Another advantage of working at lower pressures is that the light output then remains more constant from flash to flash. In fact a high degree of reproducibility can be obtained. In Fig. 13 the degree of decomposition per flash as obtained with a uranyl oxalate actinometer is plotted against flash number. In these experiments a lamp of type L5 was used at 500 μF and 5 kV. Before the first flash the lamp was filled with argon to 22 mm Hg and oxygen to 1 mm Hg. It is seen that the light output increases about 2% from the first to the fifth flash and then remains virtually constant.

The light output was measured at constant energy for different voltages. One such curve is given in Fig. 14 for a lamp of type L5 at 5000 joules. It is seen that at fixed energy the light output is higher for higher voltages, however, for voltages higher than 5 kV a rather marked levelling off is observed. It is therefore evident that an increase in voltage at constant energy is more favourable with regard to light intensity than to total light output.

At constant voltage it was found that the light output increases linearly with the capacity. This is indicated in Fig. 15 which shows curves obtained both with the uranyl oxalate and the ferrioxalate actinometer. In these experiments the lamp-pair of type L7 was used and the voltage was 5 kV. At the lowest capacities the energy is so small that no continuum is formed. From these curves it is also seen that the light absorbed in the ferrioxalate actinometer solution is about 3.3 times higher than in the uranyl oxalate actinometer solution. From the absorption curves of these solutions, Fig. 11, it is evident that this result is in general agreement with the already mentioned fact that the light intensity does not vary very strongly with the wave length.

With the final lamp and cuvette mounting shown in Fig. 6 and in cross-section in Fig. 16 measurements of the total light emitted and the fraction thereof absorbed in cuvettes of different sizes have been carried out. The reflector was removed and a cuvette *M*, with an entrance slit 10 mm × 155 mm, was mounted below one of the lamps so that the free surface of the actinometer solution (thickness 25 mm) was exposed to the flash. The other lamp was masked off with a black vertical screen. By moving the cuvette along the lamp in four steps it was found that the light inten-

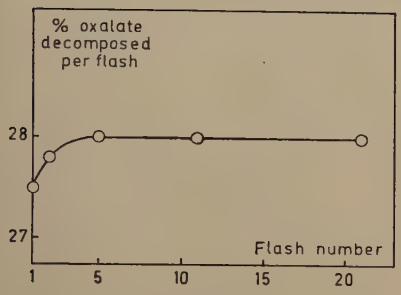

Fig. 13. Diagram showing the constancy of light output after the first few flashes for the photolysis flash lamp L5. Lamp filling, oxygen and argon, 1 and 22 mm Hg resp.

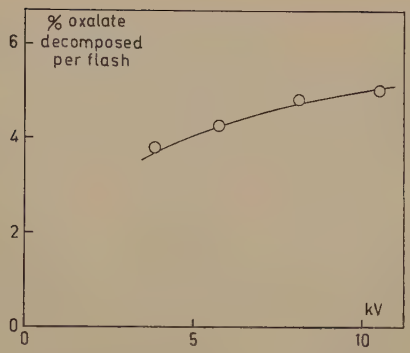

Fig. 14. The light output as a function of voltage at constant energy, 5000 joules, for the photolysis flash lamp L5. Lamp filling, oxygen, 5–10 mm Hg.

sity was constant throughout the length of the lamp. The cuvette contained 100 ml of uranyl oxalate actinometer solution and gave a decomposition of 7.1% for ten flashes at 5 kV and 500 μF (1000 μF were discharged with one lamp masked off) corresponding to 3.6×10^{19} quanta. From the geometry of the mounting one can then calculate that the total light emitted from the lamp-pair is 6.6×10^{20} quanta or 1.1×10^{-3} Einstein per flash for 1000 μF and 5 kV.

The light absorbed by the uranyl oxalate actinometer solution in the cylindrical quartz cuvettes *A* and *B* (length 610 mm; inner diameter: *A*, ca. 25 mm, *B*, ca. 11 mm; volume: *A*, 290 ml, *B*, 55 ml; thickness of annular liquid filter space: *A*, 5 mm, *B*, 10 mm; outside diameter: *A*, 43 mm, *B*, 39 mm; cf. Fig. 16) was measured under normal working conditions, i.e. using both lamps with the reflector in place. To avoid excessive decomposition smaller flashes (600 μF, 5 kV) were used, and for one such flash, with water in the liquid filter space, a decomposition of 9.1% was observed in cuvette *A* and 29.3% in cuvette *B*. This shows that the total amount of light absorbed in cuvette *A* is 1.6 times higher than in cuvette *B*; on the other hand the amount of light absorbed per unit volume is 3.2 times higher in cuvette *B* than in cuvette *A*. From these and the previous results it is also found that the amount of light absorbed in cuvette A is about $\frac{2}{3}$ of the total light emitted by the lamp-pair.

As the light intensities employed in this work are much higher than in previous investigations it is questionable if it is valid to assume the normal quantum yield for the uranyl oxalate actinometer in the calculations. Christie and Porter (16) have already shown that the quantum yield is constant up to light intensities about one tenth of those used by us. This, together with the finding that the decompositions obtained with the uranyl oxalate and ferrioxalate actinometers are directly proportional to each other even at the highest intensities (p. 546, Fig. 15), lends support to the assumption of a normal quantum yield. Furthermore, it was found that solutions containing only oxalic acid (0.005 *M*) did not undergo any perceptible decomposition under analogous conditions. Therefore the different quantum yield for the direct decomposition does not have to be taken into account.

However, as a further check, the light output was determined by integrating the intensity curves obtained with the phototube and oscilloscope arrangement already

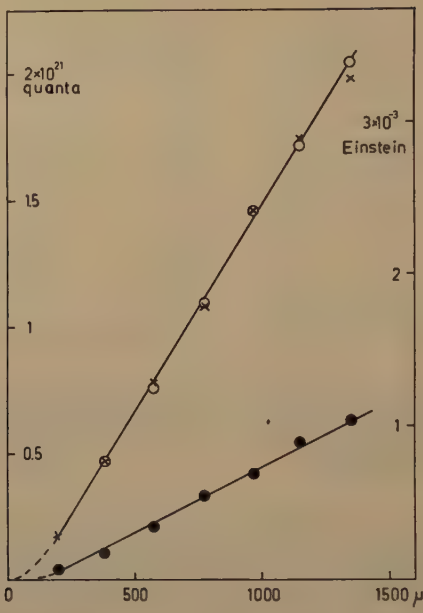

Fig. 15. The number of quanta absorbed by the actinometer solution in cuvette *A* (cf. Figs. 6 and 16) as a function of capacity at constant voltage, 5 kV. ●, Uranyl oxalate; ×, potassium ferrioxalate; ○, values from integrated phototube intensity curves (cf. Fig. 7). Lamp filling, oxygen and argon, 2 and 20 mm Hg resp.

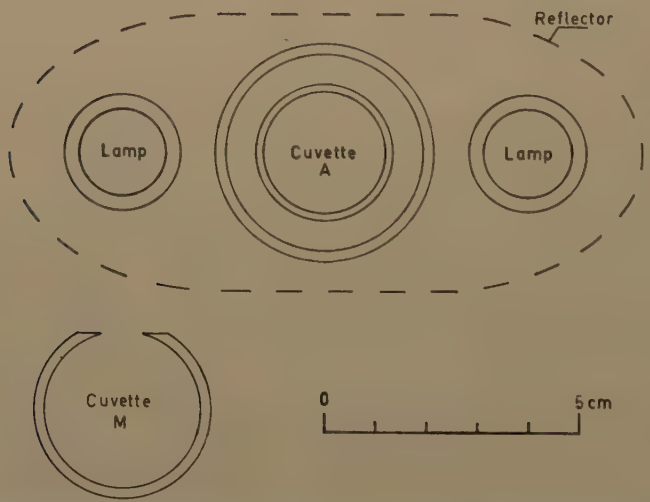

Fig. 16. Section (to scale) through the cuvette and lamp system in Fig. 6. The extra cuvette *M* was used with the reflector removed for the measurements of total light output,
p. 546 and Table 2.

Table 2. Maximum* light output per flash, and intensity available at 1370 μF and 7 kV. Flash duration time 150 μsec

	Uranyl oxalate $\lambda < 350$ mμ	Potassium ferrioxalate $\lambda < 480$ mμ
Total light output from lamp-pair	0.0033 E	0.011 E
Light absorbed in cuvette *A*		
total	0.0023 E	0.0075 E
per unit volume	0.0079 E/litre	0.026 E/litre
Light absorbed in cuvette *B*		
total	0.0014 E	0.0046 E
per unit volume	0.025 E/litre	0.084 E/litre
Average intensity from lamp-pair		
total	22 E/sec	71 E/sec
per unit volume in cuvette *A*	53 E/litre sec	170 E/litre sec
per unit volume in cuvette *B*	170 E/litre sec	560 E/litre sec
Average flux		
cuvette *A*	0.033 E/cm² sec	0.11 E/cm² sec
cuvette *B*	0.046 E/cm² sec	0.15 E/cm² sec
Electrical energy	33,600 joules	
Average power	200,000 kW	
Average current	65,000 amp	

* These values were extrapolated to 7 kV (according to Fig. 14) from the curves for 5 kV in Fig. 15 at 1370 μF as the decompositions of the actinometers were too high at 7 kV.

described (p. 542) and compared with the decomposition of the ferrioxalate actinometer. By using gauge screen of known transmittance at different light intensities, the response of the phototube and oscilloscope arrangement was found to be linear. No absolute calibration of the phototube was carried out. It is seen from Fig. 15 that by a suitable choice of the arbitrary unit the curves for the phototube arrangement and the ferrioxalate actinometer could be brought into coincidence demonstrating the proportionality between the two sets of values.

Although these arguments are not conclusive it seems permissible to use the normal value of 0.6 for the quantum yield of the uranyl oxalate actinometer.

From the data given in this section it is possible to calculate the light output available when the maximum electrical energy at our disposal is discharged. It is given in Table 2, where only that portion of the light which is actually absorbed in the actinometers has been taken into account, that is, the light emitted in the regions 200–350 and 200–480 mμ (cf. the transmission curve in Fig. 11). Some related quantities are also included in the table. It is obvious that this lamp arrangement is ideally suited for a wide variety of problems in flash photochemistry due both to its high total light output and to its high intensity. As already pointed out by Porter (10) the efficiency of this type of lamp is very high. In our case about 14% of the electrical energy is emitted as light in the region 200–480 mμ. If constant spectral distribution throughout the visible part of the spectrum is assumed one can get a rough idea of the average luminous flux from the lamps. It amounts to about 10^{10} lumen or more than 50 lumen per watt. This is of the same order of magnitude as the limiting value at high pressures for the most efficient high pressure mercury lamps (17).

The equipment for photographic recording of absorption spectra

When recording absorption spectra photographically it is necessary to have a very short exposure time in order to get good time resolution. It is then convenient to use a small flash discharge tube as spectrograph lamp. By using a special electrical circuit it is possible to trigger this lamp at any desired time after the photolysis flash. The time interval is also recorded independently, because of the somewhat irreproducible firing characteristics of the lamp. Hilger medium quartz and glass spectrographs are normally used for recording the spectra. Stray light from the photolysis flash is prevented from entering the spectrograph by the use of narrow stops at both ends of the cuvette. Furthermore, the spectrograph is placed at a fairly long distance from the cuvette, and a lens with long focal distance produces a real image of the spectrograph lamp, which is then projected by the condenser lens on the spectrograph slit.

Spectrograph lamp

The photometric work will be greatly simplified if the spectrograph lamp produces a continuous spectrum. This can be achieved by taking advantage of the pressure broadening during the flash. By using short capillary lamps, see Fig. 17, filled with oxygen, we have found it possible to achieve spectra which are suitable for photometry. A typical emission spectrum from such a lamp is shown in Fig. 18. In addition to the continuum there are a few lines which are due to absorption of the silicon vapour formed in the lamp during the flash (cf. p. 544). The dimensions of the lamp capillary are: inner diameter 2 mm, length 40 mm, wall thickness 3 mm. The electrode holders are constructed according to Fig. 5A. The lamp is normally used with 15 μF at 4.5 kV and with enough self inductance in the leads to give a flash duration time of $\sim$20 μsec. This time is still short enough to give sufficient resolution, but permits when necessary the use of capacities up to 100 μF at 4.5 kV without explosion.

The triggering electrode is wound around the capillary. If the oxygen pressure in the lamp is adjusted to be just high enough to prevent spontaneous firing, the time lag between firing pulse and light flash ($<$10 μsec) will be insignificant.

To get constant firing properties the pressure of the oxygen in the lamp is kept constant by a ballast volume of about 2 litres.

This lamp gives a very reproducible light output from flash to flash.

Circuits for lamp synchronization and time interval measurements

As already mentioned the lamps are triggered by means of a high voltage pulse. A suitable pulse is obtained by discharging 2 μF at 1.2 kV through the primary side of an ordinary automobile induction coil. The high voltage end of the secondary coil is connected to the triggering electrode via a resistance of 50,000 Ω to prevent the condenser bank from discharging through the coil (see Fig. 4).

Because of the somewhat irreproducible time lag between pulse and flash of the photolysis lamp we do not normally synchronize the lamps by means of the triggering pulses directly. Instead a coil was mounted close to the leads of the photolysis lamp (cf. Fig. 4). The very rapid current increase at the beginning of the photolysis flash causes a pulse in this coil and this pulse is fed into a phantastron circuit where it can be delayed from 20 μsec to 1 sec. The outgoing pulse is then used for triggering the

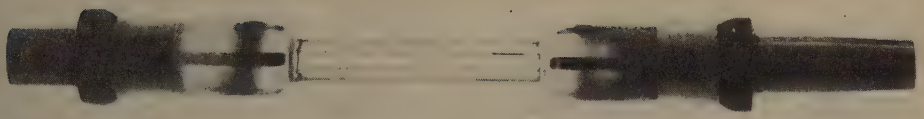

Fig. 17. The spectrograph flash lamp. The capillary tube is used to get pressure broadening.

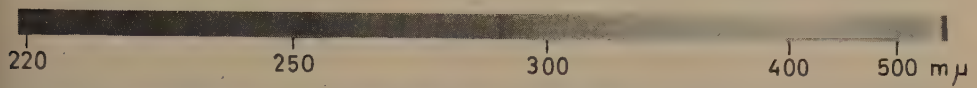

Fig. 18. The emission spectrum of the spectrograph flash lamp. Capacity 15 μF, voltage 4.5 kV. Lamp filling, oxygen, 28 mm Hg. Hilger medium quartz spectrograph, Ilford Selochrome plate.

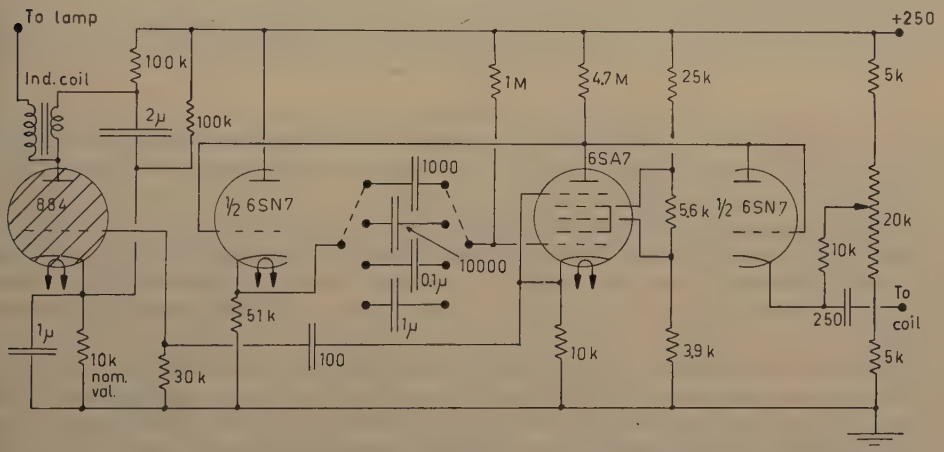

Fig. 19. The time delay (phantastron) and the spectrograph lamp triggering (thyratron) circuits.

grid of a thyratron which closes the triggering circuit for the spectrograph lamp. This triggering circuit is similar to the one used for the photolysis lamp but the condenser voltage used is 230 V instead of 1.2 kV. The time delay and triggering circuits for the spectrograph flash lamp are shown in detail in Fig. 19.

The triggering pulse to the photolysis flash lamps is obtained on closing a relay-operated high voltage switch, the "firing switch" in Fig. 4. Another switching system has also been developed for use when investigating turbid solutions. In this case unwanted stray light from the solution may enter the spectrograph during the photolysis flash. In order to cut off this stray light a rotating shutter wheel has been placed in front of the spectrograph slit. The synchronizing is done as follows. In the trigger circuit of the photolysis flash lamp is inserted a spark gap which consists of two pins, one mounted on the perifery of the wheel (30 cm in diameter, 2400 r.p.m.) and the other fixed in such a way that a very short gap between the pins is obtained when the rotating pin passes the stationary one. If the relay switch is closed the lamp will then fire when the shutter wheel has reached such a position that the short gap is formed. By suitable positioning of the pin in relation to the opening in the shutter

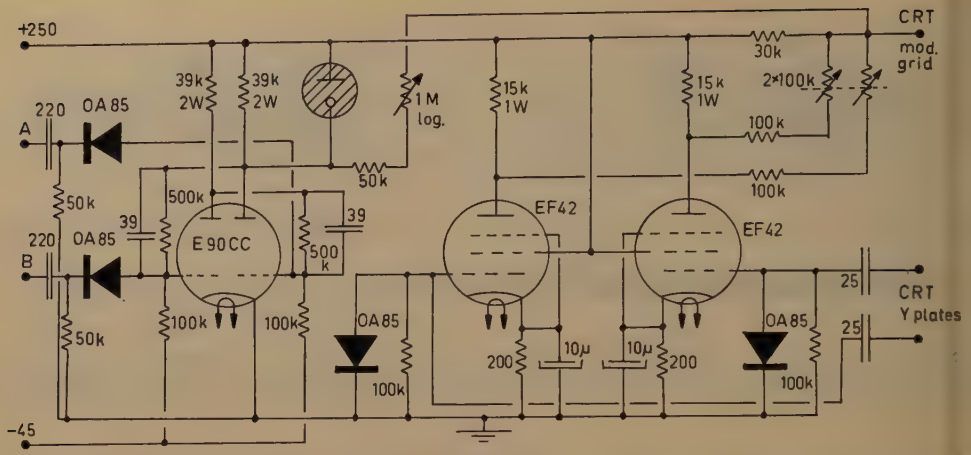

Fig. 20. The intensity modulator circuit for obtaining constant brightness along the cathode ray trace.

wheel, no light will fall on the spectrograph slit when the photolysis flash is on but when the spectrograph flash lamp fires via the time delay circuit the opening is in front of the spectrograph slit.

As indicated earlier (p. 542), a complication in the use of a mechanical shutting device in connexion with the photolysis flash lamp arises from the fact that the flash lamp gives a time lag effect in firing. In order to use the shutter wheel at its maximum resolution, about 100 μsec, it is necessary to use flash lamps filled with a mixture of oxygen and argon.

Because of the time lags in lamp firing, a recording of the exact flash time interval is necessary and is made in the following manner. Two coils, electromagnetically coupled to the photolysis lamp circuit and the spectrograph lamp circuit respectively, are connected via a voltage divider to the Y input of an oscilloscope (Furzehill 0.100, bandwidth 0–1 Mc/sec) (Fig. 4). The Y amplifier is balanced; one input receives the coil signals and the other a signal from a square wave generator. The amplitude of this time marking signal is adjusted to give a barely perceptible square wave character to the oscilloscope sweep. The current surges in the lamp circuits produce pulses in the coils which correspond to the current derivatives with respect to time. The pulse obtained from the photolysis lamp current is also used for starting a time base single stroke.

When recording flash intervals of some length the sweep must be slow. The flash pulses will then appear very thin on the screen and will not be visible on the oscillograms unless the cathode ray intensity is increased when the pulses appear. Therefore an intensity modulator has been developed, Fig. 20, which provides a uniform trace intensity, independent of the trace shape. This intensity modulator also includes a circuit which eliminates exposure due to the quiet cathode ray spot.

The cathode ray is continuously modulated with a voltage which is proportional to the instantaneous writing speed, i.e., proportional to the absolute value of the derivative with respect to time of the input signal function. The push-pull signal obtained directly from the Y deflection plates is differentiated, rectified and amplified in a one-stage pulse amplifier and then fed to the

CRT modulating grid. Rectification is carried out in such a way that the differentiated signals will be applied with positive values on the grid. Two ganged resistors of 100 kΩ adjust the amplitude of the modulating signal. A more detailed description of a similar oscilloscope intensity modulator may be found in reference (18).

If the brightness of the quiet cathode ray spot is reduced to zero with the brightness control, a positive voltage must be applied to the CRT modulator grid when a sweep is triggered, in order to render the sweep visible. This voltage pulse should have the same duration as the sweep. A bistable multivibrator (the E90CC circuit in Fig. 20) is used for producing such square pulses. The input *A* is connected to a coil which is electromagnetically coupled to the photolysis lamp circuit. The current rise at the start of the flash discharge produces a voltage pulse of negative polarity at *A* and thus at the grid of the right hand side of the multivibrator. (This side should be conducting before the application of the pulse, and the neon bulb is inserted for controlling the conducting position.) The multivibrator will switch over and a positive voltage is obtained at the CRT modulator grid. The sweep, which starts at the same instant, shows up on the screen with an intensity depending upon the setting of the 1 MΩ variable resistor. At the return stroke the time base circuit furnishes a negative pulse which is fed to the input *B*. The multivibrator switches back to its original position and the intensity is reduced to zero.

The equipment for photoelectric recording of the changes in light absorption

Arrangements have been made for continuously following, within a narrow wave length region, the changes in absorption of a substance exposed to an intense photolysis flash. The spectrograph flash lamp and the spectrograph, described above, are replaced by a continuous light source, a monochromator, and a phototube connected to an oscilloscope (Fig. 21).

During the photolysis flash, light is scattered by the substance under investigation. This leads to difficulties, especially in the case of turbid solutions, since the stray light obscures the recordings and may even overload the phototube or the oscilloscope amplifier. As described previously, the stray light effect can be greatly reduced by using a long optical path. Further reductions are effected by using vacuum phototubes instead of multiplier phototubes as well as by introducing a stray light compensating phototube.

In order to obtain a favourable signal-to-noise ratio when using vacuum phototubes it is necessary to employ a high intensity light source for monitoring the phototube. A high pressure xenon lamp, Osram XBO 301 (15 V, 20 A dc) was chosen for this purpose as it emits an essentially white light of very high intensity. After passage through the cuvette the light is focussed, by means of two lenses, on the entrance slit of the quartz monochromator (Zeiss Spiegelmonochromator). The long distance, 5 m, between the lenses reduces the stray light to a very low level in normal cases. A vacuum phototube (*M* in Fig. 21) is mounted at such a distance from the exit slit as to be filled with light and is connected to the Y input of the oscilloscope (Tektronix 541). The load resistance is chosen to yield a high signal without decreasing the time resolution (0.1–1 MΩ). The Y input shunt capacity amounts to about 100 pF. (If it would be necessary to reduce the shunt capacity a cathode-follower could be inserted between the phototube and the oscilloscope.)

A second phototube (*S* in Fig. 21) picks up only the unfocussed stray light via a mirror system not reproduced in the figure. The two phototubes are so coupled that their photocurrents oppose each other. A stop in front of this second phototube ad-

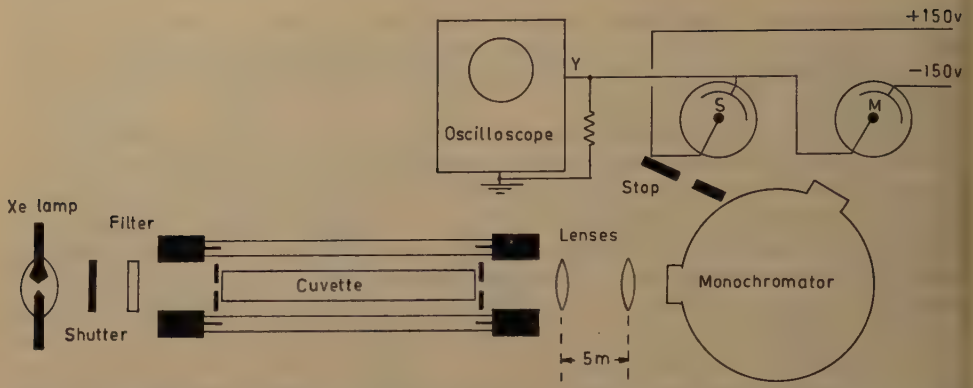

Fig. 21. Equipment for continuous recording of light absorption at a given wave length. The phototube to the right, *M*, measures the light from the monochromator, the one to the left, *S*, compensates for possible stray light during the photolysis flash, thus preventing the oscilloscope from being overloaded.

justs the stray light illumination to such a value that the opposed photocurrents cancel.

In order to avoid decomposition of the substance under investigation by the full light of the xenon lamp, a filter and shutter, which is only opened when recording, are inserted between the lamp and cuvette. The filter suppresses the injurious light.

In Fig. 25 an oscilloscope recording with the arrangement described is reproduced.

Performance of the apparatus

In the development of this apparatus the aim has been to make it as generally useful as possible for flash photolysis work. From the preceding sections it is seen that our final design combines a very high total light output and a very short flash duration time with a high degree of reproducibility and reliability. It is therefore felt that this equipment will be very suitable for the study of a great variety of systems, including those where the photochemical sensitivity is not very high. The apparatus also seems to be of value in such cases where one wants to observe saturation effects in respect to light intensity. Furthermore, the light output achieved here is sufficient for preparative work.

To illustrate the functioning of the equipment two experiments will be described; the first with photographic recording of the absorption spectra, and the second with photoelectric recording of the changes in light absorption. They have been taken as typical examples from a rather large amount of experimental material on chlorophyll which will be described in detail in later publications. Recent flash photolysis work on chlorophyll is found in references (4) and (19–22).

The first experiment was carried out with a solution of chlorophyll *b* in benzene (about 2.3×10^{-7} molar). The solution was made free from oxygen by several cycles of freezing and degassing in a high vacuum and transferred to the cuvette used for the measurements also under vacuum. This cuvette, *B* on p. 547, is 60 cm long, made of quartz with plane windows at the ends and provided with an annular space, 10 mm thick, for a filter solution. The filter solution contained 1 g of $NH_4Fe(SO_4)_2 \cdot 12\,H_2O$

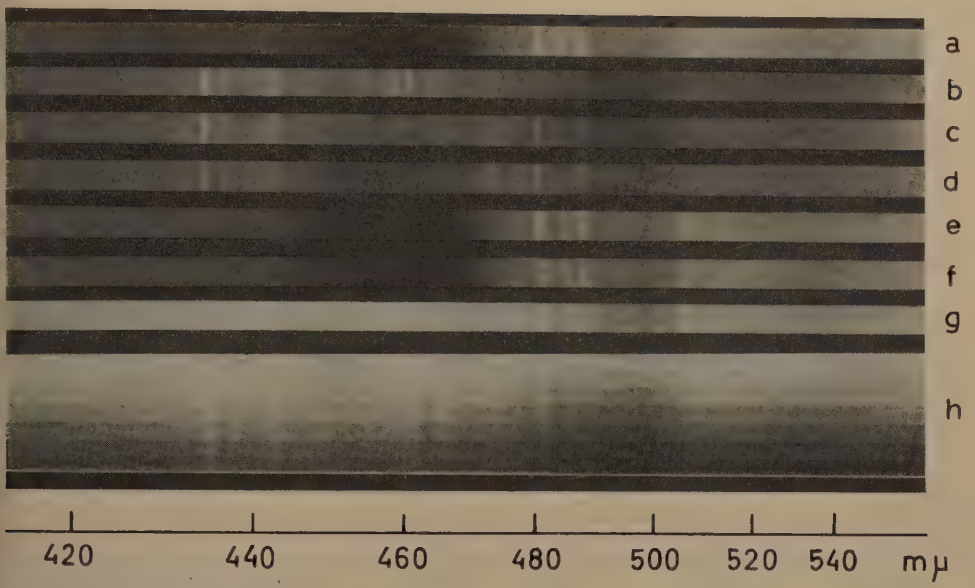

Fig. 22. Absorption spectra of chlorophyll *b* and its excited states in oxygen-free benzene solution taken before (*a*) and 60 μsec (*b*), 270 μsec (*c*) and 600 μsec (*d*) after the corresponding flashes (200 μF, 5 kV). The "after" spectrum (*e*) was taken about 5 min. after the flash, the "after + stray light" spectrum (*f*) was used for determining the amount of stray light from the exciting flash. The spectrum (*g*) is for pure benzene. For determining the blackening curve a spectrum (*h*) was taken with a seven-step neutral filter in front of the spectrograph slit with solvent in the cuvette. Hilger medium glass spectrograph, Ilford H.P.S. plate.

dissolved in 100 ml 2 *M* sulfuric acid. It will transmit light of wave length longer than about 270 mμ. For the photolysis flashes 200 μF and 5 kV were used and the absorption spectrum of the excited chlorophyll solution was photographed 60, 270 and 600 μsec after the corresponding flashes (see Fig. 22) with a Hilger medium glass spectrograph on an Ilford H.P.S. plate. Absorption spectra were also taken before the first flash and about 5 minutes after the last flash to make sure that the irreversible change of the chlorophyll *b* was small. The spectrum (after + straylight) above that of the pure benzene is an "after" spectrum which was then exposed to the stray light from one photolysis flash. The stray light is then determined as the difference between this and the previous "after" spectrum. This is better than to photograph the stray light alone, since it will then not be on the linear part of the blackening curve. In the present case the stray light was found to be negligible. The blackening curve is determined for each individual plate by placing a seven step neutral filter in front of the spectrograph slit (bottom part of Fig. 22) with solvent in the cuvette.

From the photometer curves (the one for 60 μsec and reference curves are given in Fig. 23) of these spectra, the decay curve of the excited state(s) was calculated from the absorption at 498 mμ, and the result is given in Fig. 24. It is seen that the decay is rather slow with an average half life time of about 1000 μsec.

If the solutions are not oxygen-free the half-life time will decrease with increasing oxygen content. In a benzene solution saturated with air the life time is so short that

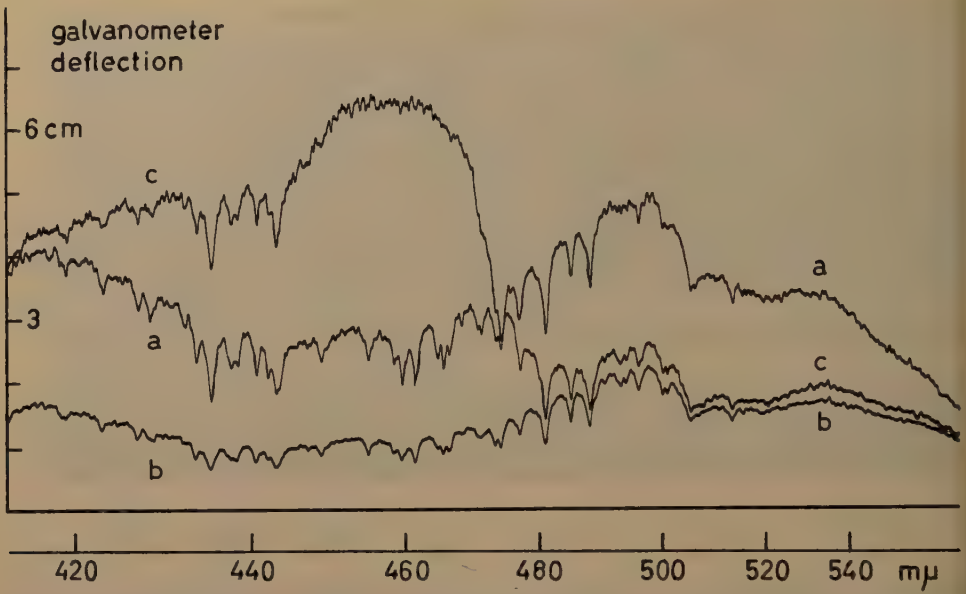

Fig. 23. Photometer tracings of the 60 μsec spectrum (*a*) in Fig. 22 and of the corresponding reference spectra for pure solvent (*b*) and original (unexcited) solution (*c*).

the change in absorption spectrum is observable almost only during the photolysis flash.

This is seen from the second experiment, where the monochromator and phototube arrangement described on p. 553 was used. The concentration of the solution of chlorophyll *b* in benzene was about 9.1×10^{-7} molar. The same cuvette and filter solution were used as before. The monochromator was set for 498 mμ where the excited states show increased light absorption compared to the ground state of chlorophyll *b*. The amount of stray light was so small that it was not necessary to illuminate the compensating phototube. Two typical oscillograms are seen in Fig. 25. The upper curve, *1*, shows the increase in light intensity due only to stray light (xenon lamp shutter closed) from the photolysis flash (800 μF, 5 kV). The lower solid curve, *2*, shows the decrease in light intensity due to the increased absorption from the excited states (shutter open). The dashed curve, *3*, is the lower curve corrected for the stray light. It is seen that the duration of the increased absorption is about the same as that of the photolysis flash. The dashed curve does not return completely to the base-line due to a small irreversible change of the chlorophyll *b*, which occurs when oxygen is present.

The light output from the photolysis flash lamp system described here is, as already mentioned, very high. The cuvettes are long and solutions of very low concentrations can then be used for the light absorption measurements. Therefore the number of quanta emitted during a flash is much larger than the number of the solute molecules. In the experiments just described the concentrations of the solutions were $< 10^{-6}$ *M*, i.e. they contained less than 10^{-9} moles/ml. The number of quanta absorbed by a ferrioxalate actinometer solution in cuvette *B* at the energies used here (200 μF and 800 μF, 5 kV) is about 3 and 20×10^{-6} Einstein/ml, cf. Fig. 15 and p. 546. Conse-

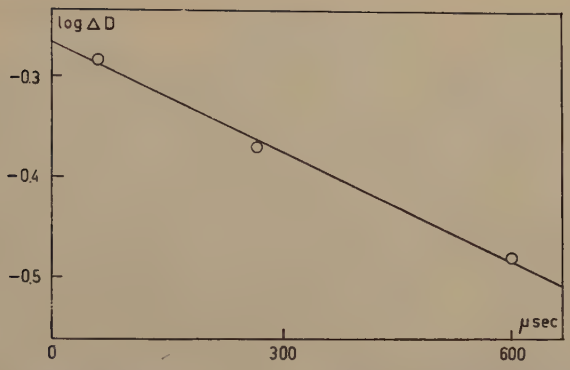

Fig. 24. Decay curve for the excited state of chlorophyll *b*. Derived from the light absorption at 498 mμ of the spectra in Fig. 22. ΔD represents the change in optical density.

quently there are several hundred and several thousand quanta per molecule even in these cases where only a small part of the totally available electrical energy is used, 7% and 29% respectively.

This is certainly highly sufficient for many types of photochemical investigations. Nevertheless it may be interesting to discuss briefly the possibilities of reaching even higher total light outputs and shorter flash duration times.

It does not seem possible to increase the light efficiency (number of quanta/joule) considerably by simple changes in lamp dimensions or gas filling. Therefore, if larger total light outputs are needed more electrical energy must be discharged through the lamps. As they are already used rather near the load which will cause them to explode, much stronger lamps must be made before they can stand higher energies. They will then be rather heavy and presumably of inconveniently large diameter. Therefore it seems better to mount more than two lamps of the type used here parallel to the cuvette. However, such an arrangement requires a very large and expensive condenser

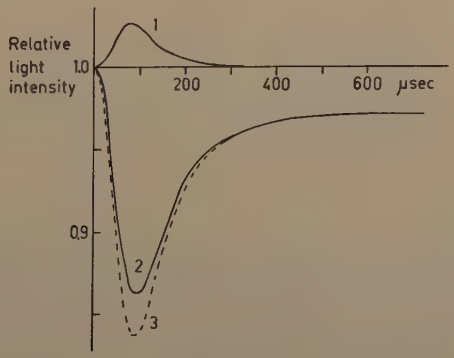

Fig. 25. Oscilloscope tracing showing the increase in light absorption at 498 mμ due to the excitation of chlorophyll *b* during the flash (800 μF, 5 kV), lower curve, *2*. The upper curve, *1*, shows the stray light from the flash alone. The dashed curve, *3*, is the lower curve corrected for the stray light. Benzene solution saturated with air.

bank and, at least at present, does not seem a very attractive proposition even if at the same time it will increase the light intensity.

A much more promising way is to try to decrease considerably the flash duration time for the same or somewhat smaller energies than those used here. That would mean reduced total light output but increased light intensity during the flash. For very short-lived products such an apparatus would be very useful. Its construction requires, however, great care in the electrical design as the flash duration time τ is roughly the same as the length of a half period for the resonance frequency ($\tau = \pi\sqrt{LC}$) of the circuit. The inductance L must therefore be made very small to make it possible to keep C reasonably large.[1] An increase in voltage will also make it possible to reduce C at constant energy as $E = \frac{1}{2} CV^2$. However, already at 10–15 kV it is possible to reach such intensities that the strength of the quartz is the limiting factor, and for many other reasons it is convenient to work at these rather low voltages. Nevertheless, if an extremely fast apparatus is required higher voltages seem to be the natural choice.

SUMMARY

An apparatus for flash photolysis work at very high light intensities and energies is described. A large condenser bank (1400 μF, 7 kV) is discharged through two photolysis flash lamps placed one on each side of the reaction vessel. During the photolysis flash, which lasts from about 30 μsec to 150 μsec depending on the number of condensers used, the number of quanta absorbed in the reaction vessel is from 4 to 45×10^{20} or from 1 to 7×10^{-3} Einstein.

The properties of such photolysis flash lamps, both with respect to mechanical strength and light emission characteristics, are described in detail and the experiments leading to the present design of such lamps are discussed.

The auxiliary equipment, both photographic and photoelectric, for flash spectroscopic work is also described.

The functioning of the apparatus is illustrated by two examples, chosen from an investigation of the excited states of chlorophyll *b*.

ACKNOWLEDGEMENTS

We wish to express our most sincere thanks to Mr. Halvard Liander, ASEA, Västerås, for arranging the generous gift of the condenser bank and for his interest in this work.

Part of this research was supported by grants from the *Rockefeller Foundation*. This is most gratefully acknowledged.

---

[1] It may be mentioned that we have designed a low inductance mounting for a specially built condenser bank (300 μF, 10 kV) which has a total inductance of 0.006 μH, lamp excluded. This is very low in comparison with the 5 μH of the present apparatus. However, the flash duration time will not be reduced in proportion as it will then be determined by the inductance in the lamp This cannot be made correspondingly small, even with coaxial design, if the lamp is to be convenient for photochemical work. It must also be pointed out that it is extremely difficult to design lamps which will not break under these extreme conditions.
This apparatus will be described in the near future.

Institute of Physical Chemistry, University of Uppsala, Uppsala, Sweden.

REFERENCES

1. Norrish, R. G. W., and Porter, G., Nature *164*, 658 (1949).
2. Norrish, R. G. W., and Thrush, B. A., Quart. Revs. (London) *10*, 149 (1956).
3. Mains, G. J., Roebber, J. L., and Rollefson, G. K., J. Phys. Chem. *59*, 733 (1955).
4. Abrahamson, E. W., and Linschitz, H., J. Chem. Phys. *23*, 2198 (1955).
5. Cook, C. L., and Clouston, J. G., Nature *177*, 1178 (1956).
6. Grossweiner, L. I., J. Chem. Phys. *24*, 1255 (1956).
7. Nelson, L. S., and Ramsay, D. A., J. Chem. Phys. *25*, 372 (1956).
8. Fueki, K., Shida, S., and Kuri, Z., J. Chem. Soc. Japan, Pure Chem. Sect. *77*, 1532 (1956).
9. Breitschwerdt, K., Förster, Th., and Weller, A., Naturwiss. *43*, 443 (1956).
10. Porter, G., Proc. Roy. Soc. (London) *A 200*, 284 (1950).
11. Bardócz, Á., and Klatsmányi, Á., Rev. Sci. Instr. *26*, 945 (1955).
12. Cloupeau, M., Compt. rend. *244*, 744 (1957).
13. Christie, M. I., and Porter, G., Proc. Roy. Soc. (London) *A 212*, 398 (1952).
14. Forbes, G. S., and Heidt, L. J., J. Am. Chem. Soc. *56*, 2363 (1934).
15. Hatchard, C. G., and Parker, C. A., Proc. Roy. Soc. (London) *A 235*, 518 (1956).
16. Christie, M. I., and Porter, G., Proc. Roy. Soc. (London) *A 212*, 390 (1952).
17. Elenbaas, W., Philips Tech. Rev. *18*, 167 (1956).
18. Kemp, R. F., Rev. Sci. Instr. *26*, 1120 (1955).
19. Livingston, R., and Ryan, V. A., J. Am. Chem. Soc. *75*, 2176 (1953).
20. Livingston, R., Porter, G., and Windsor, M., Nature *173*, 485 (1954).
21. Livingston, R., J. Am. Chem. Soc. *77*, 2179 (1955).
22. Terenin, A. N., Karyakin, A. V., Lyubomudrov, E. B., Dmitrievskiĭ, O. D., and Sushinskiĭ, P. E., Optika i Spektroskopiya *1*, 456 (1956).

Tryckt den 25 oktober 1957

Uppsala 1957. Almqvist & Wiksells Boktryckeri AB

ARKIV FÖR KEMI Band 11 nr 61

Communicated 5 June 1957 by Arne Fredga

The spectral distribution of oxygen-filled photolysis flash lamps as determined by chemical actinometry

By Stig Claesson and Gunnar Wettermark

With 3 figures in the text

A flash photolysis apparatus similar to the one originally designed by Norrish and Porter (1, 2) but for higher energies and intensities was recently described by Claesson and Lindqvist (3). There a large condenser bank (1400 μF, 7 kV) could be discharged through a pair of oxygen-filled flash photolysis lamps.

For many photochemical investigations it is desirable to know the spectral distribution of such lamps integrated over the whole flash time. From photographs of spectra Christie and Porter (4) showed that the emission from their krypton-filled lamps was rather constant over the whole ultraviolet spectrum if expressed as energy. Strong and Willard (5), also using the photographic method, investigated a small xenon-filled lamp in the region 450 mμ to 650 mμ and found a minimum around 500 mμ due to the grouping of xenon lines. Berchtold (6) used a thermopile for intensity determinations in the region 400–2000 mμ. Cloupeau (7) has studied the changes which occur in the spectral intensity curve during the actual flash by a photographic method using a rotating mirror.

However, when such lamps are used for photochemical studies, the spectral region used is normally isolated by means of suitable filters and not by means of a monochromator. The region isolated will therefore be rather wide and include groups of lines plus the strong continuum. Therefore we have considered it more useful to determine the spectral intensity distribution for our lamps by means of chemical actinometry using a series of suitable filters, rather than to determine the detailed spectral intensity curve by spectrographic methods. This has been done for the region 240–430 mμ which, for photochemical work, is the most useful part of the spectrum emitted.

The filters used were cut-off filters (Jena glass filters and a few liquid filters) with transmission curves $T(\lambda)$ of the type seen in Fig. 1 A. The wavelength for which the transmission was 0.5 is found in Table 1 for the various filters. Two Zeiss filters, D and E, with maximum transmission at 402 and 370 mμ were also used. The transmission curves were measured in a Beckman DU spectrophotometer.

For actinometry the ferrioxalate actinometer developed by Hatchard and Parker (8) was used exactly as described in their paper. The concentration used was 0.006 M. The light absorption curve $A(\lambda)$ for a one cm layer of this actinometer solution is given in Fig. 1 B. It was measured in the Beckman DU spectrophotometer. The quantum yield as a function of wavelength, $\phi(\lambda)$, for

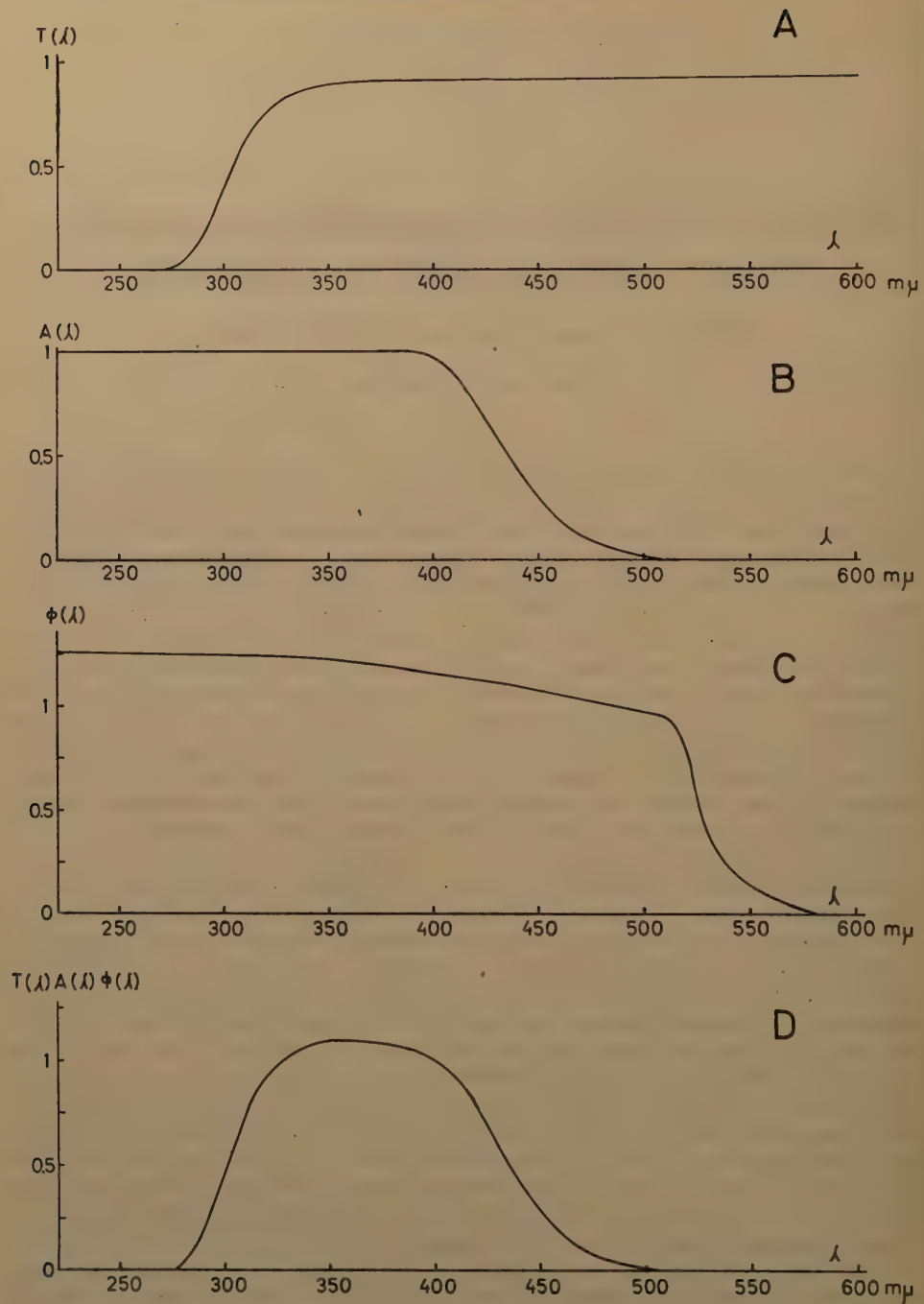

Fig. 1. The wavelength dependence of (A) the fraction of light, $T(\lambda)$, transmitted by one of the filters used (WG6); (B) the fraction of light absorbed, $A(\lambda)$, by the actinometer solution (0.006 M $K_3Fe(C_2O_4)_3$); (C) the quantum yield, $\phi(\lambda)$, for the actinometer solution; (D) the product $T(\lambda)A(\lambda)\phi(\lambda)$.

Table 1. A comparison of the experimentally determined number of quanta, Q, absorbed in the actinometer solution with the values calculated from the curve in Fig. 2 for the various filters used. Unit chosen arbitrarily.

Filter	Wavelength for 50 % transmission (mμ)	Q Mean value from actinometry	Q Calculated value from Fig. 2
GG 3	435	0.13	0.14
GG 15	430	0.14	0.15
GG 13	385	0.45	0.45
WG 1	379	0.50	0.49
GG 18	371	0.57	0.56
WG 9	364	0.61	0.61
WG 2	359	0.63	0.63
WG 3	340	0.70	0.71
BG 26	328	0.78	0.79
WG 4	328	0.78	0.77
WG 5	307	0.91	0.90
WG 6	304	0.94	0.94
WG 7	294	1.00	1.02
CCl_4	272	1.16	1.15
NaAc, 2 M	243	1.25	1.25
Zeiss D		0.12	0.13
Zeiss E		0.08	0.08

this actinometer as determined by Hatchard and Parker is shown in Fig. 1 C. The values for wavelengths longer than 436 mμ have been calculated from the values given by Hatchard and Parker for a 0.025 M solution. However, this part of the curve has very little influence on the final results.

In the experiments a plane parallel quartz cell of thickness 1 cm, diameter 4.3 cm, was placed in front of one of the lamps of the pair (the other was masked off and no reflector used, cf. ref. (2)). A metal plate with an opening 2.5 cm$\times$2.5 cm was placed immediately in front of the cell and the appropriate filter in front of that. The light absorbed in the cell could be considered as parallel.

The flashes were obtained by discharging 800 μF at 5 kV through the lamps. The lamp filling was pure oxygen at a pressure of 5 mm Hg. Depending on the filter used one to three flashes were necessary to get actinometer decompositions for best analytical results.

If we denote by $I(\lambda)d\lambda$ the number of quanta emitted from the lamp in the wavelength region λ to $\lambda+d\lambda$, it is obvious that the number of these quanta absorbed in the cell will be proportional to $I(\lambda)T(\lambda)A(\lambda)d\lambda$ and the decomposition dQ is proportional to $I(\lambda)T(\lambda)A(\lambda)\phi(\lambda)d\lambda$. For the total decomposition Q in the cuvette we then get

$$Q = k\int I(\lambda)T(\lambda)A(\lambda)\phi(\lambda)d\lambda$$

where k is a constant. For each filter used, Q was determined and the product $T(\lambda)A(\lambda)\phi(\lambda)$ could be obtained from the corresponding known curves (cf. Fig. 1 D). The curve $I(\lambda)$ could then be calculated by means of successive approximations.

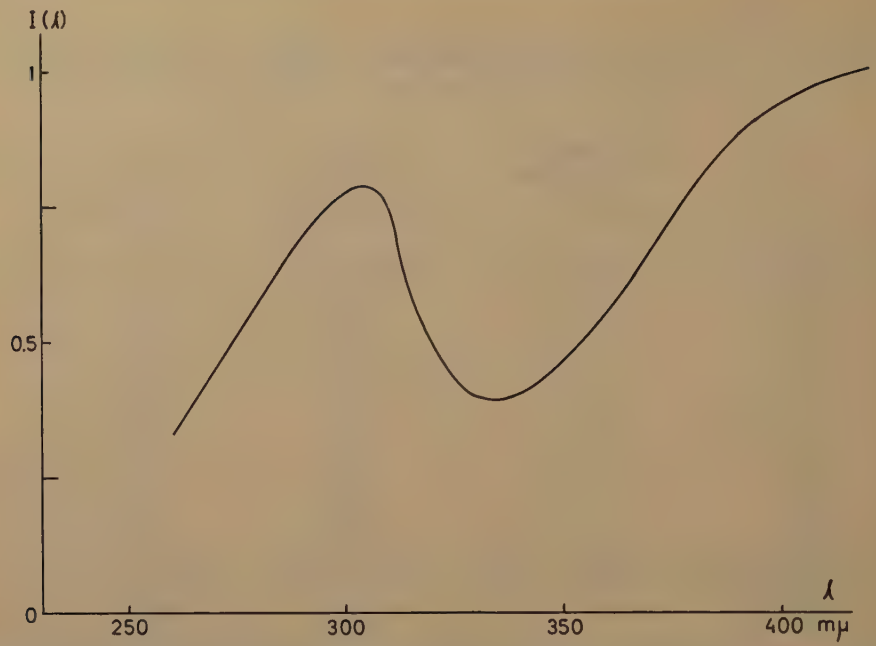

Fig. 2. The number of quanta emitted as a function of wavelength for a high intensity photolysis flash lamp filled with pure oxygen (5 mm Hg) as obtained by chemical actinometry. Energy, 800 μF, 5 kV.

This was done on a mechanical product integrator built at this Institute and following a design due to Van den Akker (9). Starting from $I(\lambda) = \text{const.}$, values for Q were calculated for the various filters. The differences between these values and those actinometrically determined were minimized by changing systematically the shape of the curve $I(\lambda)$. After a few trials the curve given in Fig. 2 (in arbitrary units) was obtained. It is thus seen that the oxygen-filled photolysis flash lamps described in ref. (3) show a maximum in the number of quanta emitted around 300 mμ, and a decrease at shorter wavelengths apparently due to the absorption of the quartz.

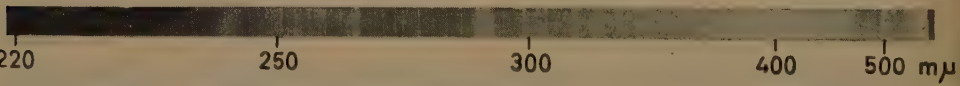

Fig. 3. Emission spectrum from the flash photolysis lamp, the smoothed spectral intensity distribution of which is given in Fig. 2. Positive print.

The agreement between the calculated and observed Q-values (Table 1) is about as good as can be expected if one takes into account the fact that the curve $I(\lambda)$ in Fig. 2 is a strongly smoothened curve compared to the actual spectral intensity curve. This is seen from the photograph of the spectrum in Fig. 3.

Institute of Physical Chemistry, University of Uppsala, Uppsala, Sweden

REFERENCES

1. Norrish, R. G. W., and Porter, G., Nature *164*, 658 (1949).
2. Porter, G., Proc. Roy. Soc. (London) *A 200*, 284 (1950).
3. Claesson, S., and Lindqvist, L., Arkiv Kemi *11*, 535 (1957).
4. Christie, M. I., and Porter, G., Proc. Roy. Soc. (London) *A 212*, 398 (1952).
5. Strong, R. L., and Willard, J. E., J. Am. Chem. Soc. *79*, 2098 (1957).
6. Berchtold, J., Diss., Nr 2376 ETH, Zürich (1954).
7. Cloupeau, M., Compt. rend. *244*, 744 (1957).
8. Hatchard, C. G., and Parker, C. A., Proc. Roy. Soc. (London) *A 235*, 518 (1956).
9. Van den Akker, J. A., J. Opt. Soc. Amer. *29*, 364 (1939).

Tryckt den 25 oktober 1957

Uppsala 1957. Almqvist & Wiksells Boktryckeri AB

ARKIV FÖR KEMI Band 11 nr 62

Communicated 22 May 1957 by Arne Fredga and Gunnar Hägg

On the reactivity of ions and ion-pairs in some base-catalysed reactions

By Arne Brändström

With 16 figures in the text

In order to explain the fact that many base-catalysed reactions have different velocity constants when measured at different dilutions, Acree [1] advanced his "dual mechanism of catalysis". In proving his statement that both the ion and the nonionized compound took part in the reaction he assumed that the conductance ratio Λ/Λ_0 was equal to the degree of dissociation. When this was proved to be incorrect the whole theory was considered as very dubious and is only seldom referred to [2]. This is, however, very unfortunate, as the "dual mechanism of catalysis" seems to be entirely correct and very useful, if only the correct degree of dissociation is used.

The calculation of the degree of dissociation is difficult even for solutions which are 0.1 normal, which often is the lower limit for the concentration of solutions which can be used with accuracy in base-catalysed reactions. It is, however, often possible to calculate the velocity of both the reaction with the dissociated and the undissociated part of the base by means of extrapolations, if the reaction velocity is measured at different concentrations and the electrolytic conductivity of the solutions measured at the same concentrations. How this can be done and how the results can be used to explain the mechanism of some base-catalysed reactions is the subject of the present paper.

The following symbols are introduced for the calculations.

Λ	equivalent conductance of electrolyte.
Λ_0	limiting equivalent conductance of electrolyte at infinite dilution.
α	degree of dissociation.
γ	activity coefficient of ion.
q	distance of closest approach of free ions.
a	distance of closest approach of ions in the ion-pair.
K	dissociation constant according to Bjerrum.
η	viscosity.
$\varkappa$	reciprocal of average radius of ionic atmosphere.
$Q(b)$	Bjerrum integral.
ε	electronic charge.
D	dielectric constant.
k	Boltzmann constant.
T	absolute temperature.

c	molar concentration.
C	initial molar concentration.
S	limiting slope of Debye–Hückel equation.
S_Λ	limiting slope of Onsager equation.
K_i	velocity constant of the reaction with the free ion.
K_m	velocity constant of the reaction with the ion-pair.
K_n	experimental velocity constant at a given concentration.
A, B, M^+	concentrations of the components A, B, and M^+.
t	time in minutes.

Bjerrum's theory

About 30 years ago Bjerrum showed that because of the interionic attraction effects, completely ionised electrolytes need not be completely dissociated at moderate concentrations [3]. Since Bjerrum's theory is now generally accepted and widely used to explain the behaviour of electrolytic solutions, it will also be used here.

The probability of finding an ion of a uni-univalent electrolyte at a given distance from another ion of the opposite charge has a minimum at a distance $q = \varepsilon^2/2\ DkT$. Bjerrum defines that two ions at a distance of $r > q$ are dissociated and those at a distance $r < q$ are associated. For the dissociation reaction Bjerrum developed the expression

$$K = \frac{c\,\alpha^2\gamma^2}{1-\alpha}. \tag{1}$$

Bjerrum further related the dissociation constant K with the dielectric constant D and the absolute temperature T by means of the equation

$$K = 1000/32\pi N q^3\, Q(b), \tag{2}$$

where

$$b = 2q/a. \tag{3}$$

The parameter a was interpreted as the distance between centers of charge in the ion pair.

In the following treatment the definition of ion association on the basis of $r < q$ is retained even if part of the associated fraction is unionized or chelated, for even in this case equation (1) is valid.

In order to demonstrate the validity of equation (1), equations for the calculations of α and γ are necessary.

The activity coefficients

In the deduction of a formula for the activity coefficients in rather concentrated solutions, use must be made of the distance of closest approach. If this quantity is taken equal to the parameter a, Debye's first approximation [4] results, which is very useful for water solutions.

In solutions with a dipole moment less than water, where the association is important, the distance of closet approach for two free ions is no longer a but q, for at a distance less than q the ions are no longer free. Thus, Debye's first approximation can be expected to be valied when $a > q$, whereas if $a < q$ another equation must be used. For the case $a < q$ Marshall and Grunwald [5] have given the formula

$$\log \gamma = \frac{-S\sqrt{\alpha c}}{(1-2.303\,S\sqrt{\alpha c})^{\frac{3}{2}}} \tag{4}$$

which can be expected to give a good approximation for those solutions where $a \ll q$ or where the concentration is not too high. If more concentrated solutions are used, the equation must contain another parameter, but it will be seen that equation (4), which contains only universal constants, can be used with success even in rather concentrated alcoholic solutions (up to $c = 0.2$ in some cases), and it will therefore be used in all the following calculations.

The conductivity equation

The most useful method to determine K is from conductivity data. For this purpose a conductivity equation which is valid even in rather concentrated solutions must be used. Such an equation can be obtained from the limiting law of Onsager

$$\Lambda/\alpha = \Lambda_0 - S_\Lambda\sqrt{\alpha c} \tag{5}$$

by dividing the term S with $(1+q\varkappa) = 1 + 2.303\,S\sqrt{\alpha c})$, as suggested by Marshall and Grunwald [5], thus giving

$$\Lambda/\alpha = \Lambda_0 - S\sqrt{\alpha c}/(1+2.303\,S\sqrt{\alpha c}). \tag{6}$$

Just as equation (4) this conductivity equation contains no adjustable parameter and is therefore very suitable for the calculation of Λ_0 and K. From the investigation of Marshall and Grunwald it can be expected that equation (6) will give an agreement between the calculated and found conductivity within 0.1 per cent when αc is less than 0.1.

The calculation of the dissociation constant

The calculation of K and Λ_0 from a set of conductivity data can be done by successive approximations. Starting with a reasonable first estimate Λ_0^{I}, α is calculated from

$$\alpha = \frac{\Lambda\,(1+2.303\,S\sqrt{\alpha c})}{\Lambda_0\,(1+2.303\,S\sqrt{\alpha c} - S_\Lambda\sqrt{\alpha c}/\Lambda_0^{\mathrm{I}})} \tag{7}$$

which is obtained from (6) by rearrangement. γ is calculated from equation (4). From the identity

$$\frac{1}{\alpha\Lambda_0} = \frac{1}{\Lambda_0} + \frac{1-\alpha}{\alpha\Lambda_0}$$

and equation (1) the following formula is further obtained

$$\frac{1}{\alpha\Lambda_0} = \frac{1}{\Lambda_0} + \frac{c\alpha\gamma^2}{K\Lambda_0} \tag{8}$$

from which follows that a plot of $1/\alpha\Lambda_0^{\mathrm{I}}$ against $c\alpha\gamma^2$ will give a straight line in the concentration region where equations (1), (4), and (6) are valid. The intercept of

this line is $1/\Lambda_0^{II}$ and the slope $1/K\Lambda_0^{II}$. If Λ_0^{II} is much different from Λ_0^{I}, the procedure is repeated until the successive approximations for Λ_0 converge. In practice the convergence is very rapid.

The plot of $1/\alpha\Lambda_0^{I}$ against $c\alpha\gamma^2$ is much more convenient than the plot of $1/\alpha\Lambda_0^{I}$ against $c\gamma^2$, as suggested by Marshall and Grunwald [5], for the latter method gives a straight line only if $c < 3 \times 10^{-7} D^3$, whereas the plot suggested here gives a straight line as long as the equations (1), (4) and (6) are correct, which is the case for much higher concentrations than $c = 3 \times 10^{-7} D^3$. This is of great importance when Λ_0 is to be determined for an alkaline solution, for in this case a correction of the conductivity data must be done to take into account the content of carbon dioxide present in the highly diluted solutions, and such a correction is always uncertain. With the plot $1/\alpha\Lambda_0$ against $c\alpha\gamma^2$ much more concentrated solutions can be used to calculate Λ_0, thus greatly reducing the corrections.

The value of K obtained can be used to calculate the parameter a by means of equations (2) and (3), but the values thus obtained are valid only if the mutual potential energy of the ion-pair is strictly coulombic, as assumed by Bjerrum. This is usually not the case if the ions are highly solvated as the free alkali metal ions, for in forming the ion-pair a considerable desolvation often occurs. This is also one of the reasons of the difference between the a values obtained from K and those calculated from Λ_0 by means of Stoke's law [6].

The validity of the dissociation equilibrium for alkoxide solutions

The validity of equations (1), (4), and (6) can be tested for the ethoxide solutions from the conductivity values of Jones and Hughes [7] for very dilute solutions, and those of Robertson [8] for more concentrated solutions. The values obtained are given in Tables 1–6 and in Figs. 1–3. The Λ values of Jones and Hughes [7] are corrected as described by them with the difference that the straight line chosen was that corresponding to equation (8) instead of that corresponding to equation

$$\Lambda = \Lambda_0 - S_\Lambda \sqrt{c}.$$

The difference between the values obtained by these two methods is very slight and of no importance for the following considerations. The Λ values of Robertson [8] are corrected to correspond to the modern standard for conductivity values [9] and for the content of carbon dioxide as described above. In Figs. 1–3 the values of Robertson [8] are plotted and the lines drawn are those obtained from Jones and Hughes

Table 1. The conductivity of $LiOC_2H_5$ at 25° [7].

$\Lambda_0 = 39.49$, $K = 5.60 \times 10^{-3}$.

$C \times 10^4$	Λ	Λ_{corr}	α	$1/\alpha\Lambda_0 \times 10^2$	γ	$C\alpha\gamma^2 \times 10^4$	$1/\Lambda_0 \times 10^2$
2.721	35.51	35.98	0.9627	2.635	0.905	2.144	2.538
6.163	33.80	33.99	0.9303	2.726	0.863	4.275	2.533
9.854	32.29	32.41	0.9021	2.812	0.835	6.197	2.532
14.584	30.77	30.86	0.8729	2.906	0.810	8.349	2.529
18.904	29.63	29.70	0.8487	2.989	0.794	10.116	2.532

Table 2. The conductivity of $LiOC_2H_5$ at 25° [8].

$C \times 10^4$	Λ	Λ_{corr}	α	$1/\alpha\Lambda_0 \times 10^2$	γ	$C\alpha\gamma^2 \times 10^4$	$1/\Lambda_0 \times 10^2$
10,000	2.67	2.67	0.1061	—	—	—	—
5,000	4.67	4.67	0.1831	—	—	—	—
2,500	6.82	6.82	0.2627	9.662	0.410	110.46	—
1,250	9.15	9.15	0.3342	7.595	0.458	87.65	—
625.0	11.95	11.96	0.4184	6.066	0.512	68.54	—
312.5	15.10	15.13	0.5064	5.012	0.569	51.24	2.70
156.3	18.65	18.71	0.5996	4.233	0.625	36.60	2.58
78.13	22.47	22.59	0.6948	3.653	0.683	25.34	2.51
39.06	26.09	26.32	0.7795	3.256	0.737	16.55	2.51
19.53	29.36	29.77	0.8529	2.976	0.790	10.39	2.51
9.767	31.77	32.50	0.9047	2.805	0.835	6.15	2.53
4.883	33.06	34.40	0.9353	2.714	0.876	3.52	2.56

Table 3. The conductivity of $NaOC_2H_5$ at 25° [7].

$\Lambda_0 = 43.12$, $K = 9.54 \times 10^{-3}$.

$C \times 10^4$	Λ	Λ_{corr}	α	$1/\alpha\Lambda_0 \times 10^2$	γ	$C\alpha\gamma^2 \times 10^4$	$1/\Lambda_0 \times 10^2$
1.857	39.00	40.67	0.9847	2.356	0.916	1.53	2.319
3.803	38.54	39.44	0.9707	2.390	0.886	2.89	2.320
7.180	37.38	37.91	0.9507	2.440	0.852	4.95	2.320
10.366	36.40	36.80	0.9349	2.482	0.829	6.66	2.320
15.050	35.20	35.49	0.9150	2.535	0.804	8.91	2.318
19.616	34.19	34.44	0.8981	2.583	0.785	10.85	2.319

Table 4. The conductivity of $NaOC_2H_5$ at 25° [8].

$C \times 10^4$	Λ	Λ_{corr}	α	$1/\alpha\Lambda_0 \times 10^2$	γ	$C\alpha\gamma^2 \times 10^4$	$1/\Lambda_0 \times 10^2$
10,000	4.98	4.98	0.1830	12.67	0.309	174.8	—
5,000	8.30	8.30	0.3005	7.717	0.327	160.5	—
2,500	11.06	11.06	0.3867	5.997	0.370	132.3	—
1,250	13.91	13.92	0.4666	4.970	0.423	104.4	2.43
625.0	17.04	17.05	0.5464	4.244	0.481	79.01	2.32
312.5	20.44	20.47	0.6262	3.703	0.545	58.14	2.29
156.3	24.00	24.12	0.7048	3.290	0.609	40.90	2.30
78.13	27.35	27.59	0.7722	3.003	0.672	27.24	2.34
39.06	30.86	31.38	0.8456	2.743	0.740	16.44	2.34
19.53	33.46	34.46	0.8979	2.583	0.786	10.84	2.32
9.767	34.77	36.71	0.9300	2.494	0.834	6.32	2.34
4.883	35.34	38.82	0.9615	2.412	0.875	3.59	2.33

Table 5. The conductivity of KOC_2H_5 at 25° [7].

$\Lambda_0 = 46.55$, $K = 10.28 \times 10^{-3}$.

$C \times 10^4$	Λ	Λ_{corr}	α	$1/\alpha\Lambda_0 \times 10^2$	γ	$C\alpha\gamma^2 \times 10^4$	$1/\Lambda_0 \times 10^2$
2.426	41.62	43.57	0.9811	2.192	0.907	1.960	2.151
3.915	41.37	42.72	0.9726	2.210	0.885	2.983	2.148
5.841	40.79	41.78	0.9616	2.236	0.865	4.203	2.148
9.025	39.82	40.54	0.9461	2.273	0.837	5.983	2.148
12.124	38.97	39.55	0.9327	2.305	0.816	7.530	2.148
16.616	37.85	38.32	0.9149	2.350	0.797	9.660	2.148

Table 6. The conductivity of KOC_2H_5 as 25° [8].

$C \times 10^4$	Λ	Λ_{corr}	α	$1/\alpha\Lambda_0 \times 10^2$	γ	$C\alpha\gamma^2 \times 10^4$	$1/\Lambda_0 \times 10^2$
10,000	6.98	6.98	—	—	—	—	—
5,000	10.44	10.44	0.3450	—	—	—	—
3,750	11.64	11.64	0.3793	—	—	—	—
3,125	12.40	12.40	0.4003	—	—	—	—
2,500	13.26	13.26	0.4228	5.081	0.361	137.7	2.20
1,875	14.47	14.47	0.4536	4.737	0.384	125.4	2.12
1,250	16.28	16.28	0.4981	4.313	0.416	107.7	2.06
937.5	17.51	17.52	0.5264	4.081	0.441	96.02	2.07
625.0	19.48	19.50	0.5710	3.762	0.476	80.86	2.07
312.5	22.97	23.01	0.6443	3.334	0.542	59.15	2.10
156.3	26.74	26.82	0.7188	2.989	0.605	41.05	2.13
78.13	30.45	30.61	0.7873	2.729	0.670	27.62	2.15
39.06	33.91	34.35	0.8513	2.523	0.731	17.77	2.15
19.53	36.64	37.42	0.8978	2.393	0.785	10.80	2.17
9.767	38.66	40.22	0.9397	2.286	0.834	6.38	2.15
4.883	39.58	42.19	0.9652	2.226	0.856	3.45	2.15

[7]. It can be seen that the points fit the lines rather well even at high concentrations. In the last column in Tables 1–6 the values of $1/\Lambda_0 = 1/\alpha\Lambda_0 - c\alpha\gamma^2/K\Lambda_0$ are calculated. From this it can be seen that the value of $1/\Lambda_0$ is only 2.5 per cent in error when calculated from a 0.25 normal solution of potassium ethoxide. From this it can be concluded that equations (1), (4) and (6) are valid even in rather concentrated solutions, and from the considerations given by Marshall and Grunwald it can be expected that equation (4) is the least correct one of the three equations tested. Equation (6)—and (7)—can thus be expected to give reasonable values of α for most solutions that can be used for kinetic purposes.

Calculation of the velocity constant of the ion-pair and the ion

If the reaction $A + B \rightarrow C$ is of the second order with the velocity proportional to both the concentration of the base B and the other reagent A, the following equation is valid:

$$\frac{dC}{dt} = K_n A B. \qquad (9)$$

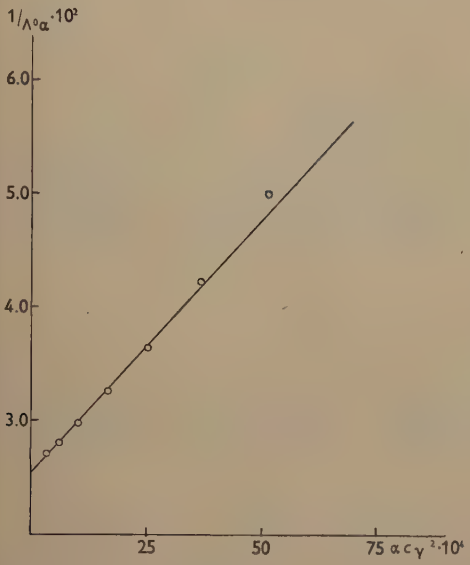

Fig. 1.

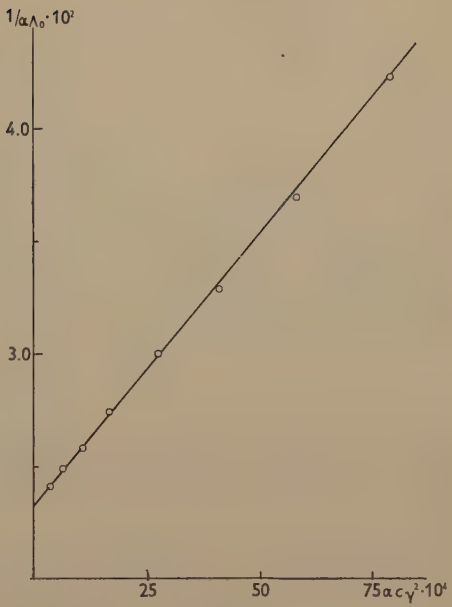

Fig. 2.

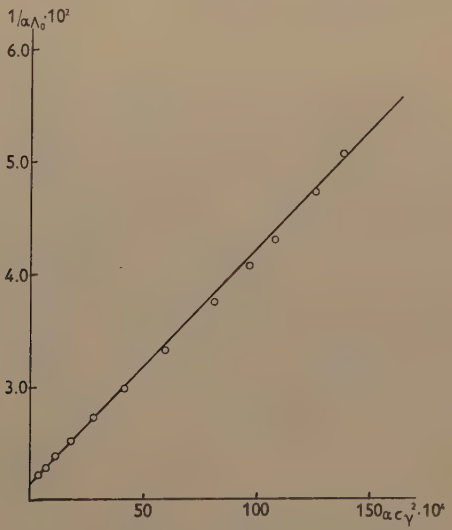

Fig. 3.

Fig. 1. The conductivity of $LiOC_2H_5$ at 25°.
Fig. 2. The conductivity of $NaOC_2H_5$ at 25°.
Fig. 3. The conductivity of KOC_2H_5 at 25°.

The value of K_n, however, is usually different at different concentrations. If the base B is only partly dissociated, it is logical to consider two reactions, one of which has a velocity proportional to the concentration of the dissociated part of the base αB and the other to the concentration of the associated part (ion-pair, chelate etc.) $(1-\alpha)B$. The differential equation for such a reaction is

$$\frac{dC}{dt} = A \cdot B[K_i \alpha + K_m(1-\alpha)] = A B K_n. \tag{10}$$

This is the Dual Mechanism of Catalysis first given by Acree [1].

From equation (10) it can be seen that if K_i and K_m are constant even if the concentration of the base B is varied, it is possible to calculate both K_i and K_m, if both the degree of dissociation α and the velocity constant K_n can be measured at two different concentrations. In practice this is usually not possible, as there may be primary salt effects too. Since the salt effect becomes less the lower the concentration of the solution, K_i and K_m can be obtained by means of extrapolation to dilute solutions in the following way.

With rearrangement equation (10) becomes

$$K_n/(1-\alpha) = K_i \alpha/(1-\alpha) + K_m. \tag{11}$$

A plot of $K_n/(1-\alpha)$ against $\alpha/(1-\alpha)$ will thus give a nearly straight line with the deviations due to experimental error or errors in α together with primary salt effects. The assymptote for low concentrations to these points has the slope K_i and the intercept K_m.

The plot of $K_n/(1-\alpha)$ against $\alpha/(1-\alpha)$ is usually much more convenient than that of K_n against α, since the former plot makes the points in the more dilute region much more important than those in the more concentrated solutions, thus rending salt effects less important. The plot suggested will also give a rather good estimate of the accuracy of K_m.

The constant K_n

In a reaction such as that of sodium ethoxide with methyl iodide the degree of dissociation may vary during the reaction, since sodium iodide is formed at the same time as sodium ethoxide is consumed, and these two sodium compounds may have different degrees of dissociation. The exact expression for the degree of dissociation of sodium ethoxide in the presence of sodium iodide is somewhat complicated and not very useful to predict the variation of α with the concentration of sodium ethoxide and sodium iodide during an experiment. From the experimental data it is usually found that K_n seems to be very nearly constant during an experiment, thus indicating that even α is constant. α is, however, not exactly constant, but in each case it is very simple to extrapolate the value of K_n to be valid at the initial concentration of the base.

The explanation for the constancy of α during the measurements is that in the dissociation equilibrium

$$\frac{\alpha M^+ \gamma^2}{1-\alpha} = K \tag{12}$$

the product $M^+\gamma^2$ is very nearly constant for small variations in M^+, which can be seen from equation (4), for γ^2 is descreasing when the concentration M^+ is increased.

The constant K_i

The constant K_i, which is obtained from the slope of the asymptote to a plot of $K_n/(1-\alpha)$ against $\alpha/(1-\alpha)$, is a measure of the reactivity of the free anion of the

base in a very dilute solution. If the cation present is varied, K_i will be the same except in those cases where the cation present is interacting with the compound with which the anion is reacting. In all reactions given in this paper K_i is constant within the experimental errors when the cation is varied.

The reactivity of the ion-pair

From the fact that electrons are withdrawn to some extent from the anion in forming the ion-pair, it might be expected that the ion-pair has a much lower reactivity than the free anion in the reaction with reagents such as methyl iodide, if there is no steric factor that makes the reaction with the ion-pair especially favoured. If no such steric factor is present, the reaction will therefore proceed mainly with the anion and only to a very little extent with the ion-pair. Such a type of reaction is observed between phenolates and alkyl halides. In other reactions such as that of alkoholates with methyl iodide, the transformation of imino-ethers into nitriles by means of alcoholates, and the alkylation of alkali compounds of ethyl acetoacetate, there is both a reaction with the dissociated part of the base and with the associated part of it. In all these cases a cyclic mechanism can be given which explains the reactivity of the ion-pair.

The alkylation of alkali phenolates

The velocities of the reaction of sodium phenoxide with methyl or ethyl iodide in alcoholic solutions have been measured by Robertson [10], and the corresponding reactions of lithium and potassium phenoxide have been studied by Shrader [11]. The conductivity of the different alkali phenoxides have been measured by Robertson [8].

The conductivity values have been corrected to correspond to the modern standard [9] and plotted in the same way as those for the ethoxides. In this way the following limiting conductivities have been obtained: $LiOC_6H_5$: $\Lambda_0^{25^\circ} = 34{,}8$; $NaOC_6H_5$: $\Lambda_0^{25^\circ} = 38.6$; KOC_6H_5: $\Lambda_0^{25^\circ} = 42.2$. From the values of Λ and Λ_0, α was calculated by means of equation (7). These values, together with those obtained from the velocity measurements, are given in Tables 7–12. Plots of $K_n/(1-\alpha)$ against $\alpha/(1-\alpha)$ indicate that K_m is very small and that the best asymptote to the points gives $K_m = 0$. The deviations from this asymptote are, however, appreciable in the most concentrated solutions, thus rendering the value of K_m very uncertain. If K_m is assumed to be 0, the deviations from the asymptote must be due to salt effects and to errors in α. Since both these errors are probably proportional to c, a plot of K_n/α against c

Table 7. The reaction $CH_3I + LiOC_6H_5$ at 25° [11].

$K_i = 0.0253$.

C	K_n	α	$K_n/(1-\alpha)$	$\alpha/(1-\alpha)$	K_n/α
0.500	0.00739	0.1917	0.00921	0.237	0.0385
0.250	0.00894	0.2856	0.01251	0.400	0.0313
0.125	0.01083	0.3869	0.01766	0.631	0.0280
0.0625	0.01317	0.4875	0.02570	0.951	0.0270
0.0313	0.01592	0.5848	0.03834	1.408	0.0272

Table 8. The reaction $CH_3I + NaOC_6H_5$ at 25° [10].

$K_i = 0.0256$.

C	K_n	α	$K_n/(1-\alpha)$	$\alpha/(1-\alpha)$	K_n/α
1.000	0.00764	0.1899	0.00943	0.234	0.0402
0.500	0.00924	0.2862	0.01294	0.401	0.0323
0.250	0.01070	0.3761	0.01715	0.603	0.0284
0.125	0.01272	0.4661	0.02382	0.873	0.0273
0.0625	0.01447	0.5552	0.03253	1.248	0.0261
0.0313	0.01678	0.6417	0.04683	1.791	0.0261

Table 9. The reaction $CH_3I + KOC_6H_5$ at 25° [11].

$K_i = 0.0258$.

C	K_n	α	$K_n/(1-\alpha)$	$\alpha/(1-\alpha)$	K_n/α
0.500	0.00937	0.3152	0.01368	0.460	0.0297
0.250	0.0105	0.3881	0.0172	0.634	0.0270
0.125	0.0124	0.4645	0.0232	0.867	0.0267
0.0625	0.0144	0.5416	0.0314	1.182	0.0266

Table 10. The reaction $LiOC_6H_5 + C_2H_5I$ at 25° [11].

$K_i = 0.0049$.

C	K_n	α	$K_n/(1-\alpha)$	$\alpha/(1-\alpha)$	K_n/α
0.500	0.001487	0.1917	0.00184	0.237	0.00776
0.250	0.001785	0.2856	0.00250	0.400	0.00625
0.125	0.002155	0.3869	0.00351	0.631	0.00557
0.0625	0.002560	0.4875	0.00500	0.951	0.00525
0.0313	0.002735	0.5848	0.00660	1.408	0.00468

Table 11. The reaction $NaOC_6H_5 + C_2H_5I$ at 25° [10].

$K_i = 0.0051$.

C	K_n	α	$K_n/(1-\alpha)$	$\alpha/(1-\alpha)$	K_n/α
1.000	0.00155	0.1899	0.00191	0.234	0.00816
0.500	0.00185	0.2862	0.00259	0.401	0.00646
0.250	0.00217	0.3761	0.00348	0.603	0.00577
0.125	0.00254	0.4661	0.00476	0.873	0.00545
0.0625	0.00290	0.5552	0.00652	1.248	0.00522

Table 12. The reaction $KOC_6H_5 + C_2H_5I$ at 25° [11].

$K_i = 0.0051$.

C	K_n	α	$K_n/(1-\alpha)$	$\alpha/(1-\alpha)$	K_n/α
0.500	0.001937	0.3152	0.00283	0.460	0.00615
0.250	0.002197	0.3889	0.00360	0.634	0.00565
0.125	0.002465	0.4645	0.00460	0.867	0.00531
0.0625	0.002795	0.5416	0.00610	1.182	0.00516
0.0313	0.003166	0.6176	0.00828	1.615	0.00512

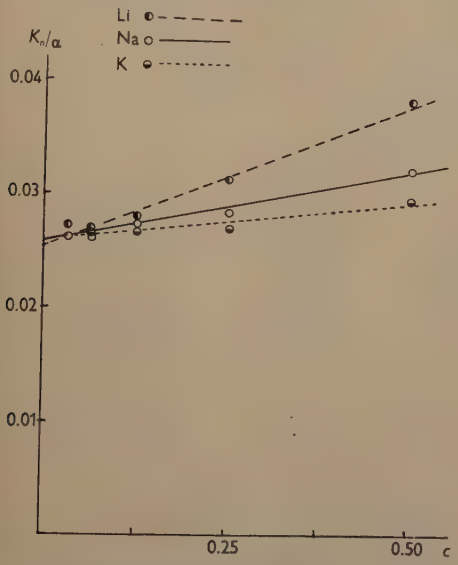

Fig. 4. The reaction of CH_3I with alkali phenoxides at 25°.

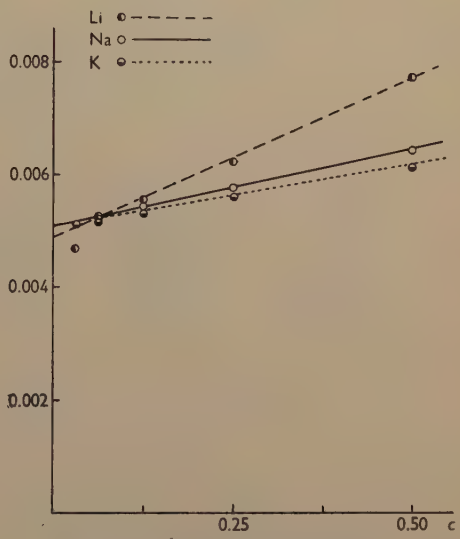

Fig. 5. The reaction of C_2H_5I with alkali phenoxides at 25°.

should give straight lines. Such plots are given in Figs. 4 and 5. From these plots it is seen that the points fit the lines drawn rather well. The intercepts for these lines at the axis $c = 0$ give K_i. The values of K_i obtained for the different alkali phenoxides are nearly equal; the deviations may well be due to experimental errors.

From the kinetic results given above it can be concluded that the reaction of the alkali phenoxides with methyl and ethyl iodides are probably pure ionic reactions. In order to prove definitely that $K_m = 0$ for this type of reaction, it is necessary to study other reactions of this type where the salt effects are much smaller. Such systems might have been investigated by Hardwick [20], Woolf [21], and by Mitchell [22] but their primary results are too scanty to be used as a basis for a recalculation.

The alkylation of alkali ethoxides

The velocities of the reactions of alkali ethoxides with methyl iodide, ethyl iodide, and methyl bromide have been measured at 25° by Shrader [11], Brown [12], Marshall and Acree [13] and Taylor [14]. The velocity constants and the degree of dissociation are given in Tables 13–21 and the values $K_n/(1-\alpha)$ plotted against $\alpha/(1-\alpha$ in

Table 13. The reaction $LiOC_2H_5 + CH_3I$ at 25° [11].

$K_i = 0.130$, $K_m = 0.034$.

C	K_n	α	$K_n/(1-\alpha)$	$\alpha/(1-\alpha)$
0.5000	0.0522	0.1831	0.0639	0.224
0.2500	0.0584	0.2627	0.0792	0.356
0.1250	0.0659	0.3342	0.0990	0.502
0.0625	0.0740	0.4184	0.1272	0.719
0.0313	0.08345	0.5064	0.1691	1.026

Table 14. The reaction $NaOC_2H_5 + CH_3$ at 25° [12].

$K_i = 0.125$, $K_m = 0.053$.

C	K_n	α	$K_n/(1-\alpha)$	$\alpha/(1-\alpha)$
0.5000	0.07470	0.3005	0.1068	0.430
0.2500	0.08005	0.3867	0.1305	0.631
0.1250	0.08610	0.4666	0.1614	0.875
0.0625	0.09202	0.5464	0.2029	1.205
0.0313	0.09893	0.6262	0.2647	1.675

Table 15. The reaction $KOC_2H_5 + CH_3I$ at 25°.

$K_i = 0.122$, $K_m = 0.063$.

C	K_n^*	α	$K_n/(1-\alpha)$	$\alpha/(1-\alpha)$
0.5000	0.0838	0.3450	0.1279	0.527
0.2500	0.0879	0.4228	0.1523	0.733
0.1250	0.0921	0.4981	0.1835	0.992
0.0625	0.0968	0.5710	0.2256	1.331
0.0313	0.1019	0.6443	0.2865	1.811

K_n^* is calculated from the values of "K_i" and "K_m" given by Taylor and the values of "α" given by Robertson.

Table 16. The reaction $LiOC_2H_5 + C_2H_5I$ at 25° [11].

$K_i = 0.0116$, $K_m = 0.0027$.

C	K_n	α	$K_n/(1-\alpha)$	$\alpha/(1-\alpha)$
0.5000	0.004300	0.1831	0.00526	0.224
0.2500	0.004863	0.2627	0.00660	0.356
0.1250	0.005660	0.3342	0.00850	0.502
0.0625	0.006344	0.4184	0.01091	0.719
0.0313	0.007159	0.5064	0.01450	1.026

Table 17. The reaction $NaOC_2H_5 + C_2H_5I$ at 25° [11].

$K_i = 0.0119$, $K_m = 0.0033$.

C	K_n	α	$K_n/(1-\alpha)$	$\alpha/(1-\alpha)$
1.0000	0.005207	0.1830	0.00637	0.224
0.5000	0.005958	0.3005	0.00852	0.430
0.2500	0.006575	0.3867	0.01072	0.631
0.1250	0.007234	0.4666	0.01356	0.875
0.0625	0.008000	0.5464	0.01764	1.205
0.0313	0.008654	0.6262	0.02315	1.675

Tabld 18. The reaction $KOC_2H_5 + C_2H_5I$ at 25° [11].

$K_i = 0.0119$, $K_m = 0.0036$.

C	K_n^*	α	$K_n/(1-\alpha)$	$\alpha/(1-\alpha)$
0.5000	0.00658	0.3450	0.01004	0.527
0.2500	0.00712	0.4228	0.01234	0.733
0.1250	0.00770	0.4981	0.01534	0.992
0.0625	0.00832	0.5710	0.01939	1.331
0.0313	0.00898	0.6443	0.02525	1.811

K_n^* is calculated from the values of "K_i" and "K_m" given by Taylor and the values of "α" given by Robertson.

Table 19. The reaction $LiOC_2H_5 + C_2H_5Br$ at 25° [11].

$K_i = 0.00550$, $K_m = 0.00135$.

C	K_n	α	$K_n/(1-\alpha)$	$\alpha/(1-\alpha)$
0.5000	0.002150	0.1831	0.00263	0.224
0.2500	0.002409	0.2627	0.00327	0.356
0.1250	0.002707	0.3342	0.00407	0.502
0.0625	0.003085	0.4184	0.00530	0.719
0.0313	0.003436	0.5064	0.00696	1.026

Table 20. The reaction $NaOC_2H_5 + C_2H_5Br$ at 25° [13].

$K_i = 0.00545$, $K_m = 0.00215$.

C	K_n	α	$K_n/(1-\alpha)$	$\alpha/(1-\alpha)$
1.0000	0.00288	0.1830	0.00353	0.224
0.5000	0.00311	0.3005	0.00447	0.430
0.2500	0.00339	0.3867	0.00553	0.631
0.1250	0.00370	0.4666	0.00694	0.875
0.0625	0.00396	0.5464	0.00873	1.205

Table 21. The reaction $KOC_2H_5 + C_2H_5Br$ at 25°.

$K_i = 0.00540$, $K_m = 0.00250$.

C	K_n^*	α	$K_n/(1-\alpha)$	$\alpha/(1-\alpha)$
0.5000	0.003600	0.3450	0.00550	0.527
0.2500	0.003772	0.4228	0.00653	0.733
0.1250	0.003957	0.4981	0.00788	0.992
0.0625	0.004152	0.5710	0.00968	1.331
0.0313	0.004367	0.6443	0.01228	1.811

K_n^* is calculated from the values of "K_i" given by Taylor and the values of "α" given by Robertson.

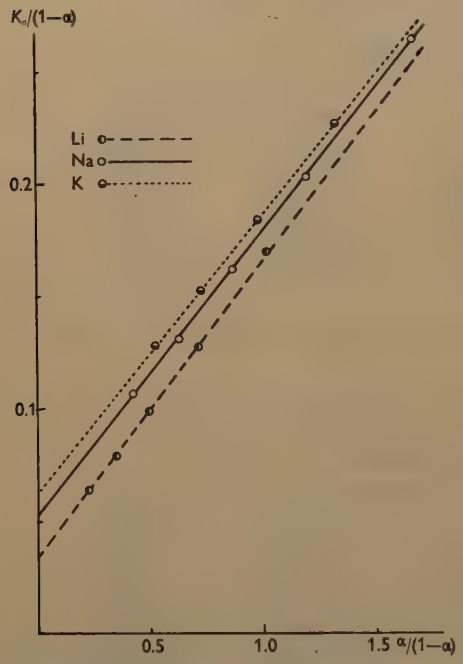

Fig. 6. The reaction of CH_3I with alkali ethoxides at 25°.

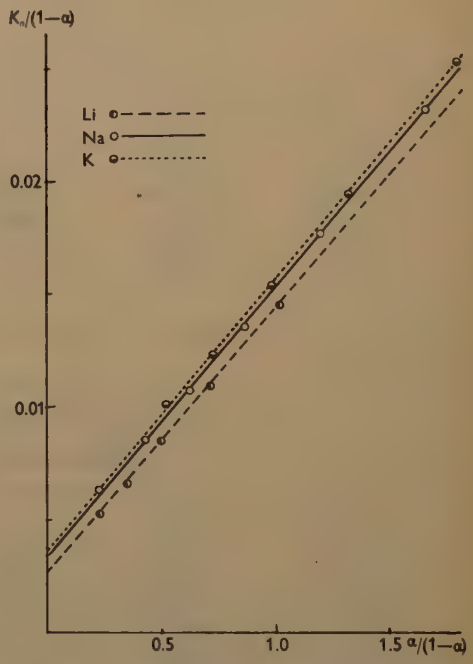

Fig. 7. The reaction of C_2H_5I with alkali ethoxides at 25°.

Figs. 6–8. From these plots it can be seen that all points fits the lines very well and that the reactivity of the ion-pair is indisputable.

The reactivity of the ion-pair in this case can be explained by the following mechanism:

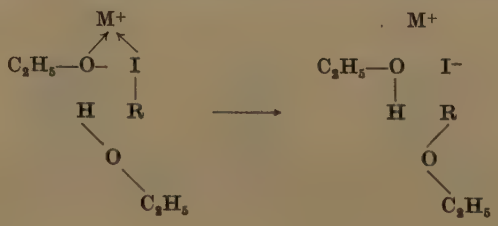

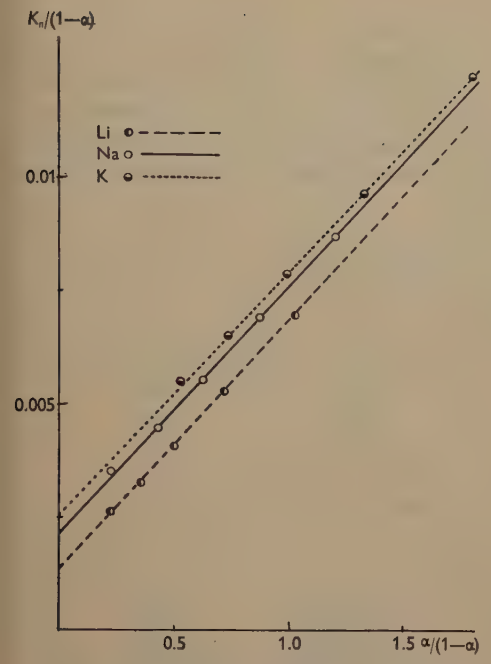

Fig. 8. The reaction of C_2H_5Br with alkali ethoxides at 25°.

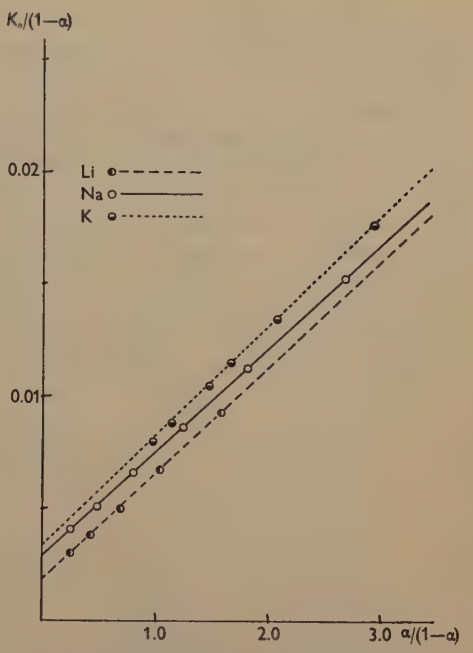

Fig. 9. The reaction of CH_3I with alkali ethoxides at 0°.

This means that the alcohol used as a solvent is alkylated by the halide with the undissociated alcoholate acting as a catalyst. As the cation takes part of the reaction, the constant K_m can be expected to be different for different cations. From the mechanism given above it can be concluded that the cation is attracting electrons both from the anion and the halide, thus rendering the former less reactive and the latter more reactive. As electrons are more easily removed from the charged anion than from the uncharged halide it can be expected that a more electron-attracting cation gives a lower constant K_n than a less electron-attracting one.

The conductivity measurements for the alcoholates indicates that the parameter a is higher for sodium ethoxide than for lithium ethoxide and still somewhat higher for potassium ethoxide. Thus, in the undissociated alcoholates, the distance between the opposite charged ions is shortest for lithium and longest for potassium ethoxide. The lithium ion is therefore more electron-attracting than the sodium ion, which in turn is a little more electron-attracting than the potassium ion. This is in agreement with the fact that K_m is highest for potassium ethoxide and lowest for lithium ethoxide.

It must be pointed out here that the relative size of the parameter a for ion-pairs of different alkali compounds are somewhat difficult to predict, as they depend to a great extent on the degree of solvation of the ions and the value of a is by no means the sum of the radii of both free ions. From the values of Λ_0 it can e.g. be concluded that the free solvated lithium ion in alcohol is bigger than the free solvated sodium ion, whereas the parameter a is higher for sodium ethoxide than for lithium ethoxide.

The reaction of the different alkali ethoxides with methyl iodide have been studied

at 0° by Brown [12]. The conductivities for the ethoxide solutions at 0° have been measured by Robertson [8]. If the conductivity values are corrected as described above, the following limit conductivities are obtained: $LiOC_2H_5$: $\Lambda_0^{0°} = 22.8$; $NaOC_2H_5$: $\Lambda_0^{0°} = 24.9$; KOC_2H_5: $\Lambda_0^{0°} = 26.9$. The values of the velocity constants and the degree of dissociation obtained are given in Tables 22–24, and a plot of $K_n/(1-\alpha)$ against $\alpha/(1-\alpha)$ is given in Fig. 9. From the figure it can be seen that the experimental points fits the line very well and that the importance of the reaction of the undissociated part of the ethoxide is still more important at 0° than at 25°. This is in good agreement with the lower attraction between the alkali ion and the ethoxide ion in the associated part at the lower temperature, which can be seen from the higher degree of dissociation at the lower temperature.

The effect of the temperature can also be found from the velocity constants of the reaction of sodium ethoxide with different alkyl iodides at different temperatures

Table 22. The reaction $LiOC_2H_5 + CH_3I$ at 0°.

$K_i = 0.00475$, $K_m = 0.0018$.

C	K_n	α	$K_n/(1-\alpha)$	$\alpha/(1-\alpha)$
0.5000	0.002406	0.201	0.003011	0.252
0.2500	0.002690	0.298	0.003832	0.425
0.1250	0.002978	0.407	0.005021	0.686
0.0625	0.003322	0.508	0.006758	1.034
0.0313	0.003619	0.613	0.009351	1.584

Table 23. The reaction $NaOC_2H_5 + CH_3I$ at 0°.

$K_i = 0.00463$, $K_m = 0.0029$.

C	K_n	α	$K_n/(1-\alpha)$	$\alpha/(1-\alpha)$
1.0000	0.003281	0.197	0.004088	0.246
0.5000	0.003435	0.328	0.005112	0.488
0.2500	0.003650	0.447	0.006606	0.810
0.1250	0.003840	0.555	0.008637	1.249
0.0625	0.004011	0.644	0.01126	1.809
0.0313	0.004169	0.728	0.01534	2.679

Table 24. The reaction $KOC_2H_5 + CH_3$ at 0°.

$K_i = 0.00490$, $K_m = 0.0033$.

C	K_n	α	$K_n/(1-\alpha)$	$\alpha/(1-\alpha)$
0.2500	0.004031	0.495	0.00799	0.981
0.1875	0.004124	0.533	0.00884	1.143
0.1250	0.004239	0.596	0.01050	1.476
0.0938	0.004346	0.624	0.01157	1.662
0.0625	0.004390	0.674	0.01347	2.067
0.0313	0.004497	0.746	0.01770	2.937

measured by Hecht, Conrad, and Brückner [15], given in Tables 25–36. Even in this case the plot of $K_n/(1-\alpha)$ against $\alpha/(1-\alpha)$ gives excellent straight lines, which can be seen from Figs. 10 and 11.

In this case the degree of dissociation is calculated from the values obtained from the measurements of Robertson [8] at 0°, 25°, and 35° by interpolation in the following way. A plot of Log α against $1/T$ was found to be linear, so that at a given

Table 25. The reaction $NaOC_2H_5 + CH_3I$ at 0°.

$K_i = 0.00523$, $K_m = 0.0024$.

C	K_n	α	$K_n/(1-\alpha)$	$\alpha/(1-\alpha)$
1.0000	0.002958	0.197	0.00369	0.246
0.5000	0.003428	0.328	0.00509	0.488
0.1000	0.003996	0.580	0.00952	1.381
0.0500	0.004348	0.670	0.001318	2.030

Table 26. The reaction $NaOC_2H_5 + CH_3I$ at 12°.

$K_i = 0.0269$, $K_m = 0.0091$.

C	K_n	α	$K_n/(1-\alpha)$	$\alpha/(1-\alpha)$
0.5000	0.01466	0.314	0.0214	0.458
0.0500	0.02014	0.620	0.0530	1.632

Table 27. The reaction $NaOC_2H_5 + CH_3I$ at 18°.

$K_i = 0.0580$, $K_m = 0.018$.

C	K_n	α	$K_n/(1-\alpha)$	$\alpha/(1-\alpha)$
0.5000	0.03020	0.308	0.04364	0.445
0.1000	0.03844	0.513	0.07893	1.053

Table 28. The reaction $NaOC_2H_5 + CH_3I$ at 24°.

$K_i = 0.126$, $K_m = 0.034$.

C	K_n	α	$K_n/(1-\alpha)$	$\alpha/(1-\alpha)$
1.0000	0.05512	0.221	0.0708	0.284
0.5000	0.06272	0.302	0.0899	0.433
0.2000	0.07182	0.412	0.1221	0.701
0.1000	0.07826	0.493	0.1544	0.972
0.0500	0.08696	0.575	0.2046	1.353
0.0250	0.09448	0.656	0.2746	1.907
0.0125	0.10226	0.735	0.3859	2.774

Table 29. The reaction $NaOC_2H_5 + CH_3I$ at 36°.

$K_i = 0.574$, $K_m = 0.14$.

C	K_n	α	$K_n/(1-\alpha)$	$\alpha/(1-\alpha)$
1.0000	0.2344	0.197	0.282	0.245
0.5000	0.2664	0.290	0.375	0.409
0.2000	0.3088	0.386	0.503	0.629
0.1000	0.3408	0.459	0.630	0.848
0.0500	0.3730	0.534	0.801	1.146
0.0250	0.4050	0.608	1.033	1.551
0.0125	0.4370	0.682	1.375	2.145

Table 30. The reaction $NaOC_2H_5 + C_2H_5I$ at 24°.

$K_i = 0.0117$, $K_m = 0.0022$.

C	K_n	α	$K_n/(1-\alpha)$	$\alpha/(1-\alpha)$
1.0000	0.004326	0.221	0.00555	0.284
0.5000	0.004946	0.302	0.00709	0.433
0.2000	0.006104	0.412	0.01038	0.701
0.1000	0.006842	0.493	0.01350	0.972
0.0500	0.007624	0.575	0.01794	1.353

Table 31. The reaction $NaOC_2H_5 + C_2H_5I$ at 36°.

$K_i = 0.0524$, $K_m = 0.0092$.

C	K_n	α	$K_n/(1-\alpha)$	$\alpha/(1-\alpha)$
1.0000	0.01817	0.197	0.02263	0.245
0.5000	0.02148	0.290	0.03025	0.409
0.2000	0.02586	0.386	0.04212	0.629
0.1000	0.02918	0.459	0.05394	0.848
0.0500	0.03234	0.534	0.06940	1.146

Table 32. The reaction $NaOC_2H_5 + n\text{-}C_3H_7I$ at 36°.

$K_i = 0.0209$, $K_m = 0.002$.

C	K_n	α	$K_n/(1-\alpha)$	$\alpha/(1-\alpha)$
0.5000	0.00739	0.290	0.01041	0.408
0.2500	0.00870	0.366	0.01372	0.577
0.1000	0.01066	0.459	0.01970	0.848

Table 33. The reaction $NaOC_2H_5 + n\text{-}C_8H_{17}I$ at 36°.

$K_i = 0.0153$, $K_m = 0.0006$.

C	K_n	α	$K_n/(1-\alpha)$	$\alpha/(1-\alpha)$
0.2500	0.00598	0.366	0.00943	0.577
0.1000	0.00734	0.459	0.01357	0.848

Table 34. The reaction $NaOC_2H_5 + n\text{-}C_{16}H_{33}I$ at 36°.

$K_i = 0.0166$, $K_m = 0$.

C	K_n	α	$K_n/(1-\alpha)$	$\alpha/(1-\alpha)$
0.2500	0.006066	0.366	0.00957	0.577
0.1000	0.00761	0.459	0.01407	0.848

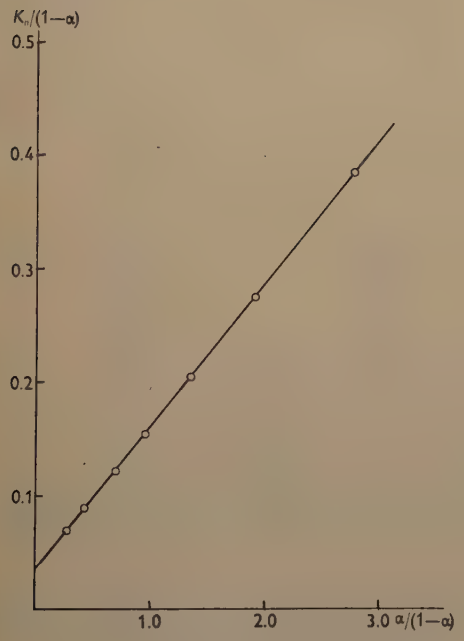

Fig. 10. The reaction of $NaOC_2H_5$ with CH_3I at 24°.

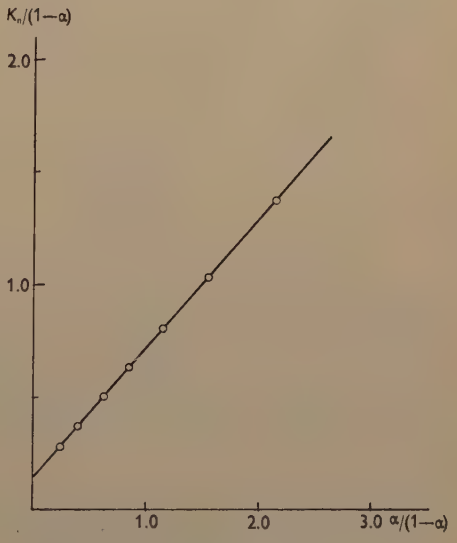

Fig. 11. The reaction of $NaOC_2H_5$ with CH_3I at 36°.

temperature α could be obtained from this plot, using the values calculated at 0°, 25°, and 35° (Fig. 12). To obtain the values of α at concentrations not given by Robertson, use was further made of the fact that a plot of α against log c was linear (Fig. 13).

From Table 35 it is obvious that the fraction K_i/K_m increases with increasing temperature in good agreement with the fact that the attraction between the two

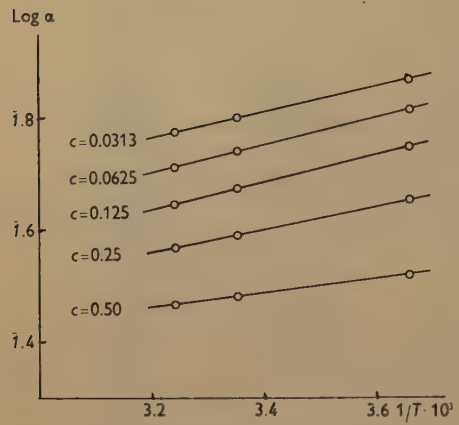

Fig. 12. The dissociation of $NaOC_2H_5$ at different temperatures.

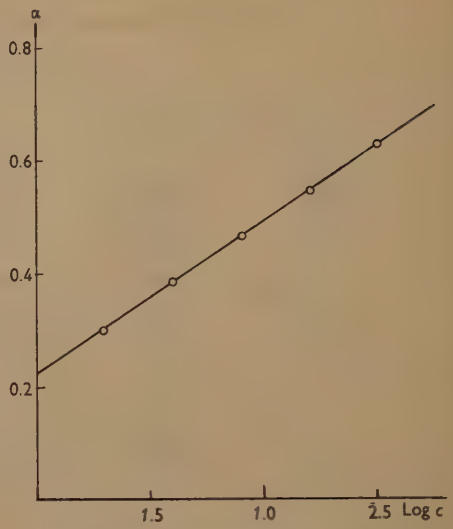

Fig. 13. The dissociation of $NaOC_2H_5$ at 25°.

Table 35. The reaction $NaOC_2H_5 + CH_3I$ at different temperatures.

Temp.	K_i	K_m	K_m/K_i
0	0.00523	0.0024	0.46
12	0.0269	0.0091	0.34
18	0.0580	0.018	0.31
24	0.126	0.034	0.27
36	0.574	0.14	0.24

ions increase (decreased dissociation) with increasing temperature, thus rendering the reaction of the undissociated part of the molecule less important.

It must be pointed out that the data obtained by Hecht, Conrad, and Brückner [15] and those of Acree *et al.* [10–14] cannot be directly compared, as the solutions usually contain different amounts of alkyl iodides and probably different amounts of carbon dioxide, which makes an extrapolation to infinite dilution somewhat uncertain.

From a comparison of the values of K_m/K_i obtained for different alkyl iodides (Table 36), it can be found that this fraction is highest for methyl iodide and decreases

Table 36. The reaction of $NaOC_2H_5$ with different alkyl iodides at 36°.

Iodide	CH_3I	C_2H_5I	n-C_3H_7I	n-$C_8H_{17}I$	n-$C_{16}H_{33}I$
K_i	0.574	0.0524	0.0209	0.0153	0.0166
K_m	0.14	0.0092	0.002	0.0006	0
K_m/K_i	0.24	0.18	0.10	0.04	0

with increasing length of the carbon chain. This is in good agreement with the mechanism proposed, for the reaction with the undissociated ethoxide for this mechanism must be very dependent on steric effects.

The reaction of imino-ethers with sodium ethoxide

The reversible reaction

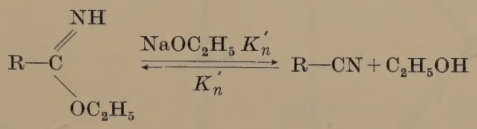

has been studied for the case R = CH_3 and R = C_6H_5 by Harrison [16]. Her results are given in Tables 37 and 38, where K_n is equal to $K_n' + K_n''$, where K_n' is the velocity of the formation of the nitrile and K_n'' the velocity constant for the reverse reaction. As can be seen from Fig. 14 and 15, a plot of $K_n/(1-\alpha)$ against $\alpha/1-\alpha)$ gives a good straight line. In this reaction the ion-pair has good reactivity, which can be explained by the following cyclic mechanism

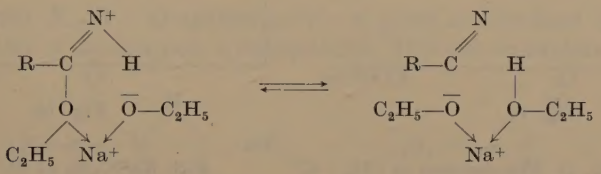

Table 37. The reaction $NaOC_2H_5 + CH_3C(=NH)OC_2H_5$ at 25° [16].

$K_i = 0.346$, $K_m = 0.208$.

C	K_n	α	$K_n/j1-\alpha)$	$\alpha/(1-\alpha)$
0.125	0.2736	0.4666	0.513	0.875
0.0625	0.2848	0.5464	0.628	1.205
0.0313	0.2944	0.6262	0.788	1.675
0.0156	0.3084	0.7048	1.045	2.388

Table 38. The reaction $NaOC_2H_5 + C_6H_5C(=NH)OC_2H_5$ at 25° [16].

$K_i = 0.118$, $K_m = 0.096$.

C	K_n	α	$K_n/(1-\alpha)$	$\alpha/(1-\alpha)$
0.1250	0.1064	0.4666	0.1995	0.875
0.0625	0.1075	0.5464	0.2370	1.205
0.0313	0.1091	0.6262	0.2919	1.675
0.0156	0.1126	0.7048	0.3814	2.388

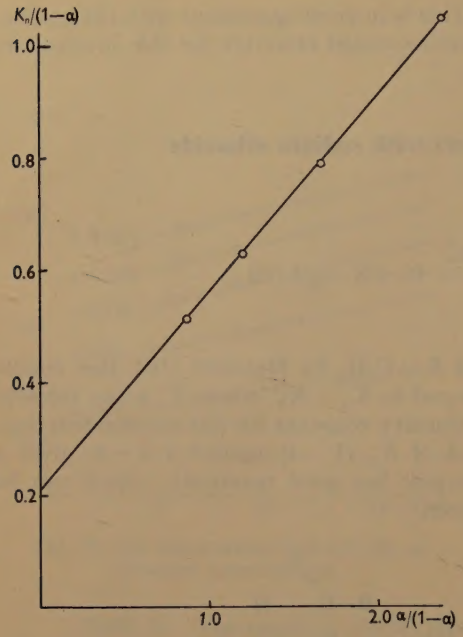

Fig. 14.

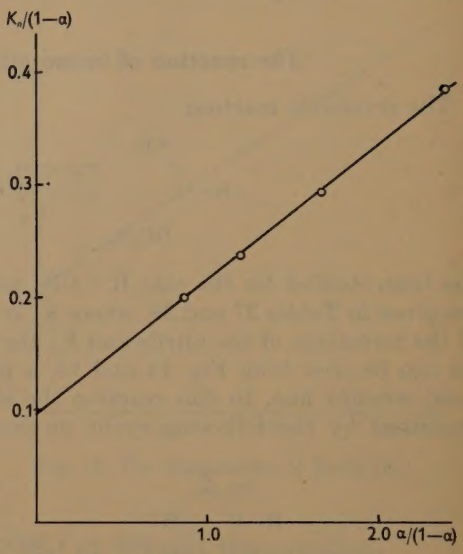

Fig. 15.

Fig. 14. The reaction of $CH_3-C(=NH)OC_2H_5$ with $NaOC_2H_5$ at 25°.

Fig. 15. The reaction of $C_6H_5C(=NH)OC_2H_5$ with $NaOC_2H_5$ at 25°.

The ethylation of 1-phenyl-3-thiourazole

The reaction of sodium 1-phenyl-3-thiourazole with ethyl iodide in alcoholic solution at 25° has been studied by Chandler [17]. The degree of dissociation has been calculated from the conductivity measurements of Robertson [8], which gives $\Lambda_0 = 38.3$. The results are given in Table 39 and Fig. 16. From the figure it can be

Table 39. The reaction of sodium 1-phenyl-3-thiourazol with ethyl iodide at 25° [17].

$K_i = 0.420$, $K_m = 0.120$.

C	K_n	α	$K_n/(1-\alpha)$	$\alpha/(1-\alpha)$
0.2500	0.2265	0.3560	0.352	0.553
0.1250	0.2575	0.4600	0.476	0.852
0.06250	0.2890	0.5518	0.645	1.231
0.03125	0.3120	0.6438	0.876	1.807
0.01563	0.3355	0.7193	1.195	2.563

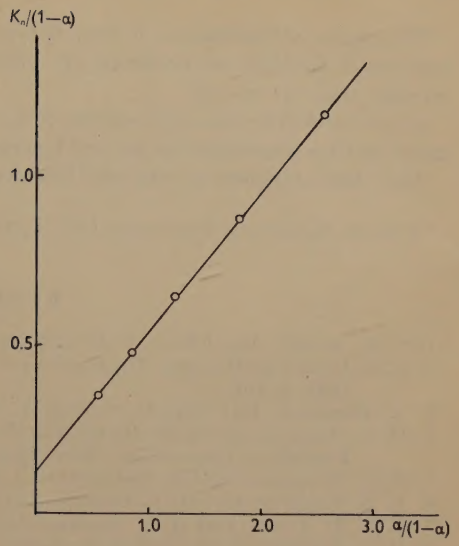

Fig. 16. The reaction of sodium 1-phenyl-3-thiourazol with ethyl iodide at 25°.

seen that the plot $K_n/(1-\alpha)$ against $\alpha/(1-\alpha)$ gives an excellent straight line, and that the reactivity of the ion-pair is indisputable. This can be explained by the following mechanism:

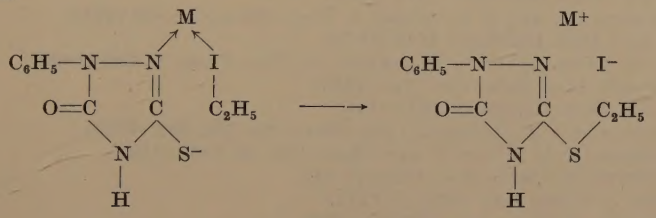

Other reactions

Certain other reactions have been studied at different concentrations of the basic reagent, but the experimental values are not of very good quality or the primary data rather scanty, so that a recalculation cannot be made. This is unfortunately the case for the measurements of Gruse and Acree [18] on the inversion of menthone and that of Myers and Acree [19] on the reaction of *p*-bromobenzonitrile with alkali ethoxides, which like most measurements of Acree *et al.* are of a very good quality. They are, however, extended to such dilute solutions that the contamination of the solvent with carbon dioxide will cause appreciable errors unless the solutions are prepared with an extreme care, and as no anlysis for the content of carbon dioxide was made, the results cannot be depended on. In both reactions the reactivity of the ion-pair is, however, unquestionable.

SUMMARY

The reactivity of some ions and ion-pairs in alcoholic solutions have been recalculated from kinetic results, using an extrapolation method that makes it possible to reduce greatly the errors which result from pimary salt effects.

The degree of dissociation of electrolytes has been calculated by means of the conductivity equation of Marshall and Grunwald (5), which seems to give good values of α even in solutions stronger than 0.1 normal.

A new method for the extrapolation of Λ_0 from conductivity data has been given that gives a linear plot for concentrations up to 0.1 normal.

The "dual mechanism of catalysis" has been found very useful to explain reaction mechanisms.

Research Laboratory, Pharmacia Ltd., Uppsala, Sweden, May 1957.

REFERENCES

1. S. F. Acree, Am. Chem. J. *48*, 353 (1912).
2. E. A. Moelwyn-Hughes, The Kinetics of Reactions in Solution. Oxford Univ. Press, London, 1933, p. 101.
3. N. Bjerrum, Kgl. Danske Selskab *7*, No. 9 (1926).
4. H. S. Harned, and B. B. Owen, The Physical Chemistry of Electrolytic Solutions, Reinhold Publishing Corporation, New York 1950, second edition, pp. 37–39.
5. H. P. Marshall, and E. Grunwald, J. Chem. Phys. *21*, 2143 (1953).
6. N. N. Lichtin, and H. P. Leftin, J. Phys. Chem. *60*, 162 (1956).
7. G. E. M. Jones, and O. L. Hughes, J. Chem. Soc. 1934, p. 1197.
8. H. C. Robertson Jr., and S. F. Acree, J. Phys. Chem. *19*, 407 (1915).
9. G. Jones, and B. C. Bradshaw, J. Am. Chem. Soc. *55*, 1780 (1933).
10. H. C. Robertson Jr., Diss. Baltimore 1910 (1913).
11. J. H. Shrader, Diss. Baltimore 1913.
12. B. M. Brown, Diss. Baltimore 1913 (1915).
13. E. K. Marshall Jr., and S. F. Acree, J. Phys. Chem. *19*, 589 (1915).
14. W. A. Taylor, Diss. Baltimore 1914 (1916).
15. W. Hecht, M. Conrad, and C. Brückner, Z. Phys. Chem. *5*, 289 (1890).
16. J. P. Harrison, Diss. Baltimore 1912 (1913).
17. J. Chandler, Diss. Baltimore 1912 (1915).
18. W. A. Gruse, and S. F. Acree, J. Am. Chem. Soc. *39*, 382 (1917).
19. C. N. Myers, and S. F. Acree, J. Am. Chem. Soc. *50*, 2916 (1928).
20. P. J. Hardwick, J. Chem. Soc. 1935, p. 141.
21. S. S. Woolf, J. Chem. Soc. 1937, p. 1172.
22. J. A. Mitchell, J. Chem. Soc. 1937, p. 1792.

Tryckt den 28 oktober 1957

Uppsala 1957. Almqvist & Wiksells Boktryckeri AB